UNIVERSITÄTSKLINIKUM HAMBURG-EPPENDORF

Klinik und Poliklinik für Neurologie

Prof. Dr. med. Tim Magnus

Enhancing the Brain's Barrier: CD73 Gene Therapy for Stroke Protection in Mice

Dissertation

zur Erlangung des Doktorgrades PhD

an der Medizinischen Fakultät der Universität Hamburg.

vorgelegt von:

Maria Stamataki

aus Hamburg

Hamburg 2026

Betreuer: Prof. Dr. Tim Magnus

Mitglieder des Thesis-Komitees:
Mitglied: PD Dr. Jakob Körbelin
Mitglied: PD Dr. Björn Rissiek

Gutachtende:
Gutachter: Prof. Dr. Tim Magnus
Gutachter: PD Dr. Jakob Körbelin

Mitglieder der Prüfungskommission:
Vorsitz der Prüfungskommission: Prof. Dr. Tim Magnus
Mitglied der Prüfungskommission: PD Dr. Jakob Körbelin
Mitglied der Prüfungskommission: Prof. Dr. Eva Tolosa

Datum der Disputation: 25.08.2026

This study was conducted between January 2023 and March 2026 at the University Medical Center Hamburg-Eppendorf (UKE) and funded via the CRC SFB1328 (DFG).

Ὁ βίος βραχύς, ἡ δὲ τέχνη μακρή,
ὁ δὲ καιρὸς ὀξύς, ἡ δὲ πείρα σφαλερή,
ἡ δὲ κρίσις χαλεπή.

Life is short, the art long, opportunity fleeting,
experiment uncertain, and judgment difficult.

— Hippocrates, *Aphorisms* I.1

Inhalt

1. Introduction

1.1 Ischemic stroke as a global health burden

Ischemic strokes still remains one of the most common and devastating neurological disorders worldwide. It is characterized by tissue injury caused by the sudden interruption of the blood supply to a certain brain region leading to oxygen and nutrients deprivation. Within minutes, cells inside the brain begin to undergo necrosis. According to the World Stroke Organization, stroke is among the three leading causes of death globally and the main cause of long-term neurological disability. Every year, more than twelve million people experience a stroke and over six million die as a result of it [1-5]. About 85% of all strokes are ischemic, which are usually caused by thrombotic or embolic occlusions of the cerebral arteries. While the remaining stroke cases are hemorrhagic [1-3].

The incidence of stroke is continuously growing despite major progress in prevention, acute treatment and rehabilitation. Some factors contributing to this increase include aging, hypertension, diabetes, dyslipidemia and smoking. The incident rate is expected to increase even more, especially in low- and middle-income countries where access to early diagnosis, specialized stroke units and acute treatment is still limited [1-3, 6]. Studies show that most stroke survivors also experience chronic consequences in the quality of their life [7, 8].

The introduction of reperfusion therapies, such as intravenous thrombolysis with recombinant tissue plasminogen activator (rt-PA) [9] and mechanical thrombectomy [10], changed the path of acute stroke treatment. Although these treatments have been beneficial for many patients by restoring the blood supply in the affected brain region, they are available only for a subset of patients. Such treatment is only feasible in case the occluded vessel is visible and accessible to the surgeon and patients need to get immediate medical attention [10]. So in reality, many patients arrive too late to the hospital or do not meet the criteria, which means that effective acute treatment is not an option for them.

Even when reperfusion is successful, recovery is often incomplete. Many survivors are left with long term motor, cognitive or emotional impairments that affect their independence and daily life [7, 8, 11-13]. Common post stroke symptoms include cognitive decline, persistent fatigue or depression. So for many patients, stroke does not end when they leave the hospital,

but It becomes a chronic condition with lasting neurological and psychological consequences [11-13].

These challenges highlight the urgent need for new therapeutic strategies that go beyond vessel reopening and address directly the downstream mechanisms of tissue injury, inflammation and repair after ischemic stroke.

1.2 The blood-brain barrier and its role in stroke pathophysiology

The main role of the blood-brain barrier (BBB) is to protect the delicate environment of the central nervous system (CNS) by regulating the exchange of molecules between the CNS and the bloodstream, keeping pathogens out while allowing vital nutrients to pass [14, 15]. The BBB consist of endothelial cells, pericytes, astrocytic end-feet and the basement membrane [16, 17].

More specifically, the endothelial cells form the physical barrier and are connected by tight junctions. The pericytes help stabilize the vasculature and suppress excessive endothelial permeability, while the astrocytic end-feet provide metabolic support and regulate endothelial polarization through secretion and even direct contact [18-20]. Lastly, the basement membrane provides a stable structure as well as a platform of signaling that influences leukocyte adhesion and migration [21].

The BBB belongs to the neurovascular unit (NVU), which is a multicellular system composed of endothelial cells, pericytes, astrocytes, microglia, neurons and the surrounding extracellular matrix [17, 19, 20, 22]. Each of these cell types contribute to the integrity of the BBB and their constant communication with each other is vital for a protected CNS. The NVU has the ability to adapt in case of pathogenic or injury related threads in order to keep the CNS protected while trying to restore homeostasis inside it [16, 17, 20].

However, during an ischemic stroke episode the sudden disruption of blood flow initiates a cascade of metabolic and inflammatory events that disrupt the BBB integrity. The deprivation of oxygen and glucose affects the energy metabolism of the endothelial cells and results in cytoskeletal changes, loss of tight junction proteins such as claudin-5, occludin, ZO-1 and increases paracellular permeability [15, 23, 24]. Even when the oxygen levels have been

restored to the affected region, it can further aggravate injury through oxidative stress, activation of matrix metalloproteinases (particularly MMP-2 and MMP-9) and inflammatory signaling pathways [15, 25]. This enables the infiltration of plasma proteins, leukocytes and water inside the brain tissue, contributing to edema formation and secondary injury [15, 23-25].

From a clinical perspective, the disruption of the BBB is linked to increased neurological damage, higher risk of hemorrhagic transformation and impaired recovery [15, 20, 26]. The involvement of the BBB and the way it can influence stroke outcomes, which will be further discussed in the next subchapter, is the reason why it has become both a key target and a major challenge in stroke research as it holds great promises for new therapeutic avenues [14, 15, 20, 26].

1.3 The BBB as an active regulator of immune cell recruitment and functional polarization

The lack of peripheral immune cells is what gives the brain its status as an immune-privileged organ. This means that under physiological conditions, the BBB does not allow the infiltration of peripheral immune cells inside the brain. This is achieved thought constant active regulatory mechanisms that control leukocyte adhesion, migration and signaling at the vascular interface [17, 20, 22, 27, 28].

Immune cell migration across the BBB is a highly coordinated process with multiple steps, including the interaction between endothelial adhesion molecules, chemokines and the cellular compartment as well as the extracellular components of the NVU. The endothelial cells that constitute part of the BBB express specific adhesion molecules and chemokines, that determine which immune cell populations are able to interact with the vessel wall and eventually are allowed into the CNS [27, 28]. During neuroinflammation, the infiltration of immune cells is still being partially controlled by the BBB rather than in an uncontrolled manner, even though the above-mentioned regulatory processes are impaired as the BBB becomes disrupted [20, 21, 28]. Especially in the context of stroke, changes in endothelial metabolism, inflammatory signaling and extracellular matrix composition result in an altered

immune environment more suitable for immune cells transmigration. The infiltrating immune cell populations often demonstrate a mix of activation states, likely because they continue to receive regulatory signals from the BBB [15, 20, 29].

So, the activation and polarization of the immune cells post infiltration are also influenced by the BBB. It is worth to mention that all components of the BBB provide signals that influence immune cell activation, polarization and retention [16, 17, 21, 28]. For example, the composition of endothelial and parenchymal basement membranes has been shown to regulate not only the entrance side of the immune cells in the brain but also how they migrate and what functional state they adopt once inside [20, 21, 28].

1.4 Neuroinflammation and immune cell responses in the CNS

An ischemic stroke initiates a neuroinflammatory response that involves both the resident immune cells of the CNS and the peripheral immune cells [29, 30]. These responses are not purely harmful or purely protective but their effects depend strongly on timing, location and the specific cell type populations involved. In the early phase, inflammatory processes usually contribute to secondary tissue damage and exaggeration of the injury. But as time passes, immune cells can also support debris clearance, tissue remodeling and recovery [30, 31]. Understanding the different immune cell populations involved and their roles in the immune response post stroke is essential for the interpretation of observed effect and the investigation of potential therapeutic strategies.

1.4.1 Resident immune cells of the CNS

Even under physiological conditions the CNS is not immunologically silent. It has its own resident immune cells that constantly monitor the tissue, maintain homeostasis and respond to potential harm. But the immune system of the CNS is very different from that of the rest of the peripheral organs [32, 33].

1.4.1.1 Microglia: the main immune cells of the CNS

Microglia are the primary resident immune cells of the CNS. They originate from primitive myeloid progenitors in the embryonic yolk sac and are found in the brain very early in development, even before the BBB is fully formed [33, 34]. What sets microglia further apart from peripheral macrophages, which are being constantly replenished by bone marrow derived monocytes, is that microglia are self-renewing [33, 35].

In the healthy brain, the microglia display a highly branched morphology and they continuously survey their environment, able to sense the most subtle changes in neuronal activity, extracellular ATP levels and tissue integrity [36, 37]. Through these activities, microglia contribute to synaptic remodeling, clearance of cellular debris and the maintenance of functional neuronal circuits [38].

Microglia express a wide range of pattern recognition receptors, purinergic receptors and cytokine receptors, which enables them to respond quickly to danger-associated molecular patterns (DAMPs) during tissue injury. After an ischemic stroke, microglia become activated and undergo both morphological and functional changes [29, 31]. It is also important to highlight that terms like “M1” and “M2” have been outdated and although the use of “M1-like” and “M2-like” are still acceptable, microglia do not switch into a single fixed state. They are highly adaptable cells and can adopt a range of different phenotypes, ranging from pro-inflammatory with tissue damaging properties to anti-inflammatory and reparative ones that support debris clearance, tissue remodeling and recovery [39, 40].

1.4.1.2 Border-associated macrophages

In addition to microglia, inside the CNS there are several populations of tissue-resident macrophages known as border-associated macrophages (BAMs). These cells are located at the interfaces between the brain and the periphery, including the meninges, perivascular spaces and choroid plexus [41, 42]. Similar to microglia, many of these macrophage populations originate from embryonic progenitors and are maintained locally, without relying on circulating monocytes for renewal [43].

Because of their location, BAMs serve as guards at the CNS barriers. They monitor the cerebrospinal fluid and perivascular compartments for pathogens or inflammatory signals and can contribute to antigen presentation as well as in the regulation of leukocyte migration across the CNS barriers [32, 42]. After an ischemic stroke, BAMs become activated and take part in inflammatory signaling. However, their exact role and how they differ from microglia or infiltrating macrophages are still not fully understood.

1.4.1.3 Astrocytes and other glial cells as immune modulators

While microglia and BAMs represent the main resident immune cells of the CNS, they are not the only ones forming the immune system of the brain. Astrocytes, which are the most abundant glial cells in the brain, are essential for the formation and maintenance of the BBB and are heavily involved in neuroinflammatory responses [44, 45].

Astrocytes undergo a process known as reactive astrogliosis when there is an inflammation or tissue injury. Astrogliosis leads to morphological changes, increased proliferation and shifts in gene expression patterns [46]. Their response is also not fixed, but rather it depends on the context and the signals they receive. Reactive astrocytes can release pro-inflammatory cytokines and chemokines that promote leukocyte recruitment or produce neurotrophic and anti-inflammatory signals that support tissue repair and recovery [45]. So astrocytes do not simply react to inflammation but they actively shape the inflammatory environment within the CNS. Other glial populations of the CNS are also part of its immune system, such as the oligodendrocyte progenitor cells that take part in immune signaling by producing cytokines, expressing adhesion molecules and interacting directly with infiltrating immune cells.

These interactions highlight that the immune response against neuroinflammation is not only driven by infiltrating peripheral immune cells, but it develops firstly from a continuous communication between multiple resident cell types within the CNS [29].

1.4.1.4 Functional roles of resident immune cells in homeostasis and injury

Under normal conditions, resident immune cells help maintain CNS homeostasis by clearing apoptotic cells, regulating synaptic connectivity and supporting vascular and neuronal

functions. But after an ischemic stroke, this changes rapidly. The same cells that normally maintain homeostasis become activated and initiate inflammatory cascades that influence both tissue damage and the later phases of repair [29, 47].

Microglia are usually among the first to respond. They sense ATP and other DAMPs from neighboring damaged or dead neurons and react within minutes to hours. This activation leads to the production of cytokines, chemokines and reactive oxygen species (ROS), which can worsen tissue injury even more, especially in the early phase. Eventually, microglia also are responsible for debris clearance and the resolution of inflammation [31, 40]. Astrocytes and BAMs detect similar signals and take part in both inflammatory and reparative processes, adjusting their behavior as the environment changes.

These immune responses are tightly linked to the state of the BBB. When endothelial cells become activated and the barrier is disrupted, the local inflammatory environment shifts and peripheral immune cells begin to enter the brain. At the same time, signals from resident immune cells influence the function of both endothelial cells and leukocytes. This constant communication between the vascular and immune compartments is a vital part of the CNS response to injury [29, 32].

In summary, resident immune cells form a dynamic and interconnected network. Under healthy conditions, they maintain homeostasis and under inflammation or injury, they help orchestrate the inflammatory response, shaping both the extent of damage and the potential for recovery.

1.4.2 Peripheral immune cell infiltration after stroke

Stroke does not only activate resident immune cells but it also triggers the recruitment of the peripheral immune cells. The activation of the endothelial cells and the release of cytokines and DAMPs leads peripheral immune cells to firstly attach to the vessel wall of the BBB and then finally infiltrate into the affected region of the brain [29, 47]. The infiltration of peripheral immune cells occurs in a rather coordinated manner and can contribute to both tissue damage and repair, depending on the cell type and stage of the inflammatory response [30, 48].

The first responders to the side of inflammation are neutrophils [49]. Once they have entered the brain, they release ROS, proteolytic enzymes and pro-inflammatory cytokines, which contribute to further disruption of the BBB and exacerbate tissue damage [29, 48].Neutrophils have also the ability to form neutrophil extracellular traps (NETs), that have been linked to the contribution of secondary injury after stroke [50]. Withing the first days monocytes do also enter the brain, where they differentiate into macrophages and initiate phagocytosis, cytokine production and tissue remodeling [29, 31]. Infiltrating monocytes/macrophages have been shown to interact closely with microglia and affecting their activation state and polarization [51]

Just like microglia, macrophages can adopt a plethora of phenotypes. [31, 40, 47]. Macrophages can exhibit both pro- and anti-inflammatory effects. It has been demonstrated that in the first week post stroke macrophages tend to adapt a more reparative phenotype promoting debris clearance and tissue protection. A more pro-inflammatory “M1-like” state has been observed in later stages of neuroinflammation, these macrophages are releasing cytokines such as TNF-α and IL-1β. It should be noted that many markers for M1 and M2 macrophages overlap and therefore making the distinction of them complicated while also supporting the theory of mixed activation states [52, 53]

Transcriptomic studies have demonstrated that macrophages exhibit strong transcriptional changes in a stroke mouse model, with gene expression patterns that are linked to neurovascular remodeling [54]. T lymphocytes (T cells) are part of the adaptive immune response and although they are passing through the BBB in a quite later stage, they also contribute in the progress of the neuroinflammation [30, 49]. $CD4^+$ T cells, such as T helper 1 (Th1) and T helper 17 (Th17) are releasing pro-inflammatory cytokines such as INF- γ and IL-17, while regulatory T cells (Tregs) support tissue repair and resolution of inflammation [29, 55, 56]. A clinical study showed that stroke patients demonstrated an altered dynamic of circulating $CD4^+$ T cells, as they migrate to the brain tissue and makes those patients more susceptible to infections [56].

In another study γδ T cells were identified to response more quickly that other T cells [57]. γδ T cells can be activated by the cytokines IL-23, IL-1β and IL-18 that are being released from dendritic cells and infiltrating macrophages. γδ T cells influence the stroke pathophysiology

by cytokine release. IL-17a producing ones have been shown to promote neutrophil recruitment and contribute in neuronal death and tissue damage [58]. While, γδ T cells producing IL-22 have been observed to exert neuroprotective effects [59]. The role of γδ T cells seems to be context-dependent and therefore their role in ischemic stroke is not yet completely understood.

Natural killer (NK) cells are another lymphocyte population that infiltrates into the brain tissue post stroke. They belong to the innate immune system and are able to release perforin and granzymes that are neurotoxic and contribute to neurodegeneration. [29, 60].

More immune cells, such as B cells and other lymphocyte subsets, have also been detected at later stages of the inflammatory response. These cells may take part in antigen presentation, antibody production and the modulation of T cell responses. But their overall contribution to stroke pathology remains less well understood [29, 30].

The progression of infiltrating immune cells reflects the constantly evolving inflammatory environment and contributes to the transition from acute injury to repair and remodeling of the brain tissue. As previously mentioned, the infiltration of the peripheral immune cells is not a random act, but there is an order in the type, number and timing of cells entering the brain parenchyma depending on the condition of the BBB. The activated endothelial cells show an alternate expression of adhesion molecules and production of chemokines and these signals are one of the most significant steps in the inflammatory response to ischemic stroke, as they are responsible for the migration of the immune cells [29, 47].

So the interaction between endothelial cells, resident immune populations and infiltrating leukocytes ultimately determines whether the inflammatory response is causing further tissue damage or supports recovery and repair.

1.5 Purinergic signaling and inflammation

Purinergic signaling is a communication system and within the CNS it allows the interaction between neurons, glial cells, endothelial cells and even infiltrating immune cells through extracellular nucleotides and nucleosides (Fig. 1).

In homeostasis, ATP acts as an intracellular energy source that is essential for metabolic processes. However, during cellular stress or tissue damage, ATP is being release into the extracellular space and acts as a signaling molecule via vesicular exocytosis, membrane channels or specific transporters. Extracellular ATP and its metabolites interact with a broad family of purinergic receptors. These include ionotropic P2X receptors and metabotropic P2Y receptors, which are found on neurons, glial cells, endothelial cells and immune cells. The activation of these receptors can influence vital functions in both healthy and diseased conditions such as neuronal excitability, vascular regulation, and immune cell behavior depending on the type of the receptor and the means of activation [61-64].

More specifically, during tissue injury, stressed and dying cells are releasing ATP into the extracellular space and it acts as a DAMP alerting the immune system. The P2X and P2Y receptors on microglia and macrophages are being activated and the release of cytokines, chemotaxis and the activation of inflammasome are being initiated. This signifies the start of the immune response against inflammation [63-67]. But if ATP signaling is excessive or prolonged, it can also contribute to secondary tissue injury. To avoid further damage, ectonucleotidases expressed on endothelial and immune cells have the ability to degrade extracellular ATP. Two of the most important enzymes in this pathway are the ectonucleoside triphosphate diphosphohydrolase-1 (ENTPD1) a.k.a. CD39 and the ecto-5'-nucleotidase (*NT5E*) a.k.a. CD73. CD39 converts ATP and ADP into AMP and then CD73 hydrolyzes AMP into adenosine. Adenosine can activate the P1 receptors, including the A_1, A_{2A}, A_{2B} and A_3 receptor subtypes creating a more anti-inflammatory and tissue protective environment [63, 68-70] (Fig. 1).

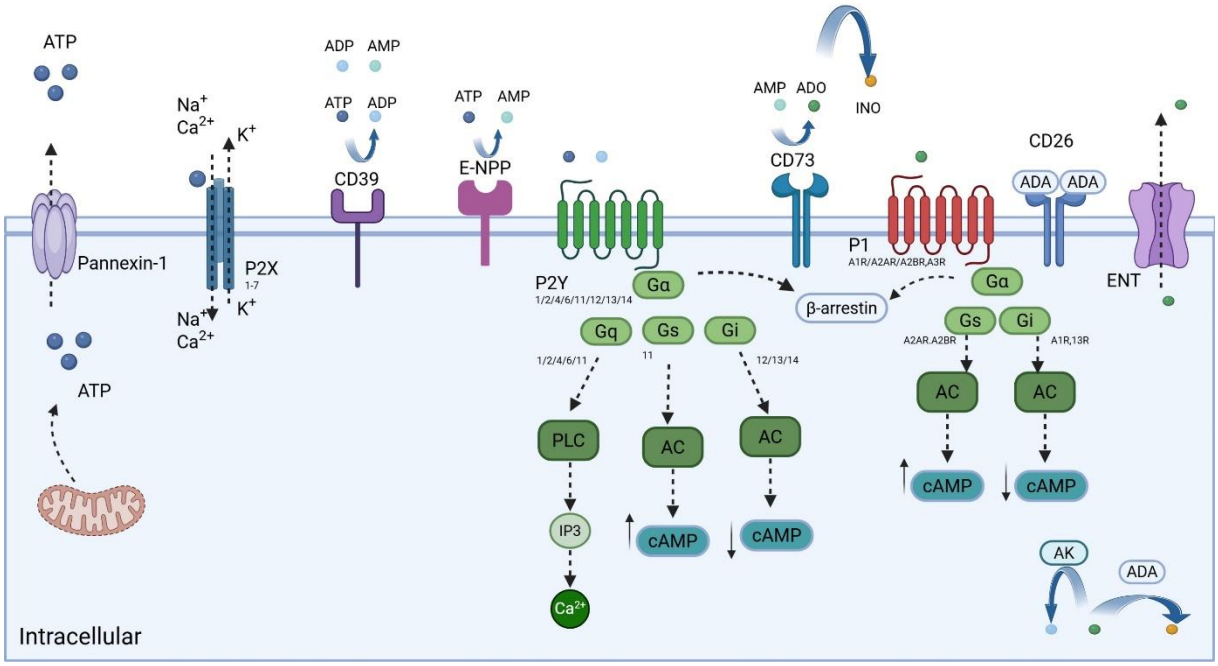

Figure 1: Overview of purinergic signaling at the cell surface.

Extracellular ATP released is hydrolyzed to ADP and AMP by CD39 and further converted to adenosine by CD73. ATP and ADP mainly signal through P2 receptors and are commonly linked to pro-inflammatory responses, while adenosine generated by CD73 shifts signaling toward P1 receptor activation, which promotes anti-inflammatory responses [61]. Reproduced from Gratal et al., 2020 [71]. *Created in BioRender.com.*

The balance between extracellular ATP and adenosine therefore becomes a critical determinant of the inflammatory environment in the ischemic brain. If ATP is not efficiently degraded, pro-inflammatory signaling may lead to endothelial exhaustion and more severe tissue injury [70, 72].

In contrast, increased adenosine production has been linked to neuroprotection, reduced leukocyte infiltration and improved outcomes in several experimental models [62-64, 73]. Brain endothelial cells mainly express A_{2A} and A_{2B} receptors. Acting on these receptors, adenosine can increase cyclic AMP (cAMP) levels and stabilize tight junctions, which supports

BBB integrity under inflammatory conditions [70, 72, 74] (Fig. 2), while the activation of P2 receptors via ATP promotes endothelial contraction and barrier leakage [65, 70, 72]. So the purinergic system functions as a dynamic balance between pro-inflammatory ATP signaling and anti-inflammatory adenosine signaling. This balance plays an important role in determining whether the vascular and immune responses after ischemia lead to further injury or support resolution, tissue protection and repair [62-64, 68].

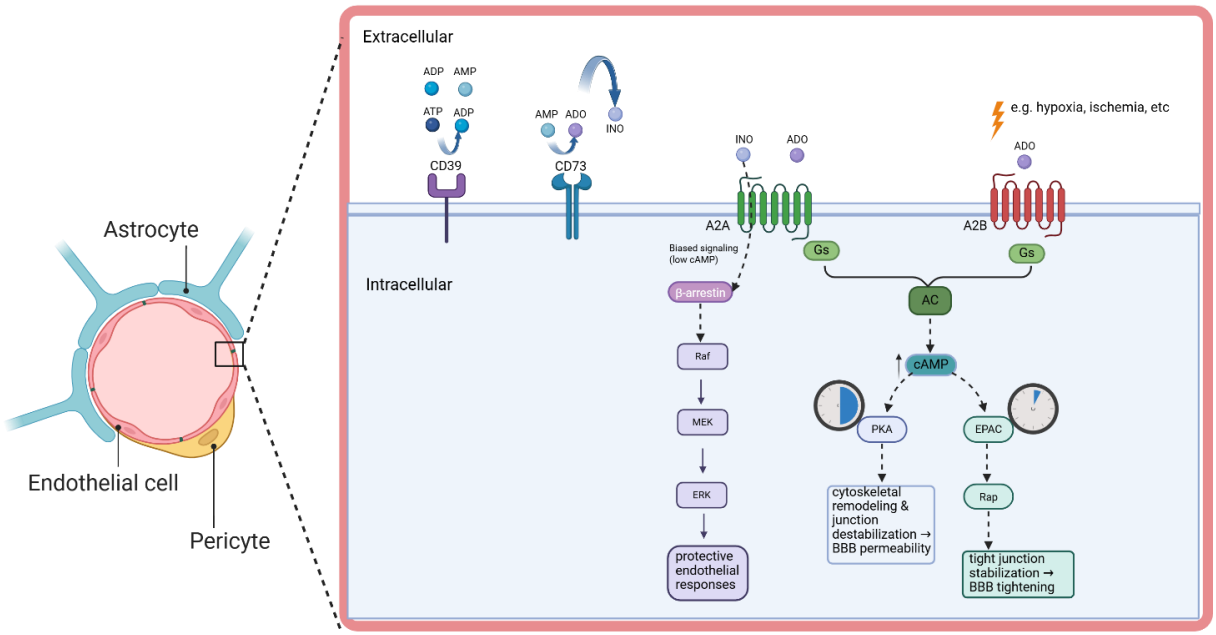

Figure 2: Adenosine receptor signaling at the BBB in humans.

Adenosine generated by CD73 activates A_{2A} and A_{2B} receptors on brain endothelial cells. A_{2A} signaling can engage β-arrestin-dependent pathways and increases intracellular cAMP via Gs-coupled signaling, while A_{2B} receptor activation mainly increases intracellular cAMP. The activation of protein kinase A (PKA) or *exchange factor directly activated by cAMP 1* (EPAC1) differentially affects cytoskeletal organization and tight junction stability and subsequently BBB permeability [75, 76]. *Created in BioRender.com.*

1.6 Ectoenzymes CD39 and CD73: function and regulation

The CD39 and CD73 cascade can control the breakdown of extracellular ATP and the generation of adenosine at the cell surface; this is why these ectoenzymes can influence the

inflammatory environment and the responses of endothelial and immune cells in stressed or injured tissues [63, 68, 69, 77, 78].

The expression of both CD39 and CD73 depends on their environment and pathological stimuli. It has been shown that under hypoxic or inflammatory conditions, CD73 is being upregulated through the hypoxia-inducible factor-1α (HIF-1α) pathway and can also be induced by transforming growth factor-β (TGF-β) resulting in enhanced adenosine production [68, 79]. However, cytokines such as TNF-α and IFN-γ, which have a pro-inflammatory effect have been shown to downregulate CD73 expression on endothelial cells, leading to reduced adenosine levels [68, 80].

CD73 is not only important because of its enzymatic activity but it also can interact with components of the extracellular matrix and adhesion molecules that influence leukocyte transmigration, endothelial barrier regulation and tissue remodeling [70, 72, 81]. On the brain endothelium, adenosine generated by CD73 promotes vasodilation, inhibits leukocyte adhesion and reduces endothelial permeability [70, 72, 74].

Within the CNS both CD39 and CD73 are expressed across multiple cell types of the NVU but their expression on brain endothelial cells differs considerably between species, an aspect that the following section will be focusing on [72, 82].

1.7 Species differences in endothelial purinergic machinery

Although purinergic signaling is a cellular communication system found in many species, the abundance and regulation of its enzymes and receptors can differ between them. These differences are especially found in the endothelium, where extracellular nucleotide metabolism plays an important role in controlling vascular tone, immune cell trafficking and barrier integrity. A previous study has demonstrated that CD73 expression at the BBB is substantially higher in humans than in mice, demonstrating important interspecies differences [82]. So the low levels of CD73 in the mouse brain endothelium may limit the conversion of AMP into adenosine and hence the levels of adenosine in the brain [72].

This low basal expression of CD73 in the mouse brain endothelium has been suggested to favor ATP-driven pro-inflammatory responses that lead to persistent activation of P2

receptors, sustained cytokine release and endothelial activation [63, 68]. The higher endothelial CD73 expression detected in humans may provide a more balanced environment by enhancing adenosine production and promoting tissue protection during cellular stress and damage, such as hypoxia or ischemic stroke [70, 79]. Moreover, species differences in ectonucleotidase activity, glycosylation and membrane anchoring may further influence enzymatic kinetics and the distribution of these enzymes at the luminal endothelial surface [69].

This difference in the purinergic signaling of the murine brain endothelium may represent a limitation when translating stroke therapies to humans and highlights the need for experimental approaches that adjust endothelial purinergic capacity to reflect the one seen in humans.

1.8 Therapeutic potential of modulating ATP-adenosine conversion at the BBB

The ATP-adenosine axis has become a potential therapeutic target as it directly links inflammatory signaling to endothelial barrier function and leukocyte recruitment at the neurovascular interface [63, 64, 68]. Shifting this balance toward a more rich in adenosine environtment may support BBB integrity and limit secondary injury post stroke, as adenosine signaling particularly via the A_2A and A_2B receptors has been linked to improved endothelial barrier stability [70, 72, 74, 83].

Experimental studies in other peripheral organs demonstrated that increasing CD73 expression or activating adenosine receptors reduced reperfusion injury as well as vascular permeability and promoted tissue recovery [63, 84-86]. For example, adenosine signaling through the A_2B receptor has been shown to protect the liver and heart from ischemic injury by stabilizing endothelial function and suppressing leukocyte recruitment [83, 85, 86].

Adenosine signaling may also influence leukocyte trafficking at the neurovascular interface. Immune cell entry into the CNS is not determined solely by endothelial activation but is also shaped by interactions with the vascular basement membrane and surrounding extracellular matrix. Another group has shown that distinct laminin isoforms within the vascular basement

membrane regulate leukocyte migration across the vessel wall and into the CNS parenchyma [21, 87].

1.9 Adeno-associated viral vectors as gene delivery tools

1.9.1 Biology and structure of adeno-associated viruses

Adeno-associated viruses (AAVs) are small, non-enveloped viruses that belong to the *Parvoviridae* family and the *Dependoparvovirus* genus. They are characterized by a single-stranded DNA genome of approximately 4.7 kilobases which is enclosed within an icosahedral capsid [39, 88]. Wildtype AAVs are replication defective and require the presence of a helper virus, such as an adenovirus or a herpes simplex virus [39, 89]. An AAV can establish a latent infection if there is no helper virus involved.

The AAV genome consists of two main open reading frames, *rep* and *cap*, that are flanked by inverted terminal repeats (ITRs). The *rep* gene encodes the replication proteins Rep78, Rep68, Rep52 and Rep40, which are involved in genome replication, packaging and integration. While the *cap* gene encodes the structural capsid proteins VP1, VP2and VP3, which form the viral particle [39, 90]. The ITRs are palindromic sequences that form hairpin structures and are essential for viral genome replication and packaging. In the case of a recombinant AAV (rAAV) vector, the *rep* and *cap* genes are removed and replaced by a therapeutic transgene cassette, while the ITRs are still preserved in order to enable vector production and genome replication [91].

AAV vectors have become one of the most used gene delivery tools due to their non-pathogenic status in (most) humans and their relatively low immunogenicity compared to other viral vectors [91]. AAVs have the ability to also establish long term transgene expression in post mitotic cells without integrating into the host genome [90]. This reduces the risk of mutagenesis while still allowing sustained gene expression, especially in tissues with low cellular turnover such as the CNS.

1.9.2 AAVs in the central nervous system

Due to the limited regenerative capacity of the neural tissue and the fact that many neurological diseases affect large parts of the brain and different types of cells, the CNS

remains a challenge for gene therapies. AAV vectors have emerged as one of the most promising tools for CNS gene delivery because of their ability to transduce post-mitotic cells [90, 91].

One of the defining features of AAVs in the CNS is their serotype tropism. Different AAV serotypes show specificity for neurons, glial and vascular cells of the CNS. For example, AAV2 was one of the first serotypes used for CNS gene transfer and has been even applied in early clinical trials for Parkinson's disease, due to its strong neuronal tropism following direct intracerebral injection [92]. Subsequent studies identified additional serotypes, such as AAV5, AAV8 and AAV9 with improved transduction efficiency and broader cellular targeting in the brain [93, 94].

A major advance in CNS gene therapy was the discovery of AAV serotypes, like AAV9, that can cross the BBB after systemic administration. In mice, systemic delivery of AAV9 resulted in a widespread transduction of neurons and glial cells throughout the brain and spinal cord when administered at early developmental stages [95]. This finding demonstrated the possibility of non-invasive CNS gene delivery.

The clinical success of AAV mediated gene therapy has been mostly observed in the treatment of inherited neurological diseases. One example is the development of the AAV9 *onasemnogene abeparvovec* therapy for spinal muscular atrophy (SMA), which delivers a functional copy of the *SMN1* gene to motor neurons post systemic administration. Clinical trials showed substantial improvements in both the survival and the motor functions of the patients [96-98].

A big limitation in systemic administration of AAVs in the CNS is that the BBB is not allowing the infiltration of the circulating AAV vectors. The different cell populations within the NVU also exhibit individual susceptibilities to AAV transduction, which further complicates the systemic delivery of the vector inside the CNS [94, 97]. Therefore efforts are being made towards the development of novel capsids with enhanced CNS tropism and improved cell type specificity [99].

The identification of the AAV capsid BR1 that has selective tropism for brain endothelial cells in mice, has enabled more precise genetic modulation of the NVU *in vivo* [100].

Overall, the ability of AAV vectors to achieve stable gene expression in the CNS combined with the continuous efforts in capsid engineering further signifies the recognition of AAV mediated gene therapies as a promising tool for clinical applications in Neurology.

1.9.3 Capsid engineering and endothelial targeting strategies

While these intrinsic properties have made AAV vectors highly effective for gene delivery to many organs, there are also challenges when specific cell types need to be targeted. For example, efficient and selective targeting of endothelial cells in the CNS has remained difficult to achieve in humans [97, 101]. Part of this difficulty comes from biological differences between endothelial cells and other CNS cell types. Endothelial cells express distinct surface receptors, rely on different endocytic pathways and handle intracellular signaling in ways that do not make neither the entry nor the transgene expression of AAVs easy.

Because the brain endothelium is a central regulator of BBB integrity and post stroke inflammation (Sections 1.2–1.3), gene delivery to endothelial cells offers a way to manipulate involved pathways at the BBB level [19, 22, 102]. So instead of focusing only on neurons, it became possible to intervene at the level of the vasculature itself. Selective modulation of endothelial signaling pathways may therefore represent a new therapeutic approach in stroke. This concept forms the basis for the CD73 overexpression in the endothelial cells of the BBB in mice investigated in this study.

The selection of more suitable endothelial cell-targeted AAV candidates usually starts with the generation of large and highly diverse AAV capsid libraries [103, 104]. The libraries are then introduced into relevant biological settings, where they undergo several rounds of selection. With each round, variants that successfully transduce the desired target cells are enriched, while less effective variants are gradually eliminated. This strategy makes it possible to identify capsids with improved specificity and higher transduction efficiency. Following this strategy, researchers have been able to develop AAV variants that are more efficiently targeting specific tissues and cells [99, 100, 105].

But an important challenge remains. Many engineered capsids are developed and selected in rodent models, while species-specific differences in receptor expression and vector tropism can limit how well these vectors perform in humans. So, capsid selection has been progressively focusing on more translational *in vivo* organisms such as non-human primates.

In a recent study of our group, AAV capsid libraries were screened in non-human primates, which led to the identification of variants with enhanced transduction efficiency in endothelial cells [106]. This approach enabled the identification of AAV variants with improved endothelial tropism compared with conventional serotypes and demonstrated that directed evolution in physiologically relevant systems can generate vectors with improved translational potential.

Such strategies provide an important foundation for endothelial targeting gene therapy and enables the translation of AAVs from animal models to humans.

1.10 Aim and hypothesis of the study

The present study was designed to investigate the role of endothelial CD73 in purinergic signaling at the BBB and to examine how it will affect the immune response and the recovery after ischemic stroke.

CD73 is a key enzyme in the extracellular ATP-adenosine conversion cascade. Based on the interspecies differences in endothelial CD73 expression described in Section 1.7, this study explores whether increasing CD73 levels at the murine BBB to a human level could enhance adenosine production and contribute to better stroke outcomes.

The “humanization” of the purinergic signaling cascade in the murine BBB was achieved by using the AAV-BR1-CD73 vector, which selectively transduces brain endothelial cells [100].

The central hypothesis of this work was that endothelial CD73 expression protects the brain during and post stroke by shifting the extracellular environment from a pro-inflammatory ATP towards an anti-inflammatory adenosine. This was expected to stabilize endothelial junctions and limit leukocyte infiltration.

To test this hypothesis, the AAV-BR1-CD73 vector and a control not expressing any transgene (AAV-BR1-empty) were generated and used *in vitro* to confirm expression and enzymatic activity. Following systemic administration in mice (Fig. 3), transgene expression and tissue specificity were examined regarding dose-dependent CD73 effects *in vivo*. Functional experiments were then performed to investigate how endothelial CD73 expression influences infarct size and survival after transient middle cerebral artery occlusion (tMCAO). Finally,

transcriptomics of brain endothelial and immune cells were performed to identify pathways associated with CD73 overexpression.

Thereby, this study was supposed to provide a mechanistic insight into how endothelial CD73 influences BBB function, immune modulation and recovery after ischemic stroke and subsequently to establish a foundation for future therapeutic strategies enhancing adenosine levels at the BBB in stroke.

2.1. Vector design and production

2.1.1. Generation of AAV-BR1-CD73 and AAV-BR1-empty vectors

To generate AAV vectors for endothelial CD73 overexpression, a codon-optimized sequence encoding murine *Nt5e* (CD73; ecto-5'-nucleotidase) was synthesized (GenScript) (Fig. 3). Codon optimization was performed to enhance expression efficiency in cells while preserving the amino acid sequence of the protein.

CD73 mus musculus (codon optimized):

atctGGGCCCTTTGTGCGGGGGGAGCGGCTCGGGGCTGTCCGCGGGGGGACGGCTGCCTTCGGGGGGGACGGGGCAGGGCGGGGTTCGGCTTCTGGCGTGTGACCGGCGGCTCT
AGAGCCTCTGCTAACCATGTTCATGCCTTCTTCTTTTTCCTACAGCTCCTGGGCAACGTGCTGGTTATTGTGCTGTCTCATCATTTTGGCAAAGAATTGgatctagtcgaTTCGAAgccaccATG
CGGCCCGCCGCCGCTAAGGTGCCCAAGTGGCTGCTGCTGGCCCTGTCCGCCCTGCTGCCCCAGTGGCCCGCCGCAAGCGCCTGGGAGCTGACCATCCTGCACACCAACGACGTCCAT
TCTAGGCTTGAGCAGACCAGCGACGACTCTACTAAGTGCCTGAACGCCTCCCTGTGCGTGGGCGGAGTGGCAAGACTGTTCACCAAGGTGCAGCAGATCAGGAAGGAGGAACCAA
ACGTGCTGTTCCTCGACGCCGGAGACCAGTACCAGGGAACCATCTGGTTTACCGTGTACAAGGGGCTGGAGGTGGCCCACTTCATGAACATCCTGGGATACGATGCTATGGCCCTGG
GGAACCACGAGTTTGATAACGGAGTGGAGGGCCTGATCGACCCCCTTCTGCGGAACGTGAAATTCCCAATCCTGTCCGCTAACATCAAGGCCAGAGGCCCTCTGGCCCATCAGATTAG
CGGGCTCTTCCTCCCCAGCAAGGTGCTGAGCGTGGGCGGCGAAGTGGTGGGCATCGTGGGCTACACTAGCAAGGAGACACCCTTCCTGAGCAACCCAGGAACCAACCTGGTGTTTG
AAGATGAAATTAGCGCTCTGCAGCCTGAGGTCGACAAGCTGAAGACCCTGAACGTGAACAAGATCATTGCCCTGGGACATAGCGGGTTCGAGATGGACAAGCTCATTGCCCAGAAG
GTGCGCGGCGTGGATATCGTGGTGGGTGGCCACTCAAATACCTTCCTGTACACCGGCAACCCCCCCTCTAAGGAGGTGCCTGCCGGCAAGTACCCTTTCATCGTGACCGCCGACGATG
GTAGACAGGTGCCTGTGGTGCAAGCCTACGCCTTCGGCAAGTACCTGGGATACCTGAAGGTGGAATTCGACGACAAGGGAAACGTCATCACCAGCTACGGAAATCCAATTCTGCTGA
ACAGCAGCATCCCAGAGGACGCCACCATCAAAGCCGACATCAACCAGTGGCGCATCAAGCTGGACAATTACAGTACTCAGGAGCTGGGACGCACCATTGTGTACCTGGATGGCTCCA
CCCAGACCTGCCGCTTTAGGGAGTGCAACATGGGTAACCTGATCTGTGACGCCATGATCAACAACAACCTGAGACATCCCGACGAAATGTTCTGGAACCACGTGTCAATGTGCATTGT
GAACGGGGGAGGCATCAGAAGTCCTATCGACGAGAAGAACAACGGAACCATCACCTGGGAAAATCTGGCCGCCGTGCTGCCCTTCGGGGGCACATTTGACTTGGTGCAGCTGAAG
GGCTCTACCCTGAAGAAGGCCTTCGAACACAGTGTGCACAGATATGGACAGAGTACCGGGGAATTCCTGCAGGTCGGCGGAATCCACGTGGTGTACGACATCAACAGGAAGCCCTG
GAACAGGGTGGTGCAGCTGGAGGTGCTGTGCACCAAGTGCAGAGTCCCTATCTACGAACCTCTCGAAATGGACAAGGTGTATAAGGTGACTCTGCCGTCATACCTGGCCAATGGCGG
CGATGGCTTCCAGATGATTAAAGATGAGCTGCTGAAGCACGACTCCGGCGACCAGGATATCTCTGTGGTGTCCGAGTACATCTCCAAGATGAAAGTGGTCTACCCCGCTGTGGAAGGC
CGGATCAAGTTCTCTGCCGCCAGCCACTACCAGGGCTCTTTCCCTCTGGTCATCCTGAGCTTCTGGGCTATGATTCTGATCCTGTACCAGTAAtgtacaagtaaaGCGGCCGCAAGCTTgatc

Figure 3. Codon-optimized murine CD73 sequence.

The *Nt5e* codon optimized sequence was placed under the CAG promoter, which consists of the cytomegalovirus (CMV) early enhancer fused to the chicken β-actin promoter. This promoter is commonly used in gene therapy vectors due to its strong and ubiquitous transcriptional activity across a broad range of cell types, including endothelial cells.

The expression cassette was inserted in a modified pFastBac1 backbone (Thermo Fisher Scientific, #10359-016). Downstream of the CD73 coding sequence, the cassette included the woodchuck hepatitis virus post-transcriptional regulatory element (WPRE) to enhance transcript stability and expression levels, followed by the bovine growth hormone polyadenylation signal (bGHpA) to ensure proper transcriptional termination and polyadenylation. The entire expression cassette was flanked by AAV2 ITRs, which are required for genome replication and packaging into AAV capsids. This construct is referred to as pFB1-CAG-CD73-WPRE.

An otherwise identical plasmid lacking the CD73 coding sequence was generated as a negative control vector. This plasmid, referred to as pFB-CAG-empty-WPRE, contained the same promoter, elements and ITR configuration as the CD73 vector to allow direct comparison.

For AAV packaging, a construct encoding the AAV2 *rep* gene and the BR1 capsid gene was used. The BR1 capsid has enhanced tropism for brain endothelial cells. The *rep* and *cap* genes were cloned into the pFastBac Dual vector (Thermo Fisher Scientific, #10712-024), which allows simultaneous expression of both components within the baculovirus system. This packaging plasmid was pFBD-AAV-BR1-Rep/Cap and was used for the generation of recombinant baculoviruses for subsequent AAV production.

2.1.2. Bacmid and baculovirus production in Sf9 cells

Recombinant AAV genomes and packaging components were produced using the Bac-to-Bac™ baculovirus expression system (Thermo Fisher Scientific), which enabled the large-scale AAV production in insect cells. For this, pFastBac-based transfer plasmids encoding either the CD73 expression cassette or the corresponding empty control genome were generated. In addition, the pFBD-AAV-BR1-Rep/Cap plasmid encoding the AAV2 Rep proteins and the BR1 capsid was used for packaging.

The transfer plasmids were transformed into DH10Bac™ *Escherichia coli* competent cells. These bacteria contain a bacmid shuttle vector as well as a helper plasmid expressing the Tn7 transposase, which mediates site-specific integration of the expression cassette from the transfer plasmid into the bacmid backbone. Following transformation, bacteria were plated on agar plates containing antibiotics, X-gal and IPTG in order to allow blue-white screening.

White colonies were picked and cultured overnight. Recombinant bacmid DNA was isolated using an alkaline lysis procedure, followed by ethanol precipitation to obtain high molecular weight bacmid DNA suitable for transfection.

Purified bacmid DNA was used to transfect *Spodoptera frugiperda* (Sf9) insect cells using TransIT® Insect Transfection Reagent (Mirus Bio) according to the manufacturer's protocol. Sf9 cells were maintained in suspension culture in serum-free Insect XPRESS™ medium (Lonza) supplemented with gentamicin (10 mg/L) at 27 °C under non-humidified conditions without CO_2 supplementation.

Primary baculovirus stocks (P1) encoding (i) the CD73 vector genome, (ii) the empty control genome or (iii) the AAV2 Rep/AAV-BR1 Cap packaging components were harvested 72 h post transfection. Cell culture supernatants containing the recombinant baculoviruses were clarified by low-speed centrifugation to remove cellular debris.

To obtain higher-titer virus stocks, primary baculoviruses were further amplified by serial infection of fresh Sf9 cultures. Briefly, Sf9 cells were infected at appropriate multiplicities of infection (MOI) and incubated for 48-72 h until signs of infection. Supernatants containing amplified baculoviruses (P2/P3 stocks) were collected, clarified and stored at 4 °C for short-term use or at -80 °C for long-term storage.

These high titer baculovirus stocks were subsequently used for large-scale co-infection of Sf9 cells.

2.1.3. AAV purification and quantification (qPCR)

For AAV production, Sf9 cells were co-infected with baculovirus encoding Rep/Cap and either the CD73 or empty vector genome. Cultures were incubated under gentle shaking (110 rpm) at 27 °C for 72 h.

Cells and supernatants were collected by low-speed centrifugation (150 × g, 5 min). Cell pellets were resuspended in PBS-MK and viral particles were released by three freeze/thaw cycles, alternating between -80 °C and 37 °C. AAV particles present in the clarified culture supernatant were concentrated by adding PEG-8000 (10 g/100 mL) and NaCl (5.8 g/100 mL), then incubating them for at least 24 h at 4 °C, followed by centrifugation (10,000 × g, 30 min). The resulting virus-containing pellets were resuspended as well in PBS-MK.

To remove contaminating cellular and baculoviral nucleic acids, the pooled lysates were treated with benzonase (MilliporeSigma; 50 U/mL, 30 min, 37 °C). After clarification (10,000 × g, 15 min), AAV vectors were purified by iodixanol density gradient ultracentrifugation. Discontinuous gradients (15%, 25%, 40% and 54% iodixanol in PBS-MK, prepared from OptiPrep™, Sigma Aldrich) were loaded with the clarified lysate and centrifuged in a 70.1 Ti rotor (Beckman Coulter) at 58,000 rpm for 70 min at 18 °C.

The band at the interface of the 40% iodixanol layer containing the AAV was carefully collected using an 18-gauge needle. This fraction was then concentrated and buffer-exchanged into PBS using Amicon Ultra 100 kDa centrifugal filter units (Millipore). Final preparations were stored at -80 °C until use.

Vector genome titers were determined by qPCR with primers targeting the CAG promoter (Forward Primer: AACGCCAATAGGGACTTTC, Reverse primer: GTAGGAAAGTCCCATAAGGTCA). Reactions were performed with SYBR Green master mix (Roche) on a LightCycler® 96 instrument (Roche). A plasmid containing the CAG expression cassette of known copy number was used to generate ten-fold serial dilution standard curves. Titers of purified vectors were expressed as vector genomes per milliliter (vg/mL). For tissues, DNA was isolated and diluted to 10 ng/µL, then a 50 ng template was used per reaction. Tissue-based vg counts were normalized to genomic input and expressed as vg per 100 ng DNA.

2.2. Cell culture and *in vitro* analyses

2.2.1. Cell lines and primary brain endothelial cells

Murine brain endothelial cells (bEND.3, ATCC #CRL-2299) were used for *in vitro* experiments.

Cells were cultured in Dulbecco's Modified Eagle Medium (DMEM) supplemented with 10% fetal bovine serum (FBS) and 1% penicillin/streptomycin. Cells were maintained at 37 °C in a humidified incubator with 5% CO_2. Culture medium was replaced every 2-3 days and cells were passaged upon reaching approximately 80-90% confluency. For passaging, cells were washed with PBS, detached with TrypLE™ (Thermo Fisher Scientific) and reseeded at appropriate densities depending on the downstream experiment.

Sf9 insect cells were used for baculovirus-based AAV production. These cells were cultured in serum-free Insect-XPRESS™ medium (Lonza) supplemented with 10 mg/L gentamicin. Cultures were maintained at 27 °C in non-humidified incubators without CO_2 supplementation, as required for insect cell culture. Sf9 cells were grown in suspension and adherence. They were passaged according to manufacturer recommendations to maintain optimal cell density and viability.

Primary human brain microvascular endothelial cells (HBMEC; ScienCell #1000) were used as a comparison model. Cells were expanded in Endothelial Cell Medium (ECM), consisting of 500 mL basal medium, 25 mL fetal bovine serum, 5 mL Endothelial Cell Growth Supplement and 5 mL penicillin/streptomycin (all components from ScienCell). Flasks were coated with fibronectin (Sigma-Aldrich) prior to seeding to promote endothelial attachment, as well as the spreading and maintenance of barrier-related properties.

HBMEC were maintained at 37 °C in a humidified atmosphere with 5% CO_2. Medium was changed every 2-3 days and cells were passaged using TrypLE™ (Thermo Fisher Scientific) when reaching near confluency. To preserve endothelial phenotype and functionality, HBMEC were used for experiments only up to passage 5.

All cells were regularly screened for mycoplasma contamination using the MycoCheck Mycoplasma PCR Detection Kit (ABP Biosciences, #A058-2) according to the manufacturer's instructions. Only mycoplasma-negative cultures were used for experiments.

2.2.2. AAV transduction efficiency and CD73 expression

For the *in vitro* evaluation of the CD73 expression via the AAV-BR1-CD73, murine brain endothelial cells (bEND.3) were seeded into 12-well plates at a density of 2.5×10^5 cells per well (n = 5 per condition). Cells were allowed to adhere and recover overnight under standard culture conditions. Twenty-four hours after seeding, when cells had reached approximately 60-70% confluency, cultures were transduced with AAV-BR1-CD73, with a multiplicity of infection (MOI) of 1×10^5 vector genomes (vg) per cell.

Viral particles were diluted in serum-free culture medium and added directly to the cells. After an incubation period of 2 h at 37 °C, complete culture medium was added to each well to reach a final volume of 2 mL. Cells were then returned to the incubator and maintained under standard conditions until further analysis.

CD73 surface expression was quantified at 48 hours post-transduction using flow cytometry. The cells were detached using TrypLE™ (Thermo Fisher Scientific), followed by neutralization with complete medium. Cells were collected by centrifugation at 170 × g for 5 min and washed twice with fluorescence-activated cell sorting (FACS) buffer consisting of phosphate-buffered saline (PBS) supplemented with 0.5% bovine serum albumin (BSA) and 0.5 mM EDTA.

Cells were stained for CD73 expression by incubation with FITC-conjugated anti-mouse CD73 antibody (clone TY/11.8; see Table 1) for 30-60 min at 4 °C in the dark. After staining, samples were washed once with FACS buffer and resuspended in 300 µL FACS buffer for acquisition.

Flow cytometric analysis was performed on a BD LSRFortessa™ flow cytometer (BD Biosciences). At least 10,000 events were recorded per sample. Non-transduced cells and isotype stained samples were included as negative controls to define background fluorescence and gating thresholds. Data were analyzed using standard forward and sidescatter gating to exclude debris and cell aggregates, followed by quantification of CD73 positive cells and median fluorescence intensity.

2.2.3 AMP-Glo assay for extracellular ATP/AMP conversion

To functionally validate CD73 enzymatic activity post transduction, extracellular nucleotide conversion was assessed using the AMP-Glo™ assay (Promega) according to the manufacturer's instructions with minor adaptations. This luminescence-based assay allows quantification of extracellular adenine nucleotides in cell culture supernatants and was used as a rapid functional test prior to targeted metabolite analysis.

Murine brain endothelial cells (bEND.3) were seeded into culture plates and transduced with AAV-BR1-CD73 at a MOI of 1×10^5 vector genomes per cell. Parallel cultures were left untransduced and served as negative controls. Cells were maintained under standard culture conditions for 48 h to allow transgene expression.

After the incubation period, cells were washed once with pre-warmed medium and subjected to stimulation with extracellular nucleotides. Cells were incubated at 37 °C for 30 min with either ATP or AMP at a final concentration of 100 µM in culture medium. In addition, control wells without any addition were included. For each experimental condition, five independent biological replicates were prepared. After incubation, supernatants were carefully collected to avoid disturbing the cell monolayer and centrifuged briefly to remove cellular debris.

For luminescence measurements, cleared supernatants were transferred in technical triplicates into opaque white 96-well plates (25 µL per well). Subsequently, 25 µL of AMP-Glo Reagent I was added to each well and plates were incubated for 60 min at room temperature

to allow conversion of remaining nucleotides according to the kit protocol. Plates were briefly centrifuged to ensure proper mixing of reagents and samples.

The kinase detection solution was prepared immediately before use by supplementing the kinase reagent with AMP-Glo Reagent II, following the manufacturer's instructions. The detection reagent was then added to each well and luminescence was measured after the recommended incubation time using a Tecan Infinite® 200 Pro microplate reader (Tecan).

Background controls included medium-only (without cells) wells containing either ATP or AMP or neither to account for baseline luminescence. An additional internal control consisting of untransduced cells without any addition, which was included for normalization. Data were expressed as mean values from five biological replicates, each measured in technical triplicates.

2.2.4 ATP/AMP degradation assays (LC-MS/MS)

To determine whether AAV-BR1-CD73 enables endothelial cells to degrade extracellular adenine nucleotides, ATP and AMP degradation assays were performed in vitro. Murine brain endothelial cells (bEND.3) and primary human brain microvascular endothelial cells (HBMEC) were seeded into 24-well plates at a density of 2.5×10^4 cells per well. Cells were transduced with AAV-BR1-CD73 or left untransduced (n = 15 per group). Cells were allowed to recover and express the transgene under standard culture conditions prior to the enzymatic assays.

Before the start of the assay, cells were washed once with pre-warmed PBS and switched to serum-free medium to avoid interference from exogenous ATP- or AMP-degrading enzymes present in serum. Cells were then incubated with either ATP or AMP at a final concentration of 100 µM. Incubations were carried out for 30 min at 37 °C under standard culture conditions (n = 5 per condition).

After incubation, supernatants were carefully collected to avoid disturbing the cell monolayer and centrifuged to remove residual cellular debris. Cleared supernatants were transferred into fresh tubes and stored at -80 °C until further analysis.

Metabolites of the ATP degradation cascade were quantified using a targeted liquid chromatography-tandem mass spectrometry (LC-MS/MS) approach, performed by Johanna

Hiefner (AG Worthmann) as previously described [107]. For sample preparation, frozen supernatants were thawed on ice and transferred into pre-cooled tubes. The internal standard $^{13}C_6$-nicotinamide (Sigma Aldrich) was added to each sample to allow normalization and correction for extraction variability. Metabolites were extracted by adding ice cold acetonitrile : water (8:2, v/v), followed by vortexing and incubation on ice to ensure efficient protein precipitation.

Samples were then centrifuged at 16,000 × g for 10 min at 4 °C and the cleared supernatants were transferred into amber high-performance liquid chromatography (HPLC) vials and tightly sealed to prevent evaporation or degradation.

Chromatographic separation was performed using hydrophilic interaction liquid chromatography (HILIC) on a Luna® NH_2 column (3 µm, 100 Å, 150 mm × 2 mm; Phenomenex) at a flow rate of 0.25 mL/min. The autosampler temperature was maintained at 4 °C and the column oven was set to 25 °C. A total volume of 10 µL of each sample was injected. Solvent A consisted of 20 mM ammonium acetate in water (pH 9.8) and solvent B consisted of 100% acetonitrile. A linear gradient from 80% to 0% solvent B over 17 min was applied, followed by a wash and column re-equilibration phase.

Detection was carried out on a QTRAP® 5500 triple quadrupole mass spectrometer (SCIEX) equipped with an electrospray ionization (ESI) source. Measurements were performed in negative ion mode using multiple reaction monitoring (MRM) for sensitive and selective detection of target metabolites. Data acquisition and processing were conducted using SCIEX OS software (version 2.0.0.45330).

Analytes were identified based on their specific MRM transitions and retention times and quantified using external calibration curves ranging from 2 nM to 2 µM. Peak areas were normalized to the internal standard to account for technical variability during sample preparation and measurement.

2.3. *In vivo* experiments

2.3.1. Animals and ethical approval

All *in vivo* experiments were carried out in wildtype C57BL/6J male mice aged 12-16 weeks, obtained via the central animal facility of the University Medical Center Hamburg Eppendorf (supplier: Charles River Laboratories). Only male mice were included in this study to minimize variability in infarct size and immune responses associated with known sex dependent differences in the transient middle cerebral artery occlusion (tMCAO) model.

Mice were housed in individually ventilated cages under standardized specific pathogen free (SPF) conditions with a controlled temperature and humidity and a 12 h light / dark cycle. The mice had ad libitum access to standard rodent chow and water throughout the study. Environmental enrichment, including nesting material and shelters, was provided according to institutional animal welfare guidelines. The mice were acclimatized to the animal facility for at least two weeks prior to any experimental procedures to reduce stress related variability.

The mice were randomly assigned to experimental groups and all procedures were performed during the light phase of the cycle. Health status and general well-being were monitored daily, as well as the body weight.

All animal experiments were approved by the competent authority (Behörde für Justiz und Verbraucherschutz der Freien und Hansestadt Hamburg; Amt für Verbraucherschutz, Lebensmittelsicherheit und Veterinärwesen, Tierversuchsantrag (TVA): N037/2023) and were conducted in accordance with German and European legislation on animal protection, as well as the ARRIVE guidelines for reporting animal research. All efforts were made to minimize animal suffering and to reduce the number of animals used.

2.3.2. AAV administration and dose-response testing

To achieve brain endothelial overexpression of CD73, mice received systemic tail vein injections of AAV-BR1-CD73 or the corresponding empty control vector. Viral doses ranged from 2.5×10^{11} to 2.5×10^{12} vector genomes (vg) per mouse in a total injection volume of 120 µL sterile phosphate-buffered saline (PBS) (n = 3 per group). The injection volume and viral

doses were selected based on previous studies using AAV-BR1 vectors to achieve efficient and selective transduction of brain endothelial cells.

Prior to injection, mice were briefly anesthetized using inhalation anesthesia with isoflurane (2-2.5% in oxygen) to minimize stress and movement during the procedure. The lateral tail vein was visualized and disinfected and the vector solution was slowly injected using a sterile insulin syringe. After injection, the mice were placed in a warmed recovery cage and monitored until full recovery from anesthesia.

For functional stroke experiments, AAV vectors were administered 14 days prior to transient middle cerebral artery occlusion (tMCAO) to allow for stable transgene expression in brain endothelial cells. This time point was selected based on previous studies demonstrating robust and sustained endothelial transduction by AAV vectors within this period.

For the dose-response experiments, mice were monitored daily for general health, body weight and potential adverse effects. Fourteen days after vector administration, the mice were sacrificed and brains were rapidly dissected. Cerebral hemispheres were processed for flow cytometry. The cerebellum was separated and snap-frozen in liquid nitrogen for subsequent DNA and RNA isolation and vector genome quantification.

To specifically assess CD73 expression in brain endothelial cells, microvessel-enriched fractions were prepared using a dextran-based isolation protocol (see Section 2.4.3). Resulting single-cell suspensions were stained with a viability dye, anti-CD31 antibody to identify endothelial cells and anti-CD73 antibody to quantify transgene expression. Samples were analyzed by flow cytometry to determine the proportion of CD73-positive endothelial cells and the corresponding fluorescence intensity.

2.3.3. Transient middle cerebral artery occlusion (tMCAO) surgery

Focal cerebral ischemia was induced using the filament-based transient middle cerebral artery occlusion (tMCAO) model. This model produces a reproducible infarct in the territory of the middle cerebral artery and is widely used to study acute ischemic stroke and post ischemic immune responses.

The mice were anesthetized using isoflurane (5% for induction, 1-2% for maintenance) in oxygen and placed in a supine position on a temperature-controlled heating pad to maintain physiological body temperature throughout the procedure. Ophthalmic ointment was applied to prevent corneal drying. The neck region was shaved and disinfected prior to surgery.

A midline cervical incision was made to expose the common carotid artery (CCA), external carotid artery (ECA) and internal carotid artery (ICA). Surrounding connective tissue was carefully removed and the arteries were isolated under a surgical microscope. The ECA was ligated distally and a small arteriotomy was performed to allow insertion of the filament.

A silicone coated monofilament (tip diameter 0.23 mm) was introduced into the ECA stump and advanced through the ICA toward the origin of the middle cerebral artery (MCA). Proper placement of the filament was confirmed by monitoring cerebral blood flow in the ipsilateral hemisphere using Laser Doppler flowmetry. Only procedures resulting in a ≥80% reduction in cerebral blood flow compared with baseline values were considered successful and included in the study.

After an occlusion period of 50 min, the filament was gently withdrawn to allow reperfusion. Restoration of blood flow was verified by Laser Doppler measurements. The surgical site was sutured in layers, disinfected and animals were allowed to recover in a warmed cage under close observation.

Supportive care included subcutaneous injections of pre-warmed Sterofundin® (0.5 mL) during and after surgery to prevent dehydration and maintain fluid balance. Analgesia consisted of buprenorphine (0.1 mg/kg, subcutaneously) and tramadol (1 mg/mL) administered via the drinking water, starting 24 h prior to surgery and continued during the postoperative period. Animals were monitored closely during recovery from anesthesia.

Postoperative monitoring was performed twice on the day of surgery and the next two days thereafter according to a predefined clinical scoring sheet, which included assessment of body weight, general appearance, mobility and neurological deficits. Animals showing severe distress or predefined humane endpoints were euthanized according to institutional guidelines.

Only mice that died before the planned endpoint (48 h post tMCAO) were excluded from infarct size and immune cell analyses.

2.3.4. Magnetic resonance imaging (MRI) for infarct volume assessment

Infarct volumes were measured 2 days after tMCAO using a 7 T ClinScan MRI system (Bruker/Siemens) (n = 16 per group). MRI was performed at the predefined experimental time point as indicated in the study design to assess acute ischemic lesion size.

For imaging, mice were anesthetized with isoflurane (3% in oxygen for induction and 0.8-1.5% for maintenance during scanning) and positioned prone on a temperature-controlled bed. The head was fixed in a dedicated holder to minimize motion artifacts. Physiological parameters, including respiration, electrocardiogram (ECG) and body temperature, were continuously monitored throughout the imaging session.

The MRI protocol included initial localization scans followed by T2-weighted imaging. In selected experiments, diffusion-weighted imaging (DWI) sequences were also acquired to confirm ischemic lesion development. T2-weighted images were obtained as a series of 24 contiguous coronal slices covering the entire brain. For contrast-enhanced imaging, scans were acquired before and after intraperitoneal injection of a gadolinium-based contrast agent (MultiHance®, 0.1 mmol/kg).

After completion of the imaging session, animals were sacrificed.

T2-weighted images were analyzed using Fiji (ImageJ, version 1.53t). Lesion areas were identified on each slice. The infarcted regions were manually outlined according to established anatomical landmarks and total infarct volumes were calculated by integrating the lesion areas across all slices. Where applicable, edema correction was applied to account for ischemia-induced hemispheric swelling.

Corrected infarct volume = measured infarct volume x (contralateral hemisphere area / ipsilateral hemisphere area)

Total infarct volume was obtained by integrating infarct areas across all slices. Infarct size was used for normalization of immune cell counts where indicated.

2.4. Molecular and cellular analyses

2.4.1. DNA and RNA extraction, cDNA synthesis and qPCR

For quantification of vector genome copy numbers, genomic DNA was isolated from murine tissues using a column based purification method (DNeasy Blood & Tissue Kit, Qiagen) according to the manufacturer's instructions. Briefly, tissues were mechanically homogenized and lysed in the provided lysis buffer containing proteinase K to ensure complete digestion of cellular proteins. After incubation, lysates were loaded onto silica-based spin columns, washed to remove contaminants and DNA was eluted in nuclease-free water. DNA concentration and purity were determined spectrophotometrically using a NanoDrop instrument and samples were stored at -20 °C until further analysis.

For gene expression analyses, total RNA was extracted from cultured cells and brain tissue using the Quick-RNA Miniprep Kit (Zymo Research) following the manufacturer's protocol. Tissues were homogenized in RNA lysis buffer and lysates were passed through spin columns to bind RNA. After several wash steps to remove proteins, genomic DNA and other contaminants, purified RNA was eluted in RNase-free water. RNA concentration and purity were assessed by NanoDrop spectrophotometry and samples were stored at -80 °C until use.

For complementary DNA (cDNA) synthesis, equal amounts of total RNA were reverse transcribed using the High-Capacity cDNA Reverse Transcription Kit (Applied Biosystems). The reverse transcription reaction was performed according to the manufacturer's protocol using random primers and a thermal cycler. cDNA was diluted to the desired concentration and stored at -20 °C for subsequent qPCR analyses.

qPCR was performed to assess expression levels of human *NT5E*, endogenous murine *Nt5e* and transgene *Nt5e*. Reactions were carried out using gene-specific primers and a suitable qPCR master mix in a real-time PCR system. Each sample was analyzed in technical replicates and water controls were included to exclude contamination.

Gene expression levels were normalized to the housekeeping gene *RPS18* or *Rps18* (depending on the sample origin). Relative expression was calculated using the comparative ΔCt method.

2.4.2. Flow cytometry and antibody panels

Flow cytometry was used for the evaluation of brain endothelial CD73 expression (n = 5 per group) and to quantify brain-infiltrating immune cell populations post MCAO (n = 8 for control group, n = 5 for CD73 group).

Immediately following MRI at 48 h post tMCAO, deeply anesthetized mice were euthanized by cervical dislocation. The cerebellum was dissected and stored in -20 °C for nucleic acid analysis, while the remaining forebrain tissue (olfactory bulb removed) was used for immune cells isolation.

For immune cell isolation, brain tissue was minced and enzymatically digested in DMEM containing collagenase (1 mg/mL) and DNase I (0.1 mg/mL) at 37 °C for 30 min with gentle shaking. Following digestion, cells were dissociated using pipetting to obtain a single-cell suspension. The suspension was filtered through a cell strainer to remove debris and undigested tissue fragments.

Leukocytes were enriched using a Percoll density gradient centrifugation step. After centrifugation, the leukocyte containing fraction was collected and residual red blood cells were lysed using an appropriate lysis buffer. The resulting single cell suspensions were washed and resuspended in FACS buffer consisting of PBS supplemented with 0.5% BSA and 0.5 mM EDTA.

For staining, cells were first incubated with a viability dye to discriminate live and dead cells. After washing, cells were incubated with antibodies targeting CD45, CD11b, Ly6G, P2Y12, CD4, CD8, NK1.1, B220, F4/80, CD11c, γδTCR, MHC II, CD39 and CD31 (for clones, fluorochromes, suppliers and dilutions see Table 1). Staining was performed at 4 °C in the dark for the recommended incubation time, followed by washing and resuspension in FACS buffer.

Data acquisition was performed on a BD FACSymphony™ A3 flow cytometer and compensation was applied using single-stained controls. Compensation beads were used where appropriate to define gating boundaries. Data were analyzed using FlowJo software.

Gating strategies were applied as follows. First, debris was excluded based on forward and side scatter properties and singlets were selected using FSC-A versus FSC-H parameters. Dead cells were excluded based on viability dye staining. Among live singlets, $CD45^+$ leukocytes were identified.

Within the $CD45^+$ population, lymphocyte subsets were defined as follows: B cells were identified as $B220^+NK1.1^-$ cells, NK cells as $NK1.1^+B220^-$ cells and T cells as $CD4^+$ or $CD8^+$ cells. γδ T cells were defined as $\gamma\delta TCR^+$ within the T-cell compartment.

Myeloid populations were identified within the $CD11b^+$ compartment. Microglia were defined as CD45^low$CD11b^+P2Y12^+$ cells, whereas infiltrating myeloid cells were defined as CD45^high$CD11b^+$ cells. The latter population was further subdivided into $Ly6G^+$ neutrophils and $Ly6G^-$ monocytes/macrophages.

Absolute cell counts were determined using counting beads added to each sample prior to acquisition. Where indicated, cell numbers were normalized to infarct volume (mm^3) to account for differences in lesion size between animals.

Antigen	Clone	Fluorochrome	Supplier	Catalog Number	Target Cell Population	Dilution
CD45	30-F11	PerCP-Cy5.5	BioLegend	103132	All leukocytes	1:100
CD11b	M1/70	BUV737	BD Biosciences	612800	Myeloid cells	1:100
Ly6G	1A8	AF700	BioLegend	127622	Neutrophils	1:100
P2Y12	S16007D	APC	BioLegend	Custom	Microglia	1:100
CD73	TY/11.8	FITC	BioLegend	127219	Ecto-enzyme marker	1:100
CD73	AD2	APC	BioLegend	127210	Ecto-enzyme marker (alt.)	1:100
CD4	RM4-5	BV785	BioLegend	100547	T helper cells	1:100

CD8	53-6.7	BV650	BD Biosciences	563786	Cytotoxic T cells	1:100
NK1.1	PK136	BV710	BioLegend	108745	NK cells	1:100
CD11c	HL3	BUV395	BD Biosciences	564080	Dendritic cells	1:100
F4/80	BM8	BV605	BioLegend	123129	Macrophages	1:100
B220	RA3-6B2	BUV805	BD Biosciences	748867	B cells	1:100
TCRγδ	GL-3	PerCP-Cy5.5	BioLegend	Custom	γδ T cells	1:100
MHC II	M5/114.15.2	FITC	BioLegend	107606	Antigen-presenting cells	1:100
CD39	Duha59	APC	BioLegend	143810	Ectonucleotidase marker	1:100
CD31	MEC13.3	BUV395	BD Biosciences	740231	Endothelial cells	1:100
Live/Dead dye	—	Near-IR	Invitrogen	L10119	Dead cell exclusion	1:1000

Table 1. Antibodies used for FACS.

2.4.3. Isolation and sorting of immune cells and brain microvessel endothelial cells

For transcriptomic analyses, endothelial (n = 3 per group) and immune cells (n = 2 per group) were isolated from brain tissue. Immediately after MRI, mice were euthanized and brains were rapidly removed. The cerebellum was dissected and snap-frozen in liquid nitrogen for

subsequent DNA and RNA isolation, while the remaining forebrain tissue was processed for cell isolation after the removal of the olfactory bulb.

For enrichment of brain microvessels, cortical tissue was processed using a dextran-based density centrifugation protocol. Briefly, tissue samples were mechanically homogenized in ice-cold buffer using a glass homogenizer. The homogenate was mixed with a 15% dextran solution and centrifuged at high speed. This step resulted in separation of myelin and parenchymal debris from the denser microvascular fraction, which formed a pellet at the bottom of the tube.

The microvessel-enriched pellet was carefully collected and subjected to enzymatic digestion to obtain a single-cell suspension. Digestion was performed using a buffer containing collagenase and DNase at 37 °C with gentle shaking. Following digestion, samples were passed through a 70 µm cell strainer to remove remaining debris and undigested tissue fragments.

For isolation of endothelial cells, magnetic-activated cell sorting (MACS) was performed using anti-CD31 and anti-CD45 microbeads (Miltenyi Biotec). Single-cell suspensions were first incubated with the microbeads according to the manufacturer's instructions. Cells were then passed through magnetic columns and $CD31^{+}CD45^{-}$ endothelial cells were collected as the flow-through or eluted fraction, depending on the labeling strategy.

For isolation of immune cells, brain ipsilateral hemispheres were digested using the same enzymatic protocol described above in 2.4.2. Resulting single-cell suspensions were incubated with anti-CD31 and anti-CD45 microbeads. $CD31^{-}CD45^{+}$ immune cells were then collected using MACS. This approach enabled enrichment of leukocyte populations while excluding endothelial cells.

After sorting, cell fractions were pelleted by centrifugation and immediately processed for RNA extraction. Total RNA was isolated from the sorted endothelial and immune cells using the Quick-RNA Miniprep Kit (Zymo Research) according to the manufacturer's protocol. Purified RNA was stored at -80 °C until further transcriptomic analysis.

2.4.4. Transcriptomic analysis of endothelial and immune cells

RNA quality was assessed using an Agilent Bioanalyzer system and only samples with a RNA integrity number (RIN) ≥ 7 were processed for sequencing. Library preparation and sequencing were performed by BGI Genomics (Poland) using their RNAref transcriptome sequencing service.

For library preparation, polyadenylated mRNA was first enriched from total RNA using oligo (dT) magnetic beads to selectively capture messenger RNA. The purified mRNA was then fragmented into short fragments under elevated temperature in the presence of fragmentation buffer. These fragments served as templates for first-strand cDNA synthesis using random N6 primers and reverse transcriptase. Subsequently, second-strand cDNA synthesis was performed to generate double-stranded cDNA.

The resulting cDNA fragments underwent end repair and A-tailing, followed by ligation of sequencing adapters. Adapter-ligated fragments were then amplified by PCR to generate the final sequencing libraries. Library quality and concentration were assessed prior to sequencing.

For sequencing, the libraries were converted into single-stranded circular DNA molecules, which were used to generate DNA nanoballs (DNBs) according to the DNBSEQ platform workflow. Sequencing was performed using paired-end 150 bp (PE150) reads. On average, each sample yielded approximately 6.8 Gb of high-quality sequencing data.

Raw sequencing reads were subjected to quality control to remove adapter sequences, low-quality reads and reads containing ambiguous bases. Clean reads were then aligned to the reference mouse genome using a suitable alignment algorithm. Gene expression levels were quantified and normalized across samples to allow for downstream comparisons.

Differential gene expression analyses were performed between experimental groups to identify genes significantly up- or downregulated in response to CD73 expression. Functional enrichment analyses, including Gene Ontology (GO) and pathway analyses, were conducted to identify affected biological processes and signaling pathways.

2.4.5. Bioinformatics and statistical analyses

The processing of RNA-seq data as sample quality information and differentially expressed genes (DEGs) analyses were performed by UKE Bioinformatics core facility. A gene is considered significantly differentially expressed if the corresponding False Discovery Rate (FDR) is smaller than or equal to 0.1 and the absolute log2-foldchange (log2FC) is larger than or equal to 1 (FDR <= 0.1 AND |log2FC| >= 1). Annotation source was Ensembl (version: GRCm39.110); quality control was performed by fastp (version: 0.23.2); Mapping and RNA quantification is performed by STAR (2.7.10a). The final transcriptomic dataset included endothelial and immune cell samples across the following groups: CD73_no_stroke, CD73_stroke, Control_no_stroke and Control_stroke.

Statistical analyses for non-sequencing experiments (e.g. qPCR, flow cytometry, infarct volumes) were performed using GraphPad Prism 8. Normality was tested using the Shapiro-Wilk or Kolmogorov-Smirnov tests. For two-group comparisons, either unpaired Student's t-test (parametric) or Mann-Whitney U test (non-parametric) was applied. For multiple groups, the Kruskal- test was used. Data are presented as individual data points with mean ± SD or mean ± SEM, as indicated. Significance levels were defined as $p < 0.05$ (*), $p < 0.01$ (**),$p < 0.001$ (***) and $p < 0.0001$ (****). Mice that did not survive up to 48 h post tMCAO were excluded from infarct and immune cells analyses.

3. Results

3.1 Humanizing the ATP degradation machinery in murine brain endothelium

The purinergic signaling environment at the BBB differs between humans and mice as the latter ones express relatively low CD73 levels in their brain endothelial cells. First both the expression of CD39 and CD73 were compared in primary human and murine brain endothelial cells as well as in a cell line of murine brain endothelial (bEND.3) cells to ensure that *in vitro* experiments done with this cell line would actually mimic similar effects as the primary murine cells. This was then followed by transduction of AAV-BR1-CD73 in bEND.3 cells. Finally, the functional activity of the expressed CD73 was verified using nucleotide degradation assays.

3.1.1 Differential CD39/CD73 expression in human and murine brain endothelial cells

To verify the differences in purinergic signaling at the BBB between humans and mice, the expression of CD39 and CD73 was compared between murine and human brain endothelial cells. Human brain microvascular endothelial cells (hBMECs) and the murine endothelial cell line bEnd.3 were cultured *in vitro*, while primary murine brain microvascular endothelial cells (mBMECs) were isolated from mouse brains. Total RNA was extracted from all cell populations, reverse-transcribed into cDNA and analyzed by quantitative PCR (qPCR).

These experiments confirmed previously reported transcriptomic datasets [108-110] and revealed clear differences in the expression patterns of the two enzymes (Fig. 4). Murine endothelial cells, including both primary mBMECs and the bEnd.3 cell line, expressed CD39 levels that were 0.3 - 0.7-fold as high as the RPS18 house keeping gene, while CD73 expression was more than one order of magnitude lower.

Human brain endothelial cells showed the opposite pattern. In hBMECs, CD73 expression was one order of magnitude higher than CD39, indicating a greater capacity for the conversion of extracellular AMP into adenosine. This difference resulted in an over tenfold lower CD73 expression in murine endothelial cells compared to their human counterparts.

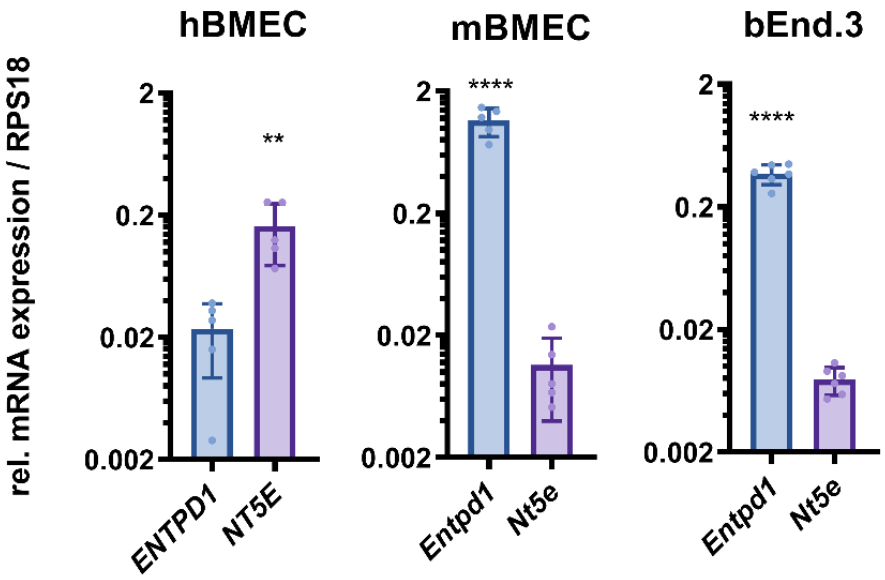

Figure 4. Differential expression of CD39 and CD73 in human and murine brain endothelial cells.

Relative mRNA expression of *ENTPD1* and *Entpd1* (CD39), as well as *NT5E* (CD73) and *Nt5e* were quantified by qPCR in human brain microvascular endothelial cells (hBMECs), primary murine brain microvascular endothelial cells (mBMECs) and the murine endothelial cell line bEnd.3 (n = 5 per condition). Gene expression levels were normalized to *RPS18* and *Rps18*. Data are shown as mean ± SD. Statistical significance was determined using two-tailed Student's t-test, , **** $p < 0.0001$.

3.3.1.2 AAV-mediated CD73 overexpression in brain endothelial cells

To increase CD73 expression in murine brain endothelial cells, an AAV vector was generated using the AAV-BR1 capsid [100]. The vector contained the CAG promoter to drive transgene expression, as well as the woodchuck hepatitis virus posttranscriptional regulatory element (WPRE) to enhance transcript stability.

To assess transgene expression, bEnd.3 cells were transduced with the AAV-BR1-CD73 vector (referred to as BR1-CD73). Total RNA was isolated 48 hours after transduction, reverse-transcription into cDNA was performed and then analyzed by qPCR. This analysis confirmed strong expression of the CD73 transgene in transduced cells, while endogenous *Nt5e* levels

remained unchanged. (Fig. 5). The levels of transgenic *Nt5e* expression reached values that even exceeded endogenous *NT5E* expression observed in human endothelial cells (refer to Figure 4 as comparison).

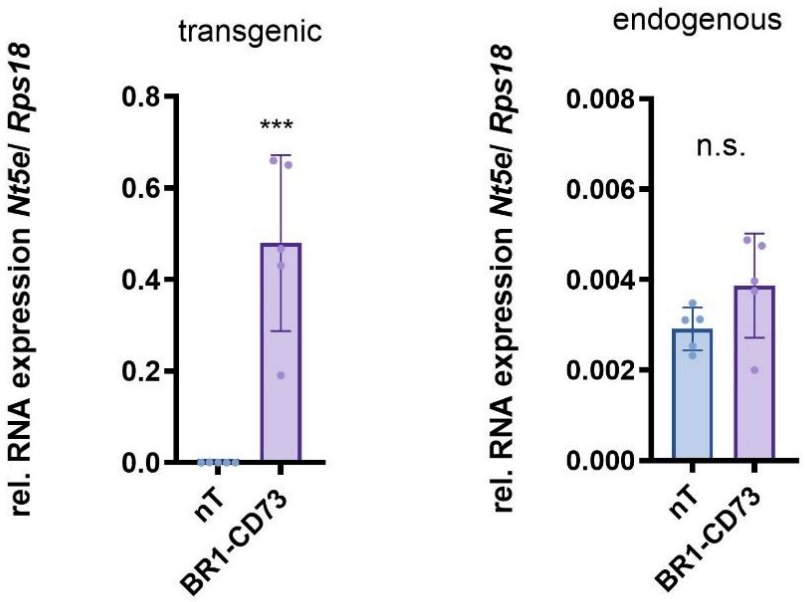

Figure 5. Transgenic and endogenous *Nt5e* (Cd73) mRNA expression in bEnd.3 cells. Relative mRNA expression of the *Nt5e* transgene (left) and endogenous *Nt5e* (right) was quantified by qPCR in non-transduced (nT) and with AAV-BR1-CD73 transduced bEnd.3 cells (n = 5 per group). Gene expression was normalized to *Rps18*. Data are presented as mean ± SD. Statistical significance was assessed using an unpaired two-tailed Student's t-test, *** $p < 0.001$.

Flow cytometry verified the efficient surface expression of CD73 protein on bEND.3 cells. The cells were transduced with AAV-BR1-CD73 and then stained with a fluorescent anti-CD73 antibody. Approximately 80% of bEND.3 cells were CD73-positive, while CD73 expression was not detected in the cells that were transduced with the control vector (Fig. 6).

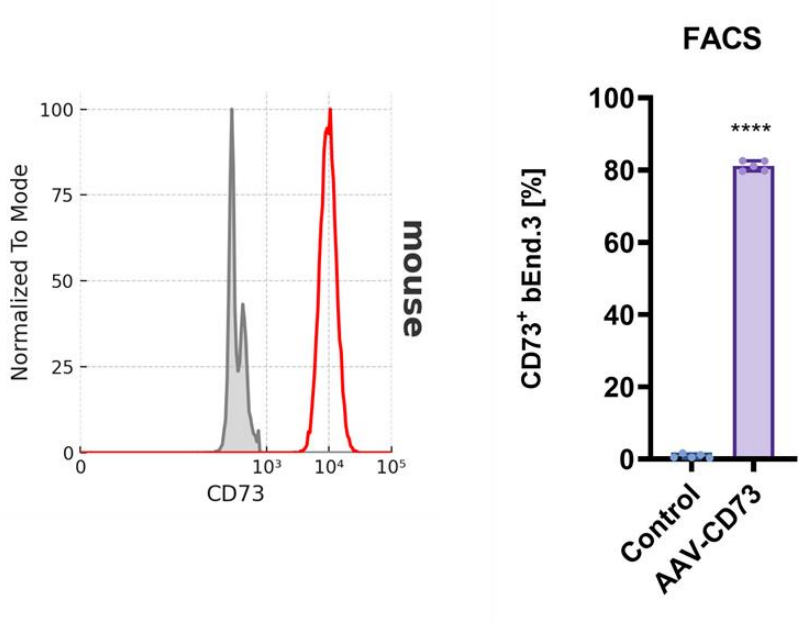

Figure 6: FACS of CD73 surface expression in bEnd.3 cells after AAV-BR1-CD73 transduction. bEnd.3 cells were transduced with AAV-BR1-CD73 or control vector and analyzed by flow cytometry for CD73 surface expression (n = 5 per group). Left: Representative histogram showing CD73 staining in control treated cells (grey) and with AAV-BR1-CD73 transduced cells (red). Right: Quantification of the percentage of CD73-positive bEnd.3 cells under each condition. Data are presented as mean ± SD.

3.1.3 Functional validation of CD73 activity using AMP-Glo assay

To investigate whether the increased CD73 expression in bEND.3 cells would lead to the conversion of extracellular nucleotides, a luminescence assay that detect AMP levels (AMP-Glo assay) was used.

bEND.3 cells were seeded and transduce for 48 hours with AAV-BR1-CD73. Untransduced bEND.3 were used as controls. ATP or AMP was added to the cells for 30 min and then the supernatants were measured for AMP levels.

Without the addition of any nucleotide, all cells showed similar baseline conditions and no apparent differences in the background signal. Control wells without cells and with only medium and either ATP or AMP showed strong luminescence signals, confirming the stability of the added nucleotides during the incubation period and validating the assays performance.

AAV-BR1-CD73-transduced bEND.3 cells showed a reduced luminescence compared to untransduced ones upon addition of ATP or AMP, indicating increase AMP degradation. As the AMP-Glo assay provides an indirect luminescence-based readout, these findings were subsequently validated and characterized in more detail using targeted metabolite analysis by HPLC, as described in the following section.

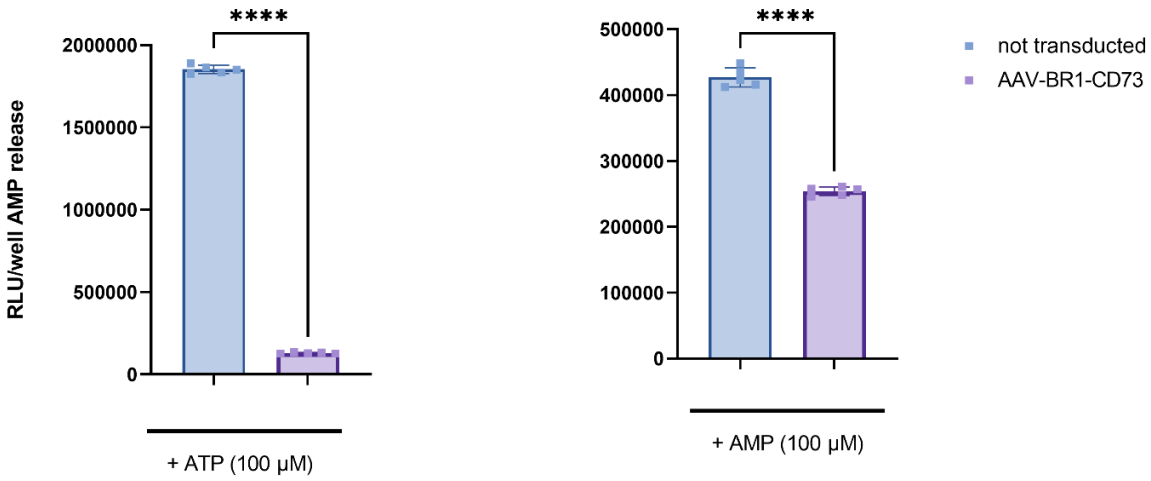

Figure 7. Functional validation of CD73 activity in bEND.3 cells using the AMP-Glo assay. bEND.3 cells were transduced with AAV-BR1-CD73 or left untransduced for 48 h, followed by incubation with either ATP or AMP (100 µM) for 30 min at 37 °C. The transduced cells showed significantly reduced AMP-derived luminescence signal compared with controls under both conditions, consistent with enhanced extracellular nucleotide conversion. Data represent mean ± SD of five biological replicates, each measured in technical triplicates. Statistical significance was determined using an unpaired two-tailed Student's t-test, **** $p < 0.0001$

3.1.4 Enzymatic validation of CD73 activity in vitro

To further investigate the functional enzymatic activity of CD73, high-performance liquid chromatography (HPLC)-based assays were performed. For this experiment, transduced and untransduce bEND.3 cells were used along with HMBECs, with the two latter serving as controls and comparison groups (Fig. 8). All three cell groups were used without nucleotide addition, ATP addition or AMP.

The samples without nucleotide addition showed no signal for ATP or its metabolites. Firstly, the degradation of ATP was measured. bEND.3 cells, both transduced and untransduced, were able to degrade ATP much faster than the hBMECs, which further supports the data in Figure 4 demonstrating that CD39 is highly expressed in murine brain endothelial cells. In the two bEND.3 groups, the entire amount of ATP was degraded successfully, while in the hBMECs 30% of ATP was still detectable. The untransduced bEND.3 cells could not further degrade AMP to adenosine, or at least only in a very small capacity (approximately 5 µM). While the bEND.3 cells that did express CD73 specifically increased levels of adenosine (approximately 20 µM), inosine (approximately 25 µM) and additional breakdown products (not shown).

This effect was further validated when AMP was added to the cells. Again, the untransduced bEND.3 cells could not degrade AMP, but the CD73-expressing ones degraded more than half of it and resembled similar levels as the hBMECs. hBMECs converted approximately 80% of the added AMP into adenosine and inosine, while transduced bEnd.3 cells converted only about 20% of the AMP into these products, which is consistent with their low endogenous CD73 expression. CD73-expressing bEND.3, however, were able to convert approximately 75% of the added AMP into adenosine (approximately 40 µM), inosine (approximately 20 µM) and other downstream metabolites

These *in vitro* experiments demonstrated that transduced bEND.3 cells with the AAV-BR1-CD73 vector can achieve similar expression and function of CD73 with that observed in hBMECs.

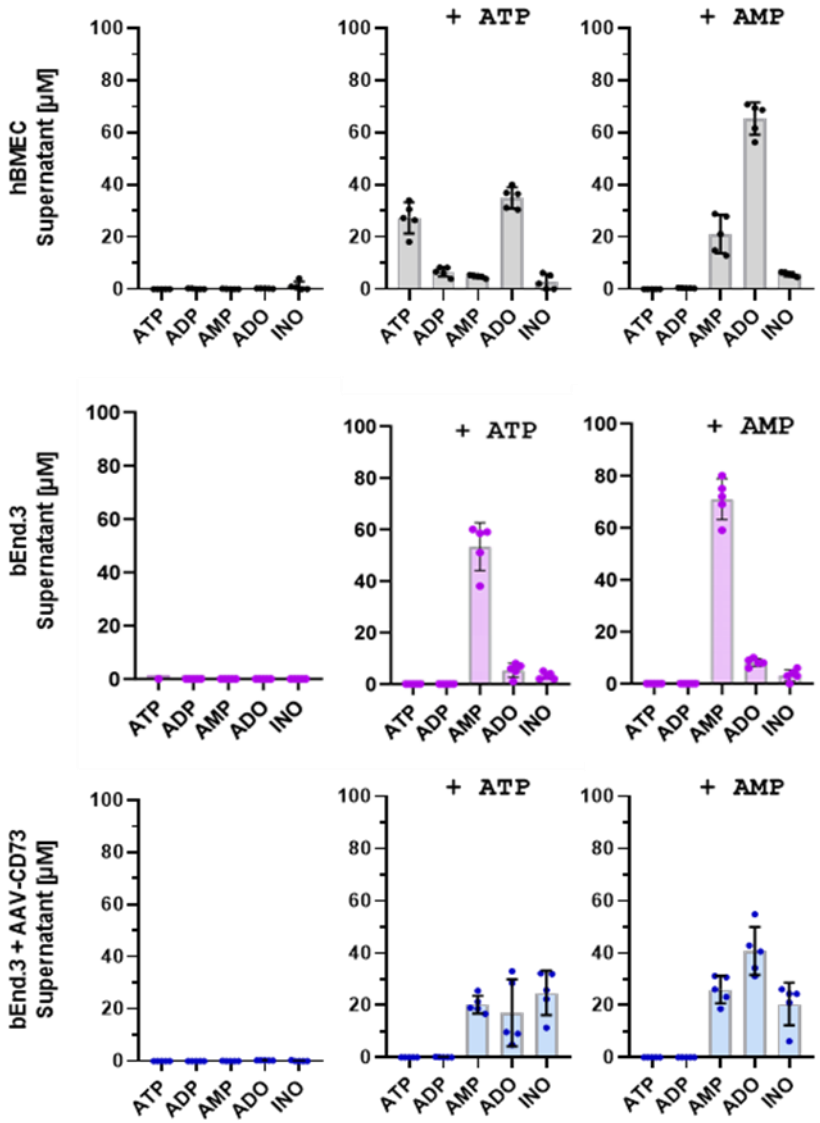

Figure 8. Enzymatic activity assay demonstrating increased nucleotide degradation after CD73 overexpression. Extracellular nucleotide conversion was measured hBMEC, bEND.3 and AAV-BR1-CD73 transduced bEND.3 cells. Cells were incubated with either ATP or AMP (100 µM) and nucleotide degradation was quantified by high-performance liquid chromatography (HPLC). CD73-expressing bEND.3 cells showed similar conversion of AMP compared to hBMECs, which is consistent with enhanced CD73 enzymatic activity. n = 5 per condition. Data are presented as mean ± SD.

3.2 In vivo AAV-CD73 expression

Following the *in vitro* validation of the expression and enzymatic activity of CD73 via the AAV-BR1-CD73 transduction, it was tested whether this vector would also work in the *in vivo* setting.

3.2.1 Dose-response testing and vector genome quantification in brain tissue

AAV-BR1-CD73 was administered to mice via tail vein injection at three different doses ranging from 2.5×10^{11} to 2.5×10^{12} vector genomes (vg) per mouse (n = 3 per group). Fourteen days after injection, brain tissues were harvested and the cerebelli were isolated and processed in order to quantify vector genome distribution and verify transgene expression.

qPCR analysis of the cerebelli revealed a clear dose dependent distribution of AAV genomes (Fig. 9). Mice that received the high vector dose exhibited the highest number of AAV genome copies per 100 ng total DNA, while the medium and low dose groups showed respectively lower vg copy numbers.

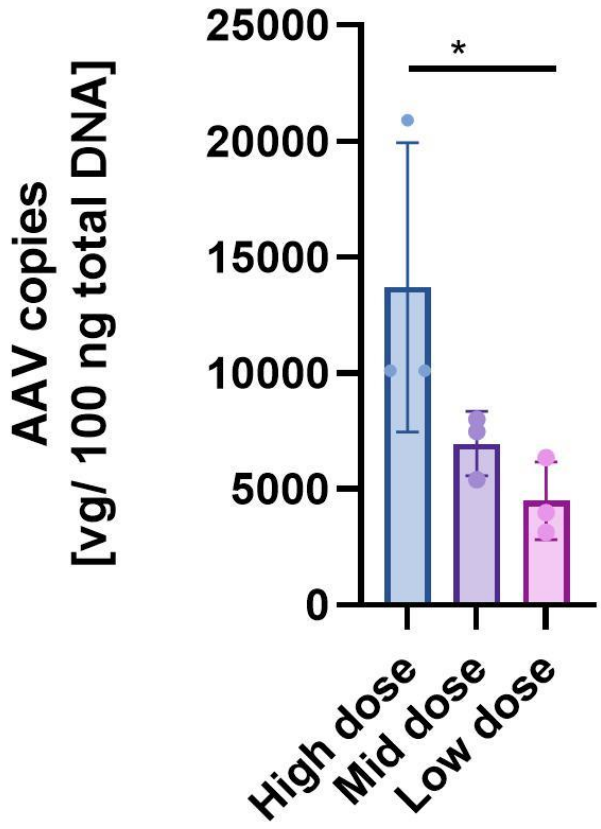

Figure 9. Dose dependent distribution of AAV vector genomes in brain tissue. Mice received systemic injections of AAV-BR1-CD73 at 2.5×10^{11} vg per mouse (low dose), 5×10^{11} vg per mouse (mid dose) and 2.5×10^{12} vg per mouse (high dose) via tail vein (n = 3 per group). Fourteen days after injection, vg copies were quantified in the cerebelli by qPCR and normalized to 100 ng total DNA. A dose dependent increase in AAV genome copies was observed, with the highest levels detected in the high dose group. Data are presented as mean ±SD, * $p < 0.1$

3.2.2 Endothelial transgene expression

To further verify the CD73 expression in the endothelial cells of the brain in mice, transgene expression was assessed at both the transcript and protein levels. Transgenic and endogenous *Nt5e* mRNA levels were measured by isolating total RNA from brain endothelial cells, followed by cDNA synthesis and qPCR.

qPCR analysis showed a dose dependent increase in transgenic *Nt5e* expression (Fig. 10). The highest transgene expression was detected again in the high dose group, with medium and low doses resulting in proportionally reduced expression levels. However, the expression of endogenous *Nt5e* remained low and did not change across the dose groups (Fig. 1), demonstrating that CD73 expression delivered via the AAV-BR1-CD73 does not alter endogenous gene regulation.

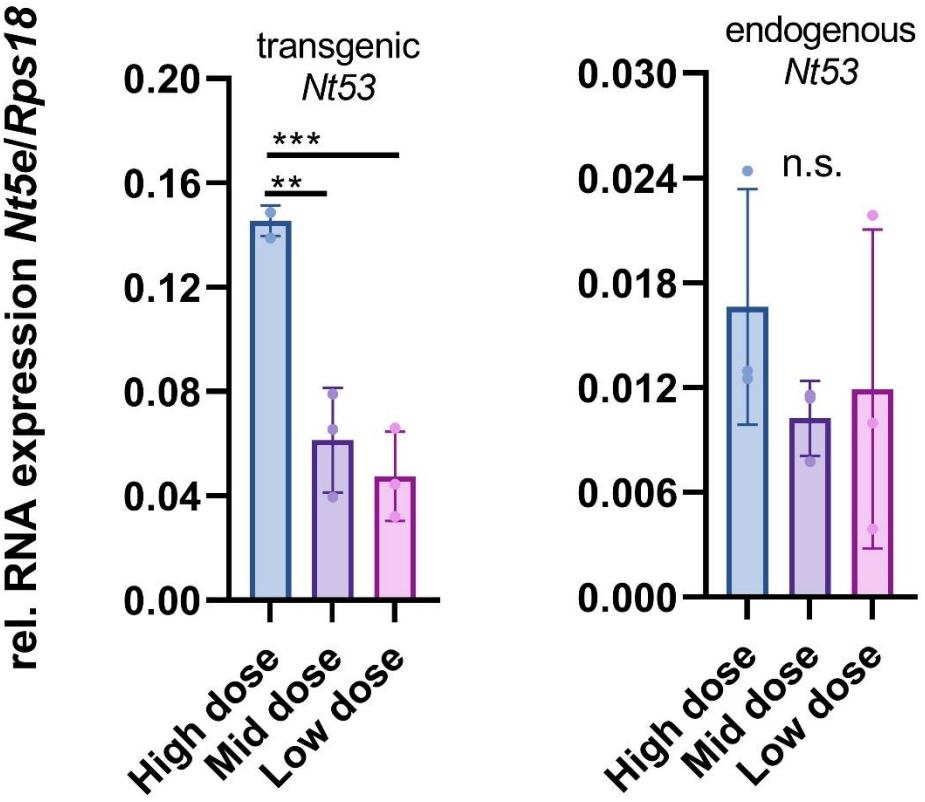

Figure 10. Transgenic and endogenous *Nt5e* expression in brain tissue after AAV-BR1-CD73 administration.

Relative mRNA expression of transgenic *Nt5e* (left) and endogenous *Nt5e* (right) was quantified by qPCR in brain tissue from mice receiving 2.5×10^{11} vg per mouse (low dose), 5 ×

10^{11} vg per mouse (mid dose) and 2.5×10^{12} vg per mouse (high dose) of AAV-BR1-CD73 (n = 3 per group). Transgenic *Nt5e* expression increased in a dose dependent manner, while endogenous *Nt5e* expression remained unchanged across all groups. Gene expression was normalized to *Rps18*. Data are shown as mean ± SD. Statistical significance was assessed using one-way ANOVA followed by Dunnett's multiple comparisons test, ** $p < 0.01$, *** $p < 0.001$

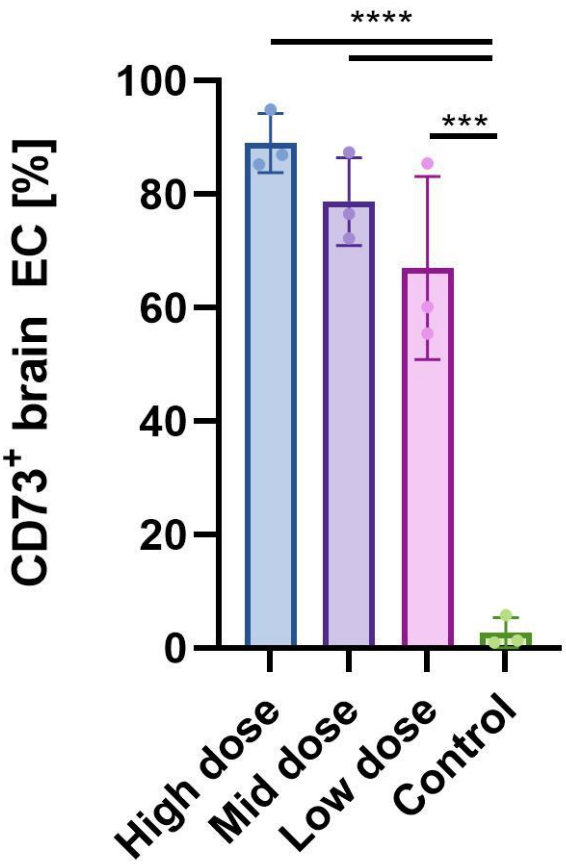

Figure 11. Dose-dependent CD73 surface expression in brain endothelial cells after the administration of AAV-BR1-CD73.

Brain endothelial cells were isolated from mice treated with high, medium or low doses of AAV-BR1-CD73 or the control vector (AAV-BR1-empty) (n = 3 per group). CD73 surface expression was analyzed by flow cytometry. A dose dependent increase in the percentage of CD73-positive endothelial cells was observed, with the highest ones detected in the high dose group. Data are presented as mean ± SD. Statistical significance was assessed using

one-way ANOVA followed by Dunnett's multiple comparisons test, *** $p < 0.001$, **** $p < 0.0001$

3.2.3 Comparison of viral biodistribution in livers

To assess the distribution of AAV-BR1-CD73 in peripheral organs, vector genome copy numbers were quantified in liver tissue from mice receiving the three different vector doses. The liver was selected as the primary organ of interest, as it represents the main site of off-target accumulation for systemically administered AAV vectors and can reveal potential hepatotoxic effects.

Fourteen days after systemic administration, liver tissues were harvested, DNA isolation was performed and then analyzed by qPCR. Vector genome copy numbers were normalized to diploid genome equivalents and are presented as vector genomes per diploid genome (vg/dg) (Figure 12).

Across all dose groups, only low levels of AAV vector genomes were detected in the liver of the mice. In contrast to the effect observed in the brain, liver vector genome levels showed only minor differences between dose groups and did not display a dose dependent trend.

These results demonstrated that increasing the injected AAV-BR1-CD73 dose does indeed enhance vector accumulation in the brain without causing any hepatotoxic effect. This distribution pattern is consistent with the endothelial tropism of the BR1 capsid and supports its suitability for targeted gene delivery to the brain endothelium [100].

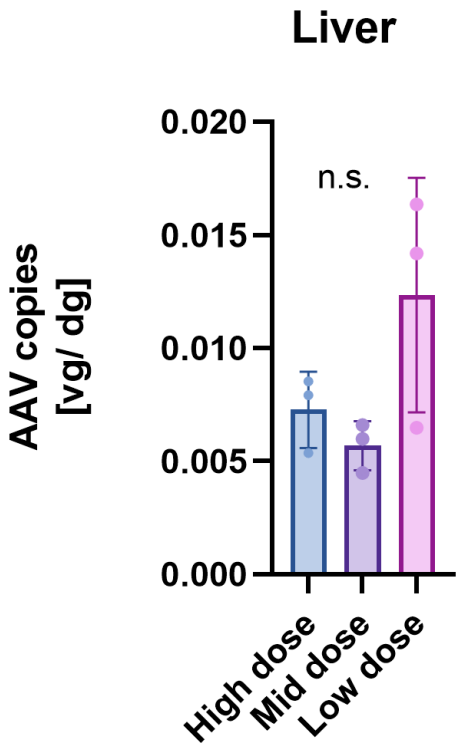

Figure 12. Biodistribution of AAV-BR1-CD73 vector genomes in the liver. Vector genome copy numbers were quantified by qPCR in liver tissue from mice treated with high, medium or low doses of AAV-BR1-CD73 (n = 3 per group). Values were normalized to diploid genome equivalents and are presented as vg per diploid genome. Comparable levels of vector genomes were detected across all dose groups with no statistically significant differences observed. Data are presented as mean ± SD.

3.3 Endothelial CD73 improves ischemic stroke outcome

After verifying the efficient expression of CD73 in the brain endothelium *in vivo,* the impact of this expression was investigated in the murine model of ischemic stroke tMCAO. The aim of these experiments was to determine whether targeted expression of CD73 at the BBB has a beneficial impact on stroke outcome during the late acute phase (48 hours).

3.3.1 Experimental design and workflow

Mice received 2.5 x 10^{12} vg of the AAV-BR1-CD73 vector or empty control systemically via the tail vein and fourteen days after they underwent tMCAO. The mice were monitored and

clinically assessed twice daily over a period of 48 hours to ensure their well-being during the acute phase of ischemic injury.

The impact of endothelial CD73 expression on stroke outcome was evaluated in the late acute phase using several readouts, including survival rate to assess overall mortality, infarct volume quantification by T2-weighted MRI, FACS of brain infiltrating immune cells and transcriptomics to investigate changes associated with CD73 expression in more detail (Fig. 13).

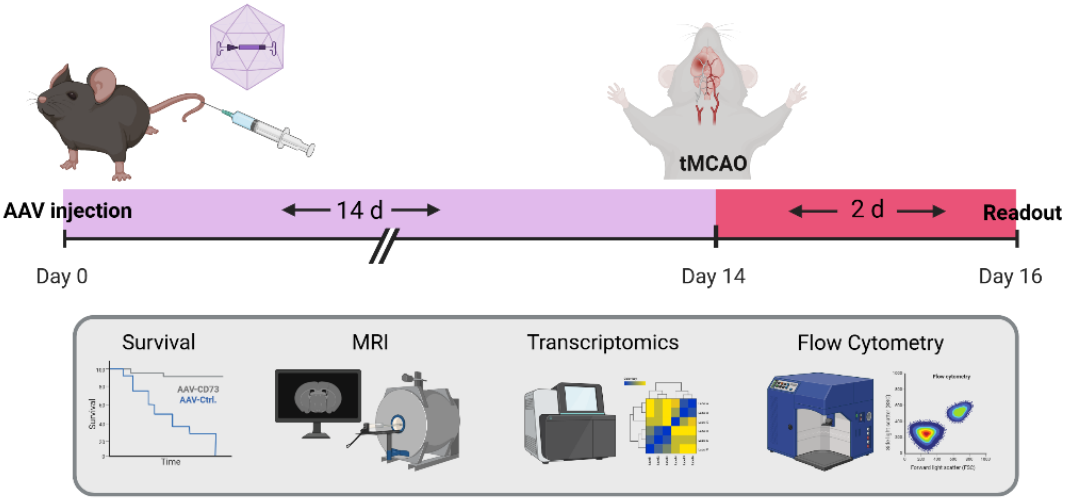

Figure 13. Experimental design for assessment of endothelial CD73 impact in ischemic stroke.

Mice received systemic administration of AAV-BR1-CD73 or an empty control vector (2.5×10^{12} vg per mouse) via tail vein injection. tMCAO was performed fourteen days after injection. At day 2 the stroke outcomes were assessed through survival analysis, T2-weighted MRI, FACS and transcriptomics. *Created in BioRender.com.*

3.3.2 Survival rate

Survival was monitored during the first two days post tMCAO until mice were sacrificed for further analysis. The CD73 group showed a significantly improved survival rate compared to the control group (Fig. 14).

In the control group, 5 out of 16 mice died within the first two days after tMCAO, corresponding to a mortality rate of 31.25%, or approximately one third of them. Noticeably all 16 mice in the CD73 group survived until they were sacrificed post MRI imaging.

These data indicate improved survival in mice expressing endothelial CD73 during the acute phase of ischemic stroke.

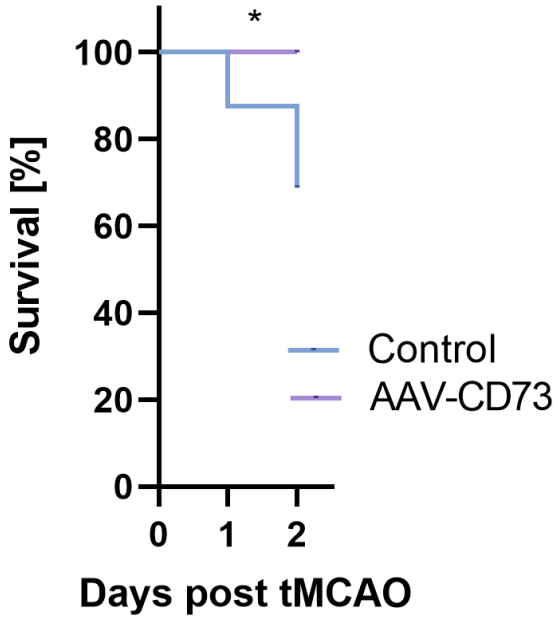

Figure 14. Survival analysis following tMCAO in control and CD73 groups. Kaplan-Meier survival curve showing survival rate after tMCAO in mice treated with either AAV-BR1-CD73 or AAV-BR1-empty (control) (n = 16 per group). The CD73 group demonstrated improved survival compared to the control group (p = 0.0166).

3.3.3 Infarct size assessment by MRI

To evaluate the extent of brain injury, infarct volumes were measured using T2-weighted MRI 48 hours post tMCAO. This time point represents the late acute phase of ischemic stroke, when infarct development is largely complete.

The mice were anesthetized and positioned in the MRI scanner with continuous monitoring of physiological parameters. T2-weighted images were acquired across the entire brain to

capture the full extent of the ischemic lesion. Representative MRI slices from control and CD73 mice are shown in Figure 14 (n = 16 per group). Hyperintense regions on T2-weighted images correspond to infarcted brain tissue and were used for further quantitative analysis of lesion volumes.

The analysis of the MRI datasets revealed significant differences in lesion size between the two groups. Control animals typically displayed larger lesions involving both cortical and subcortical structures within the ipsilateral hemisphere. While, the CD73 mice mostly exhibited smaller and more confined lesions, suggesting that CD73 expression in the brain endothelium attenuates the damage caused by stroke.

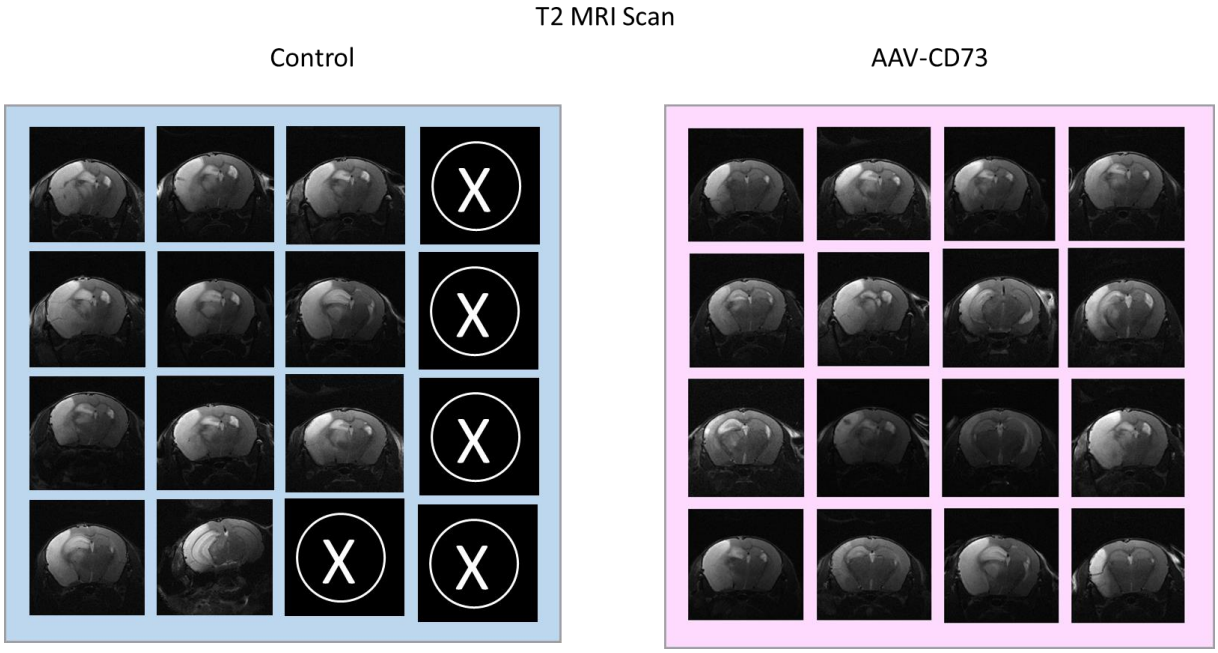

Figure 15. Representative T2-weighted MRI images 48h post tMCAO. Representative coronal T2-weighted MRI slices obtained two days after tMCAO induction in mice treated either with AAV-BR1-CD73(n = 16) or AAV-BR1-empty control (n = 11). Hyperintense regions indicate infarcted brain tissue. Black boxes with a white X indicate deceased mice. Mice treated with AAV-BR1-CD73 display visibly smaller infarct lesions compared to control mice.

Quantitative analysis of the lesion size revealed an infarct volume of X +/- Y mm^3 in the control group, whereas the infarct volume was significantly ($p < xxx$) reduced to A +/- B mm^3 in the CD73 treatment group (Fig. 16).

The infarcts seen in the ipsilateral hemisphere of the CD73 group were approximately by 40% smaller than those observed in the control group. The relatively tight clustering of infarct sizes in the CD73 group further supports that endothelial CD73 expression consistently attenuates tissue damage.

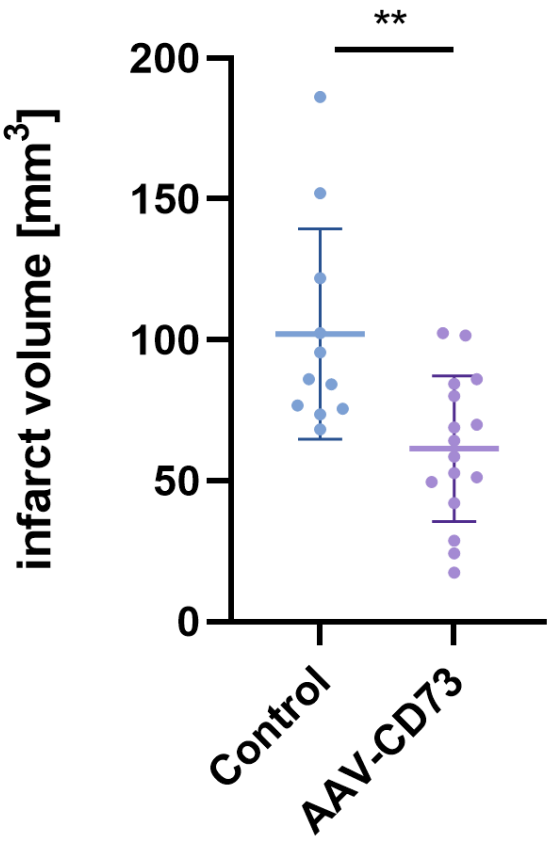

Figure 16. Quantification of infarct lesions 48 hours post tMCAO.

Infarct lesions were quantified from T2-weighted MRI scans two days after tMCAO in mice treated either with AAV-BR1-CD73 (n = 16) or AAV-BR1-empty (control) (n = 11). Lesion areas were measured across consecutive slices (how many) using Fiji/ImageJ and infarct volumes were calculated with edema correction as described in the Methods. Mice that received the AAV-BR1-CD73 vector showed reduced ischemic damage compared to control animals. Data

are presented as mean ± SD with animals shown as individual data points. Statistical significance was assessed using an unpaired two-tailed Student's t-test, ** $p < 0.01$.

3.3.4 Independent validation of stroke outcome by a second surgeon

The stroke experiments were independently repeated by a second surgeon using the same experimental design. This approach would not only reveal potential surgeon-dependent variability but also confirm the observed effect in the CD73 group.

As in the initial experiment, mice received systemically either AAV-BR1-CD73 or the corresponding control vector fourteen days prior to tMCAO. Consistent with the previous stroke experiment, survival analysis again showed a similar pattern of the improved survival in the CD73 mice compared to the controls (Fig. 17A). While two out of six animals died from stroke in the control group all six mice in the CD73 treatment group survived. This finding showed that the protective effect of endothelial CD73 expression on early mortality was reproducible across independent surgical procedures.

Representative T2-weighted MRI images obtained two days post tMCAO further supported this observation. The analysis of the images revealed yet again significantly ($P < XXX$) smaller infarct lesions (X +/- Y mm^3) in the CD73 group compared to the control mice (A +/- B mm^3; Fig. 17B & C), consistent with the protective effect observed in the initial cohort. While the absolute infarct sizes differed from those observed in the first experimental setting, this variability is consistent with the known sensitivity of the tMCAO model to subtle procedural differences between surgeons. However, the relative reduction in infarct volume in the CD73 group was comparable to that seen in the initial experiment despite the differences in absolute lesion size. This independent validation strengthens the conclusion that AAV-BR1-CD73 provides a protective effect in the acute phase of ischemic stroke.

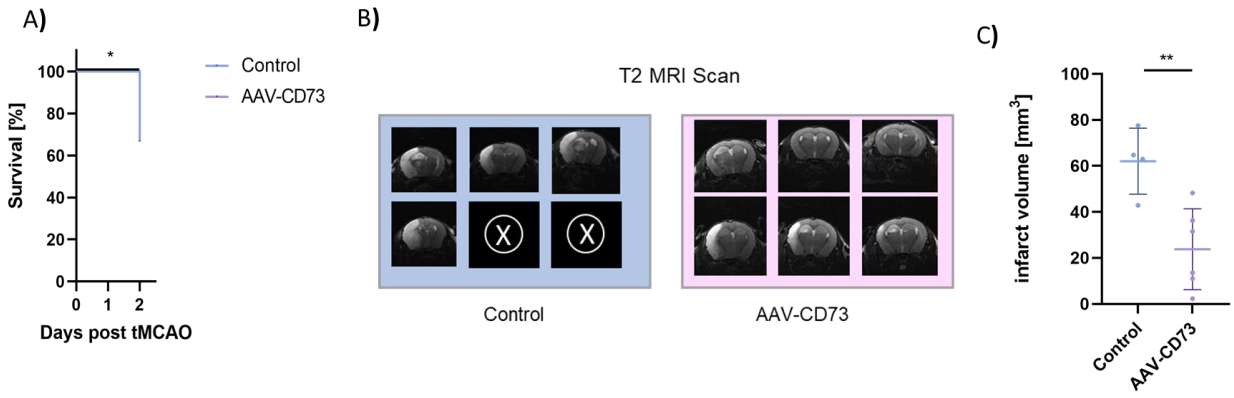

Figure 17: Independent validation of stroke outcome by a different operator. (A) Kaplan-Meier survival curve post tMCAO in mice treated either with AAV-BR1-CD73 or AAV-BR1-empty (control) (n = 6 per group), * $p < 0.1$. (B) Representative coronal T2-weighted MRI slices obtained two days post tMCAO. Hyperintense regions indicate infarcted brain tissue. (C) Quantification of infarct volumes measured by T2-weighted MRI. Data are presented as mean ± SD with individual animals shown. Statistical significance was assessed using an unpaired two-tailed Student's t-test, ** $p < 0.01$.

3.4 Transcriptomic assessment of brain endothelial cells after CD73 expression

After demonstrating that endothelial CD73 overexpression improves survival and reduces infarct size post tMCAO, the next aim was to investigate whether this protective effect is associated with transcriptional changes in brain endothelial cells. As mentioned in the introduction section, the endothelium plays an important role in the regulation of neuroinflammation, barrier integrity and immune cell migration, it was important to determine whether CD73 expression induces broader gene expression changes within the endothelial cells.

3.4.1 Endothelial bulk RNA-seq reveals no significant DEGs

To determine whether endothelial CD73 expression induces transcriptional changes in brain endothelial cells, bulk RNA sequencing was performed on isolated brain endothelial cells from mice treated with either AAV-BR1-CD73 or AAV-BR1-empty (n = 3 per group). Differential expression analysis was conducted using predefined significance thresholds (FDR ≤ 0.1 and $|\log2FC| \geq 1$) to identify genes with robust and biologically relevant changes in expression.

Under these criteria, no genes met the threshold for differential expression (Figure 18). The volcano plot illustrates that, although individual transcripts showed variation in fold change and nominal p-values, these changes did not reach statistical significance after multiple-testing correction. Most genes were distributed near the center of the plot, indicating only minor expression differences between the CD73 and control groups.

Because of these results, the following analyses focused on understanding how endothelial CD73 expression influences the response of immune cells in the acute phase of ischemic stroke.

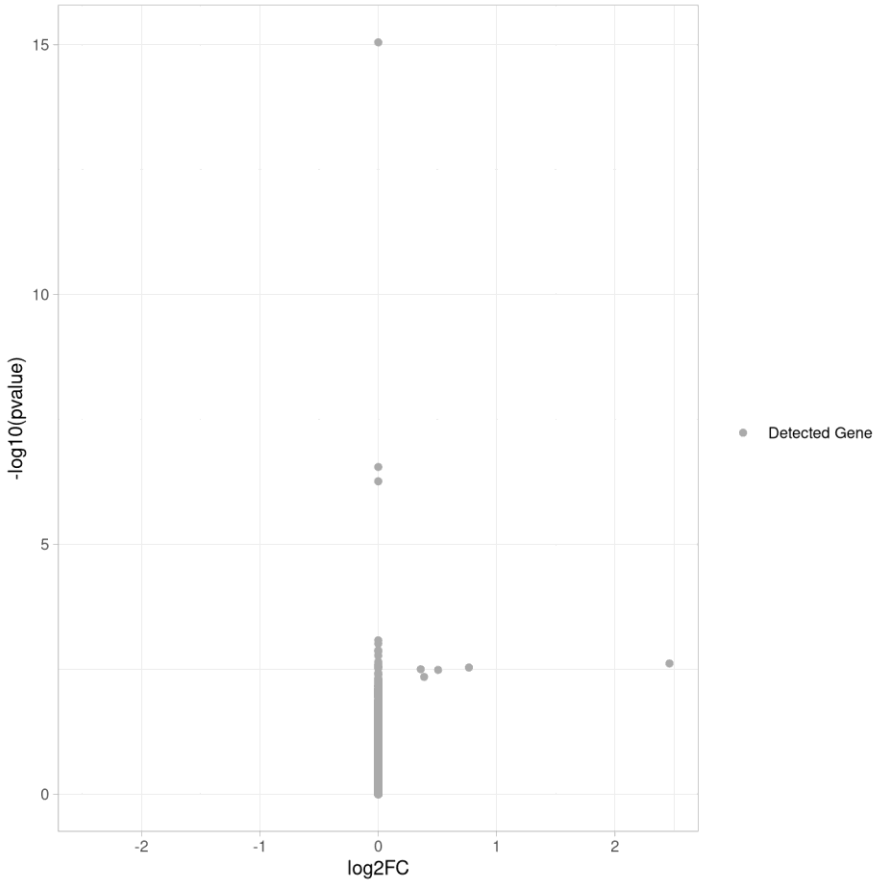

Figure 18: Differential expression analysis of brain endothelial bulk RNA-seq.

Volcano plot demonstrating the differential gene expression in brain endothelial cells from AAV-BR1-CD73 vs. AAV-BR1-empty mice (n = 3 per group). Genes are plotted by log2 fold change (x-axis) and −log10(p-value) (y-axis). No genes met the differential expression threshold of FDR ≤ 0.1 and |log2FC| ≥ 1. Statistical analysis was performed as described in the Methods.

3.5. CD73-induced immune cell recruitment and polarization

Flow cytometry-based immune profiling was combined with bulk RNA sequencing of infiltrating immune cells in order to investigate whether the endothelial CD73 expression affects immune cell recruitment and both their activation and polarization states post stroke. Infiltrating and resident immune cells were isolated from the ipsilateral hemisphere 48 hours post tMCAO.

This combined approach enabled the evaluation of potential differences in immune cell composition between the experimental groups, as well as the identification of CD73-dependent transcriptional programs within the immune cell populations.

3.5.1. Flow cytometry analysis of infiltrating leukocytes

To quantify the cerebral immune cell populations post tMCAO, single-cell suspensions from the ipsilateral hemispheres were analyzed using multicolor flow cytometry and a broad gating strategy (Fig. 19).

Cells were first gated to exclude debris, doublets and dead cells. $CD45^+$ leukocytes were then subdivided into lymphoid and myeloid populations. Within the lymphoid compartment, T cells, NK cells and γδ T-cells were identified based on CD4, CD8, NK1.1 and TCRγδ expression. Within the myeloid compartment, microglia, infiltrating monocytes/macrophages and neutrophils were classified based on CD11b, CD45, CD11c and Ly6G expression.

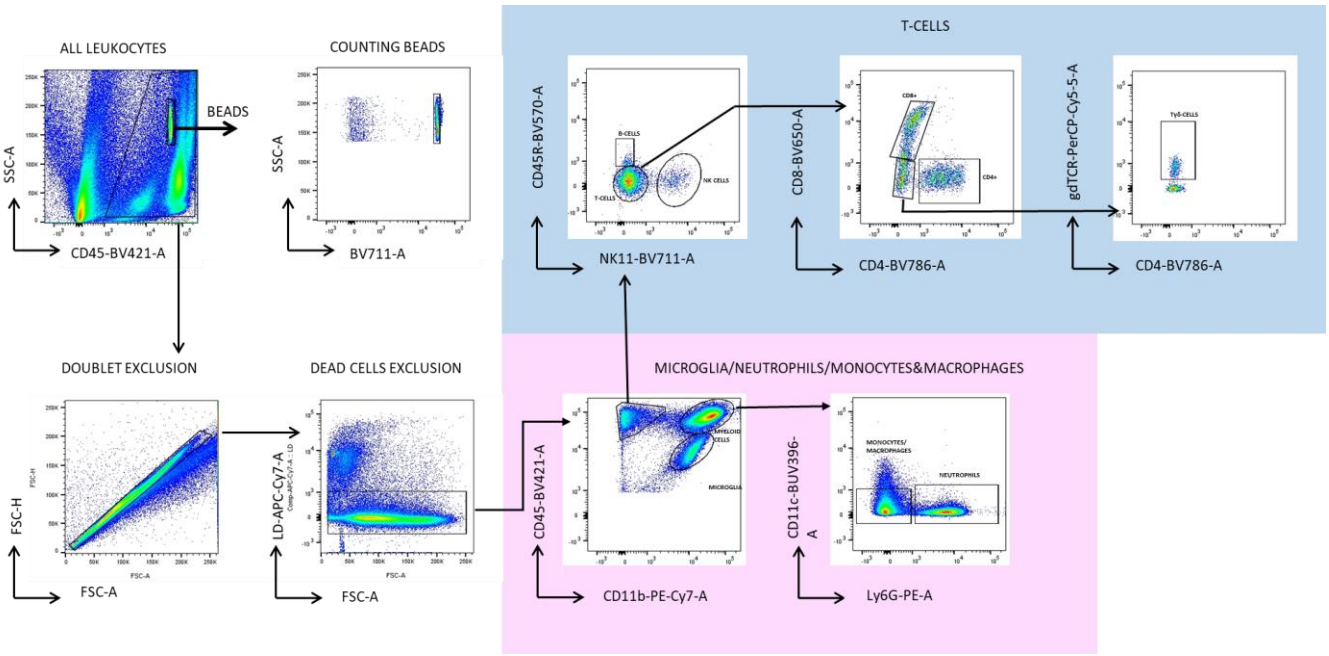

Figure 19. Gating strategy used to identify immune cell populations inside the ipsilateral hemisphere of ischemic brain tissue. After exclusion of debris, doublets and dead cells, $CD45^+$ leukocytes were subdivided into lymphoid and myeloid compartments. Lymphoid populations included T cells, NK cells and γδ T cells, identified based on CD4, CD8, NK1.1 and TCRγδ expression. Myeloid populations were divided into microglia, infiltrating monocytes/macrophages and neutrophils based on CD11b, CD45, CD11c and Ly6G expression.

Quantitative analysis of infiltrating immune cells revealed distinct changes in specific populations between the AAV-BR1-CD73 and control groups (Fig. 20). A trend towards increased amounts across all cell types was observed in the CD73 group, with a significant enrichment in the populations of monocytes/macrophages and γδ T cells compared to the control group.

These findings suggest that immune cell infiltration is not suppressed but rather enhanced by endothelial CD73 expression.

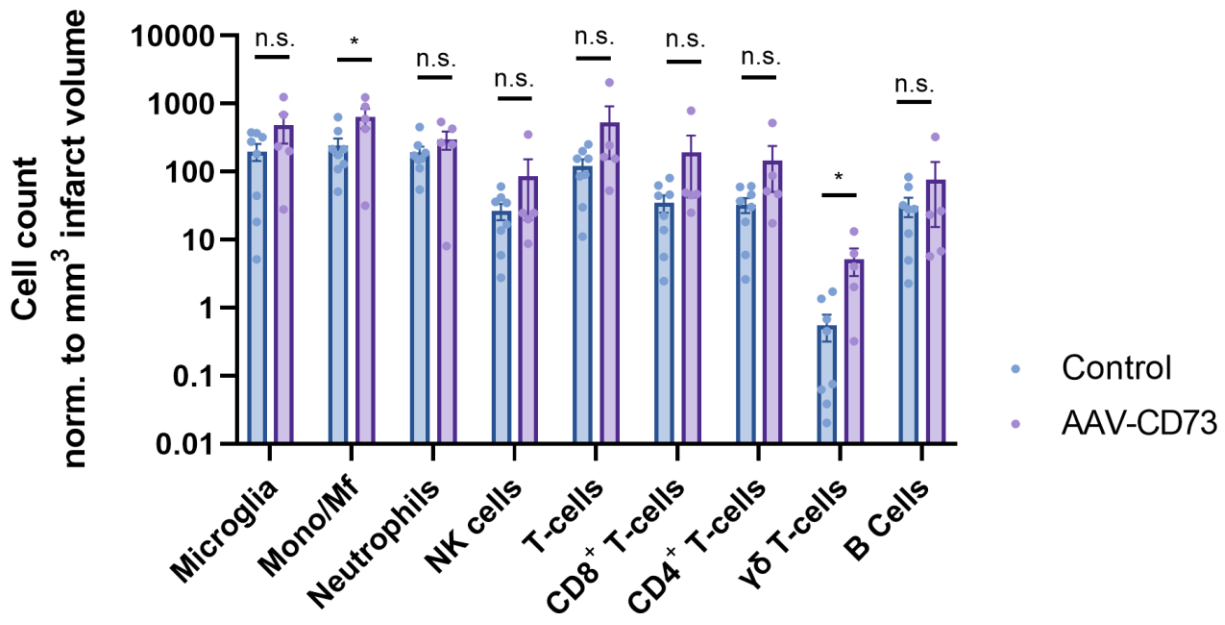

Figure 20. Quantification of brain immune cell populations post stroke. FACS quantification of immune cell populations isolated from the ipsilateral hemisphere 48 hours after tMCAO in CD73 (n = 5) and control (n = 8) mice. Bars represent mean ± SEM with individual data points shown. Monocyte/macrophage and γδ T-cell populations were significantly increased in the CD73 group, while also the rest of populations showed a trend toward higher numbers compared to controls. Statistical significance between Control and AAV-CD73 groups for each cell population was assessed using unpaired two-tailed Student's t-tests. * $p < 0.05$.

3.5.2. Bulk RNA sequencing of cerebral immune cells

In order to investigate how the CD73 expression in murine brain endothelial cells influences the transcriptional state of the immune cells inside the brain tissue, $CD45^{+}/CD31^{-}$ cells were isolated from the ipsilateral hemispheres, RNA was extracted from the sorted immune cell fractions and then sent for bulk RNA-sequencing. This enabled the selective analysis of immune cells that are inside the brain parenchyma while excluding endothelial cells. The analysis was designed as an explorative study (n = 2 per group) to get first hints on possibly affected transcriptional programs in immune cells by CD73 overexpression post tMCAO.

The results revealed profound differences between the CD73 and control groups (Fig. 21) that align with the changed immune cell composition revealed by flow cytometry. The majority of DEGs were myeloid genes upregulated in the CD73 group, confirming a prominent shift in the immune cell composition.

Among the most strongly upregulated genes were *Chil3*, *Cd14*, *Il1rn*, *Lcn2* and *Cxcl2*, which are associated with myeloid activation, innate immune responses and inflammatory signaling.

These genes represent key regulators of macrophage and neutrophil functions and are involved in processes such as cytokine signaling, chemotaxis, innate immune activation and tissue remodeling.

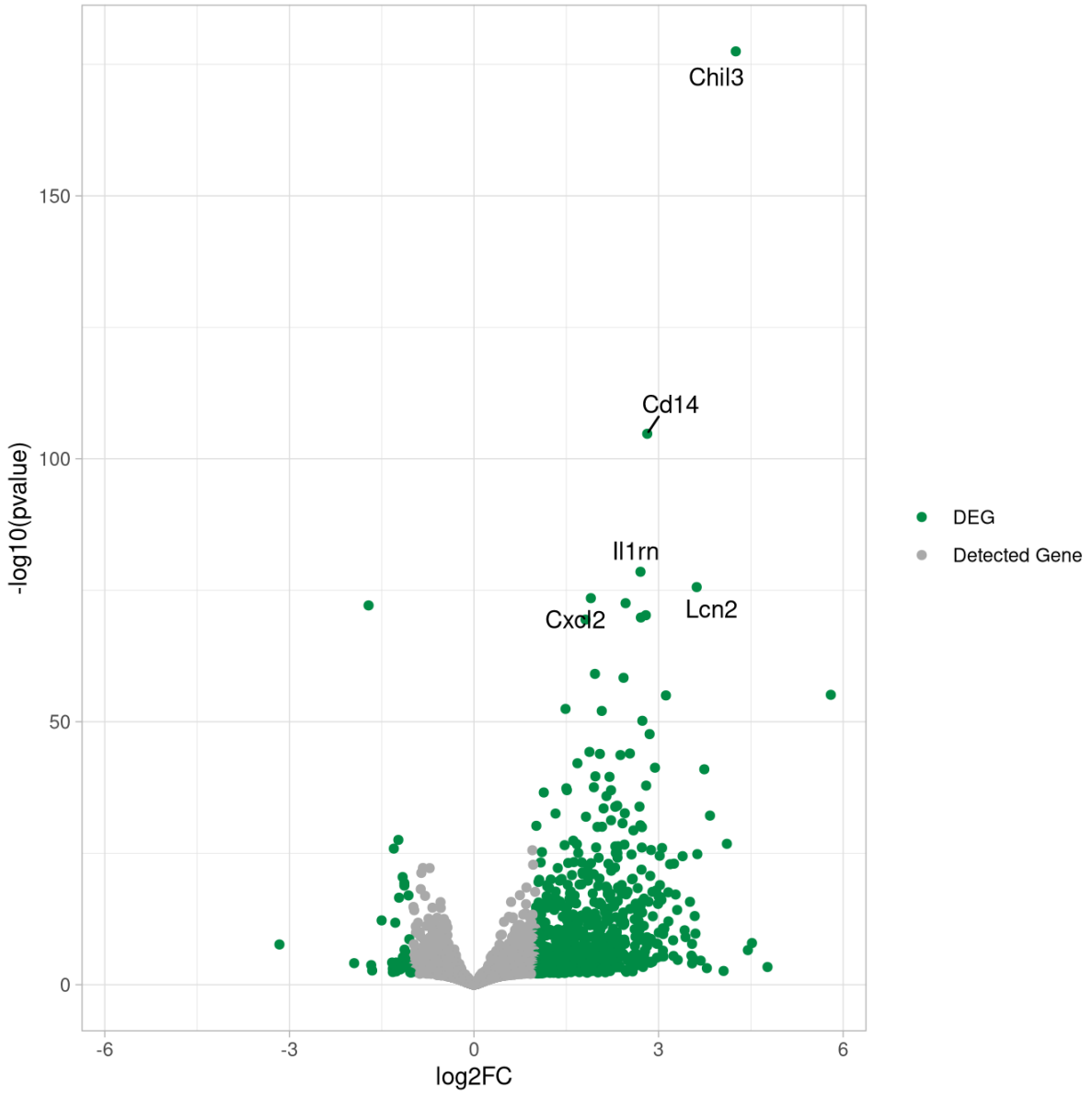

Figure 21. Differential gene expression in immune cells inside the ipsilateral hemisphere.

Volcano plot showing differential gene expression in $CD45^{+}CD31^{-}$ immune cells isolated from ipsilateral hemispheres of CD73 and control mice, 48 hours post tMCAO (n = 2 per group). Each dot represents a gene plotted by $\log_2$ fold change versus $-\log_{10}$(p-value). Significantly upregulated genes in the CD73 condition are highlighted, including *Chil3*, *Cd14*, *Il1rn*, *Lcn2* and *Cxcl2*.

3.5.3. Regulation of inflammatory, chemotaxis and myeloid activation genes

To focus on biologically relevant and highly expressed transcripts, differentially expressed genes (DEGs) were filtered based on mean expression thresholds. For most analyses, a threshold of 100 normalized counts was applied to exclude genes with low expression. This filtering step ensured that analyses were driven by genes with biologically meaningful expression levels. However, for the identification of more robust changes, a more strict threshold of 2000 normalized counts was used, especially since the number of biological replicates in this explorative approach was very small (n = 2). This higher cutoff allowed the identification of important genes that define the overall immune response.

A heatmap of the highly expressed DEGs revealed an upregulation of genes associated with innate immune activation, myeloid cell function and inflammatory signaling in the CD73 group (Fig. 22). These included genes such as *Chil3*, *S100a8*, *S100a9*, *Cd14*, *Il1b*, *Csf3r* and *Socs3*, which are commonly associated with activated myeloid cells and inflammatory responses. The strong expression of *S100a8* and *S100a9* is typically observed in neutrophils and inflammatory monocytes. *Csf3r*, which is the receptor for granulocyte colony-stimulating factor, is associated with granulocytic lineage. The simultaneous upregulation of *Cd14* and *Il1b* further indicates activation of innate immune signaling pathways. While, the upregulation of *Socs3* (negative regulator of cytokine signaling) suggests the presence of feedback regulatory mechanisms.

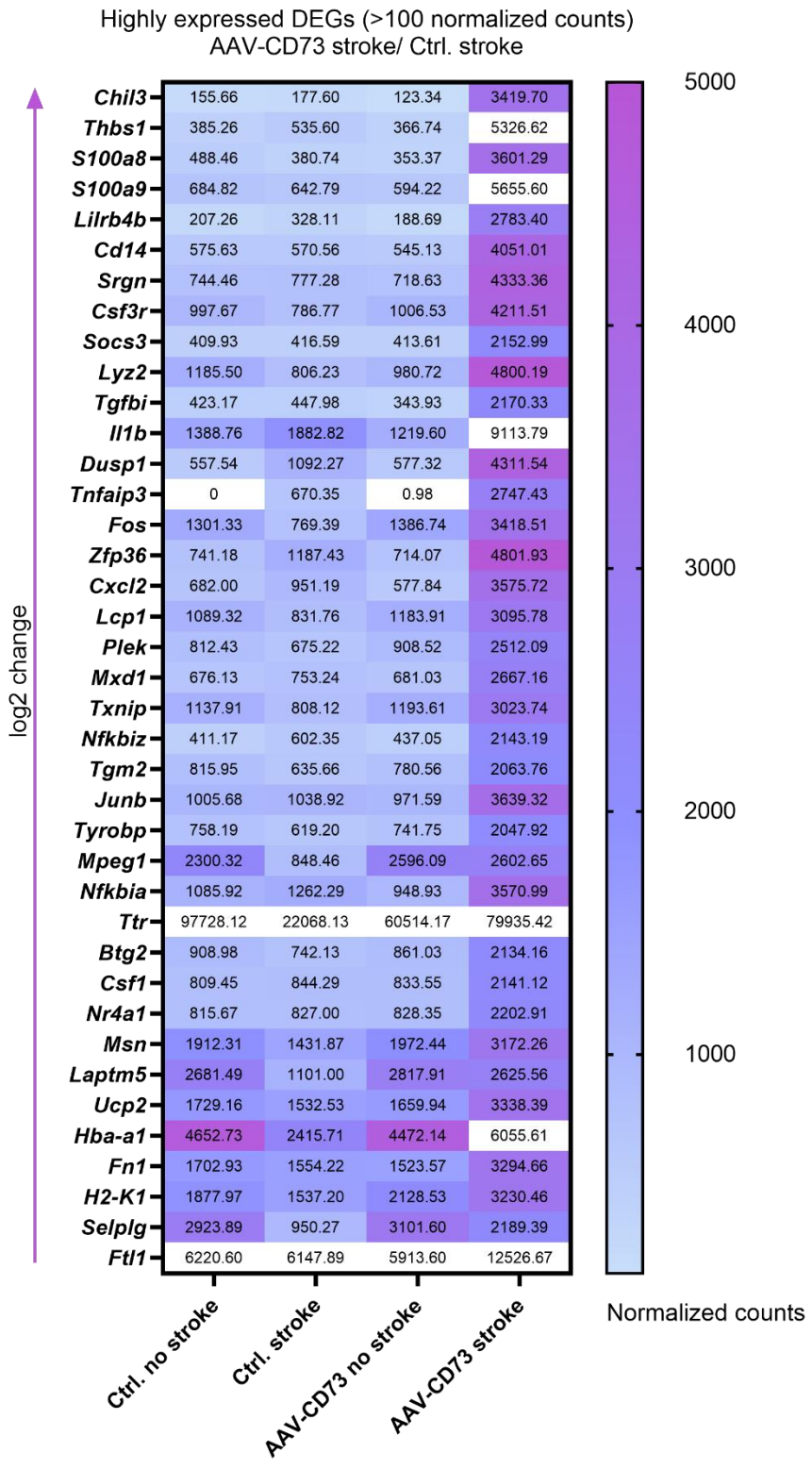

Figure 22. Highly expressed DEGs in immune cells in the ipsilateral hemispheres post tMCAO. Heatmap showing DEGs with mean expression levels above 2000 normalized counts across experimental groups. Rows represent genes and columns represent individual conditions. The

CD73 group showed increased expression of multiple genes associated with innate immune activation and myeloid cell function.

Consistent with this pattern, the top differentially expressed genes included *Saa3*, *Chil3*, *F10*, *Mefv*, *Wfdc17* and *Mmp8* (Fig. 23). Many of these genes are linked to acute phase responses, neutrophil activation and extracellular matrix remodeling. *Saa3* is an acute phase protein associated with inflammatory responses, while *Chil3* has been associated to myeloid cell activation and tissue remodeling. *F10* is a component of the coagulation cascade and *Mefv* encodes pyrin, a regulator of inflammasome activity. *Wfdc17* is associated with innate immune responses, whereas *Mmp8* encodes a neutrophil-derived collagenase involved in extracellular matrix degradation.

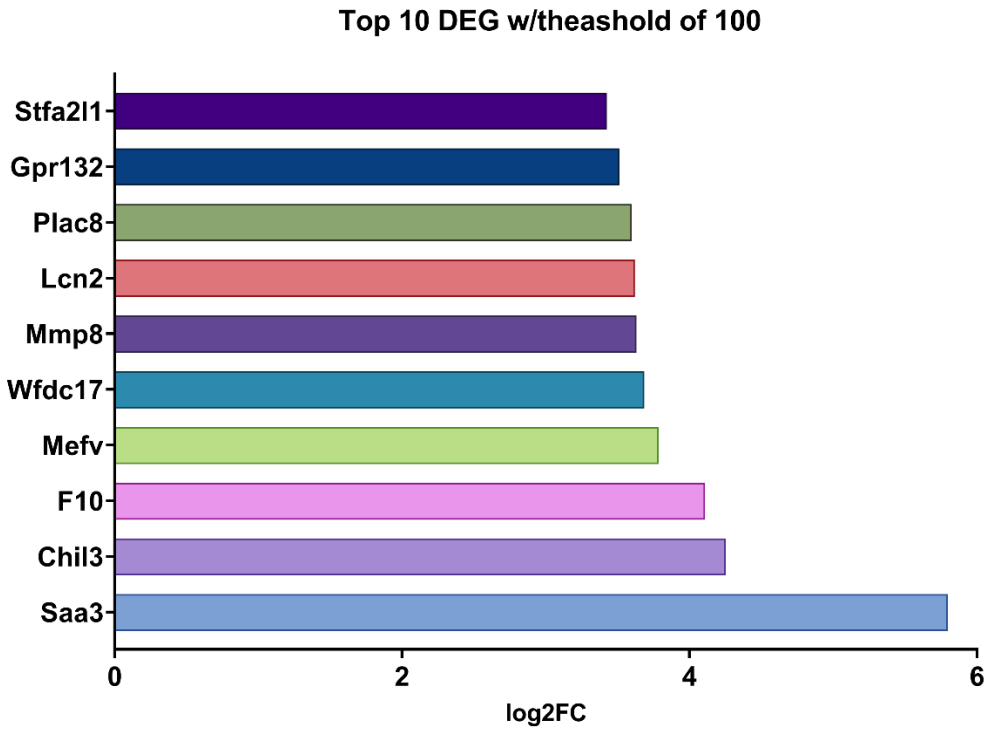

Figure 23. Top DEGs in immune cells in the CD73 group. Bar plot showing the top upregulated DEGs (mean expression >100 normalized counts) in CD73 mice compared to control mice 48 hours post tMCAO. Genes include acute phase proteins, myeloid activation markers and ECM-associated factors.

Further analysis revealed a simultaneous upregulation of genes involved in negative regulation of NF-κB signaling and innate immune responses (Fig. 24). These included *Il1rn*, *Socs3*, *Tnfaip3*, *Nfkbia* and *Nfkbie*. All these genes act as feedback inhibitors of inflammatory signaling pathways. *Il1rn* encodes the IL-1 receptor antagonist, while *Tnfaip3* and the NF-κB inhibitors *Nfkbia* and *Nfkbie* are classical regulators of NF-κB dependent transcription.

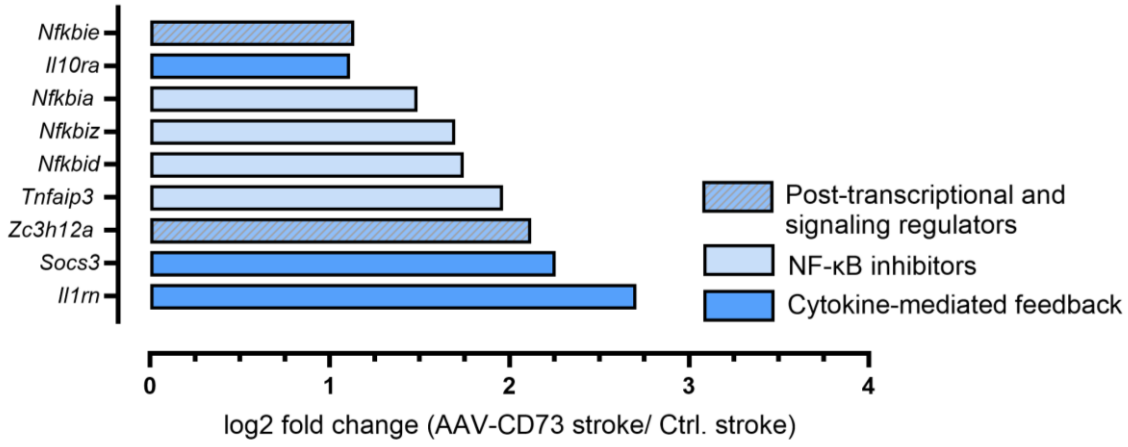

Figure 24. Negative regulation of NF-κB and innate immune signaling.

Log_2 fold change of selected genes involved in negative regulation of NF-κB signaling and cytokine mediated feedback in CD73 mice compared to control mice 48 hours post tMCAO. Genes include cytokine feedback regulators, NF-κB inhibitors and post-transcriptional signaling regulators.

Genes associated with alternative or reparative myeloid activation states were also upregulated (Fig. 25). These included *Chil3*, *Arg1*, *Lgals3*, *Mrc1*, *Lpl* and *Stab1*, which are linked to phagocytosis, lipid handling and tissue remodeling. *Arg1* is involved in L-arginine metabolism, *Mrc1* encodes the mannose receptor CD206 and *Lgals3* encodes galectin-3. All these three genes are associated with myeloid cell activation and phagocytic functions. *Lpl* and *Stab1* are involved in lipid metabolism and scavenger receptor mediated clearance processes.

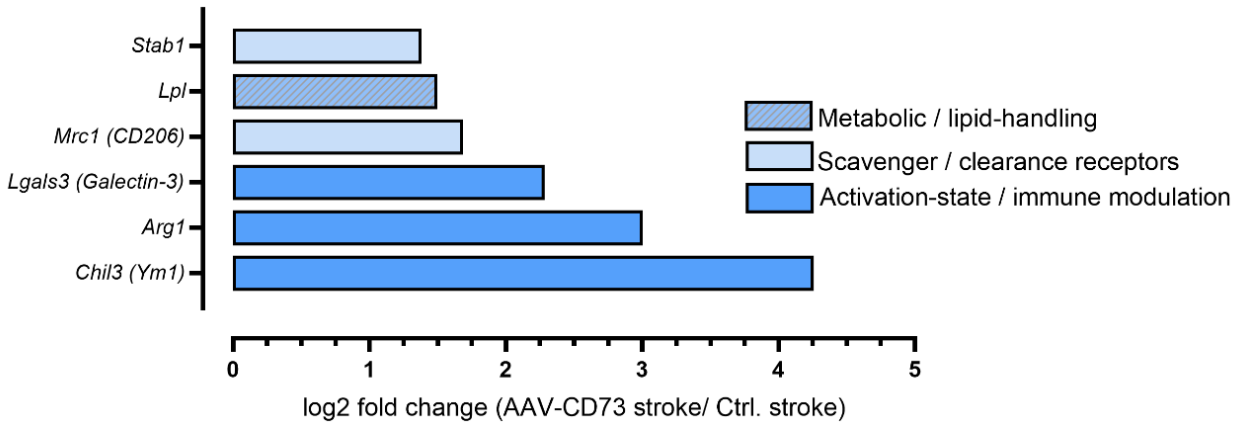

Figure 25. Myeloid activation state markers. Log_2 fold change of selected myeloid activation state markers with mean expression >100 normalized counts in CD73 mice compared to control mice 48 hours post tMCAO. Genes are associated with macrophage scavenging, lipid handling and immune modulation.

Finally, the analysis of upregulated DEGs in the CD73 group also revealed the upregulation of several inflammatory mediators and matrix-remodeling enzymes, including *Il1b*, *Tnf*, *Mmp8* and *Mmp19* (Fig. 26).

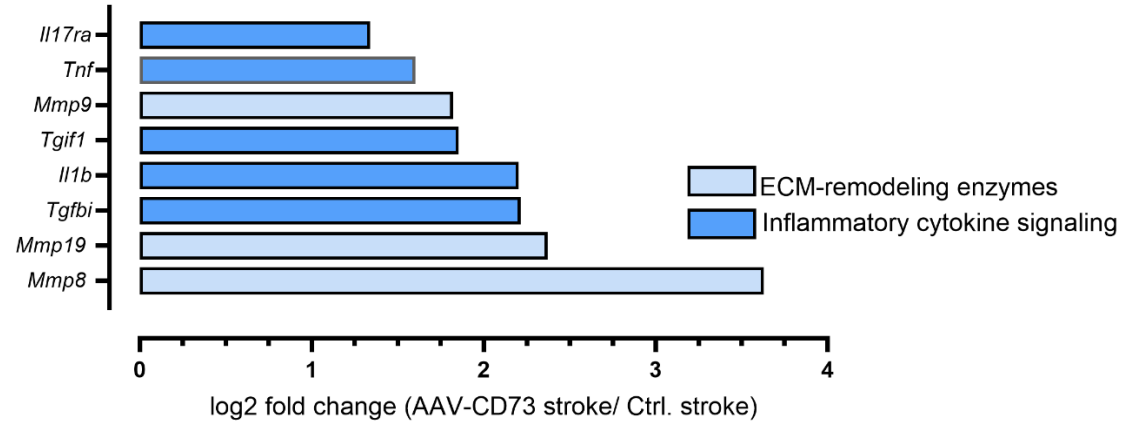

Figure 26. Inflammatory cytokine and ECM-remodeling-associated genes.
Log_2 fold change of selected inflammatory cytokine signaling components and matrix metalloproteinases with mean expression >100 normalized counts in CD73 mice compared to control mice 48 hours post tMCAO. Genes shown are associated with cytokine driven extracellular matrix remodeling and immune-ECM interactions in inflamed tissues [21].

4. Discussion

In this study, the expression of CD73, a key enzyme for the degradation of extracellular ATP, in brain endothelial cells in mice was investigated in the context of ischemic stroke and its outcome. Surprisingly, it has been shown that the CD73 expression in the brain endothelium of mice is very low, especially compared to the human counterpart [82]. To address this species-difference, an AAV vector that enables the expression of CD73 specifically in endothelial cells of the mouse brain was generated. AAV-mediated CD73 expression was assessed *in vitro* and *in vivo* before analyzing its effect on the post-ischemic immune reaction in the tMCAO mouse stroke model [100].

During ischemic stroke, ATP is being released and accumulated in the extracellular space of the brain, creating a pro-inflammatory environment [111]. Two enzymes that are part of the purinergic signaling, a communication system between cells, can degrade extracellular ATP to adenosine, which has shown to have anti-inflammatory properties [112, 113]. More specifically, CD39 (*ENTPD1*) degrades extracellular ATP into ADP and AMP, while CD73 then converts AMP further to adenosine. The overexpression of CD73 in the BBB *in vitro* has demonstrated enhanced adenosine production and restriction of leukocyte transmigration [114-116].

The role of both CD39 and CD73 has been investigated in multiple studies and although several studies have already been referred to in the introduction section, there are even more that are worth mentioning. In one study, a global knockout of CD73 resulted in increased leukocyte accumulation and larger infarct sizes in mice upon photothrombotic arterial occlusion, indicating that CD73-derived adenosine has indeed a tissue-protective effect [117]. Similarly, hypoxia-induced vascular leakage was also worsened in another study using a CD73 knockout mouse model, further supporting CD73's involvement in repair and restoration [84].

CD39 has also been investigated and shown to reduce infarct size, decrease platelet aggregation and improve neurological outcomes in experimental stroke models [118]. A recent study, also used endothelial-targeted delivery of CD39, using a nanobody, which demonstrated that selective modulation of purinergic signaling can reduce infarct size and improve outcomes in stroke models[119].

In addition to enzyme-targeting approaches, others have investigated the role of adenosine receptors in stroke pathophysiology. Adenosine signals through four G-protein-coupled receptors (A1, A_{2A}, A_{2B} and A_3), each with distinct expression patterns and functions [108, 120]. Brain endothelial cells do mainly express the receptors A_{2A} and A_{2B}. Both the activation and the inhibition of A_{2A} receptors have been reported to promote neuroprotection depending on the timing, cellular context and receptor localization [121-123]. Early receptor activation may reduce excitotoxicity and inflammatory signaling, while later modulation can influence leukocyte recruitment and secondary injury.

Other studies have highlighted the importance of adenosine signaling in regulating immune cell entry into the CNS [124]. For example, CD73 has been shown to be required for efficient lymphocyte migration into the CNS during neuroinflammation, highlighting yet again its role as a key regulator of immune cells recruitment [125].

The main drive of this study was the hypothesis that shifting the balance of the stroked brain from ATP to adenosine would result in a more stable BBB, less immune cells infiltration into the brain parenchyma and limited secondary injury [126-128].

4.1. Endothelial CD73 and BBB integrity after stroke

Systemic administration of AAV-BR1-CD73 resulted in robust and highly specific transgene expression in brain endothelial cells. Mice treated with the AAV-BR1-CD73 vector showed a 100% survival rate in the late acute phase following tMCAO (48 h), while in the control group approximately one third of the mice did not survive until the scheduled MRI appointment. T2-weighted MRI revealed also a significant reduction in infarct volumes between the two experimental groups. Mice that received the AAV-BR1-CD73 vector displayed approximately 40% smaller infarct sizes than the mice that received the control vector, AAV-BR1-empty. This protective effect was even reproduced in an independent experimental series performed by a different operator to avoid procedural variability. Since the disruption of the BBB during a stroke episode has been shown in multiple studies to contribute to the formation of edema in the affected regions of the brain, the infiltration of immune cells and subsequently to secondary injury [14, 22, 102, 129-131], we assumed that the beneficial effect of endothelial CD73 expression would be linked to BBB integrity.

CD73 is an ectoenzyme, so its function and effects are driven through extracellular nucleotide metabolism and receptor-dependent signaling, rather than through direct transcriptional regulation [114-116, 125]. Hypoxia-reoxygenation in bEND.3 cells demonstrated a time-dependent manner of CD73 upregulation and downregulation, suggesting that it may contribute to adaptive vascular responses in the context of stroke [132]. Many studies have been focused on adenosine signaling and its effects. Adenosine is an endogenous regulator of BBB permeability and it has been shown that the activation of adenosine receptors can influence tight junction stability, cytoskeletal organization and leukocyte transmigration across the BBB [128]. In another study, the antagonism of the A_{2A} receptors has been reported to reverse BBB dysfunction induced by sleep restriction [134], while in a different study, the endothelial-specific inactivation of A_{2A} receptors demonstrated to have a protective effect in mice post stroke [133]. In contrast, other studies have demonstrated protective effects of A_{2A} receptor agonists in ischemia models [134, 135]. The activation of A_2 receptors has also been used to increase BBB permeability for drug delivery in oncological settings [75].

Despite the strong observed protective effect, bulk RNA sequencing of isolated brain endothelial cells did not reveal any differentially expressed genes between the CD73 and control groups 48 hours post tMCAO. This might indicate that endothelial CD73 expression does not result in additional transcriptional changes at the BBB. However, it should be noted that the endothelial cells were isolated from both brain hemispheres, cerebellum and olfactory bulb excluded, and not only from the ipsilateral hemisphere. This might mask potential transcriptional changes in the stroked region. In addition, bulk transcriptomic approaches may not be suitable for gene detection in specialized BBB subpopulations [136]. Further, the number of biological replicates (n = 3) sent for sequencing was low due to limited resources and the cDNA samples sent for sequencing were distributed to different sequencing runs. Bioinformatic analysis revealed a massive batch effect between the sequencing runs that might have masked actual changes in gene expression.

Overall, adenosine does not act in a uniform manner but displays a range of effects that depend on receptor subtype, cellular localization, adenosine concentration, and the phase of the injury, proving its complex and context-dependent nature. Although the expression of CD73 via the AAV-BR1-CD73 vector may not have changed the transcriptome of the endothelium itself, it certainly changed the adenosine concentration, hence the activation of

adenosine receptors. It may also have affected the interaction between the BBB and the peripheral immune cells. Such effects can be exerted post-transcriptionally, which may explain the absence of detectable endothelial DEGs despite clear functional benefits [137]

4.2. Mechanistic insights: adenosine signaling and immune modulation

As the transcriptomic analysis of endothelial cells did not indicate any DEGs, the focus of this study was shifted to the immune cells inside the ipsilateral hemisphere.

Bulk RNA sequencing of immune cells showed clear transcriptional differences between CD73 and control groups post tMCAO. The findings of the bulk RNA sequencing experiment were further supported by FACS.

Although being of an explorative nature with a highly limited number of biological replicates (n = 2) due to limited resources, the sequencing data strongly suggest that the observed protective effect is more likely driven by the modulation of the immune response. Rather than directly altering endothelial gene programs, endothelial CD73 expression appears to reshape the inflammatory environment at the NVU, resulting in altered immune cell recruitment and activation states.

4.2.1 Adenosine signaling as a regulator of immune responses

Adenosine can play an important role in resident immune cell activation, peripheral immune cells migration and polarization. The outcome of adenosine signaling in leukocytes is depended on the adenosine concentration, the receptor, the cell type as well its activation state [138]. While the activation of adenosine receptors, particularly A_{2A} and A_{2B} receptors, has been demonstrated to reduce pro-inflammatory cytokine production, leukocyte adhesion and also to promote resolution in many tissues [74, 121, 139-141].]. Other scientist used chimeric mice which underwent middle cerebral artery occlusion (MCAO) and saw that the inactivation of the A_{2A} receptor in bone marrow-derived cells (BMDC) actually exhibited tissue protective effects and simultaneously proved that the A_{2A} receptor can also have a pro-inflammatory role as its inactivation resulted in the suppression of pro-inflammatory cytokines such as IL-1, IL-6 and IL-12 in the brain [142, 143]. Another study however showed that the a

and activation of the A_{2A} receptor in BMDC actually exhibited tissue protective effects in the spinal cord [142, 144].

In macrophages and microglia, adenosine signaling has often been linked to anti-inflammatory or reparative phenotypes, sometimes referred to as “M2-like” states. These cells are characterized by phagocytosis, debris clearance and tissue repair functions [40, 145]. It has also been demonstrated that the chemotactic orientation of macrophages depends significantly on the activation of the A_3 and A_{2B} receptors and when these are absent there seems to be a disorientation [146]. A recent study showed that CD73 overexpression can reduce astrocyte pyroptosis after cerebral ischemia-reperfusion injury through an A_{2B} receptor-dependent mechanism involving suppression of NF-κB signaling [147]. Adenosine also affects the expression of endothelial adhesion molecules, cytoskeletal changes and the transmigration of peripheral immune cells into the CNS [124, 128].

Taking these into account, the effects of adenosine cannot be interpreted strictly as anti-inflammatory in the context of neuroinflammation as leukocytes express multiple adenosine receptor subtypes with divers downstream effects.

4.2.2 Transcriptional reprogramming of infiltrating immune cells by endothelial CD73

According to our data, neuroinflammation does not simply appear stronger or weaker after CD73 expression in the brain endothelium but rather reprogrammed.

The transcriptional analysis demonstrated that mostly DEGs were upregulated in the CD73 group compared to the controls. Among the most strongly upregulated genes were *Chil3*, *Cd14*, *Lcn2*, *Cxcl2*, *S100a8*, *S100a9* and *Il1b*, all of which are associated with myeloid activation, innate immune signaling and neutrophil recruitment. The proteins encoded by *S100a8* and *S100a9* form the calprotectin complex, which is a well-known marker of neutrophil activation and acute inflammation [50, 148]. *Cd14* acts as a co-receptor for toll-like receptor (TLR) signaling, suggesting the activation of innate immune pathways [29]. *Il1b* encodes a key pro-inflammatory cytokine that promotes immune activation and tissue injury post stroke [29, 149]. *Lcn2* is linked to neutrophil activation and acute phase responses in neuroinflammatory

conditions [150], while *Cxcl2* is a chemokine that promotes recruitment of neutrophils and other myeloid cells to the region of injury [29].

Several negative regulators of inflammatory signaling were upregulated as well, including *Il1rn*, *Socs3*, *Tnfaip3*, *Nfkbia* and *Nfkbie*. These genes encode classical feedback inhibitors of cytokine and NF-κB dependent pathways. *Il1rn* produces the interleukin-1 receptor antagonist, which competes with IL-1 ligands and decreases IL-1-mediated signaling, has been shown to exert protective effects in stroke [151]. *Socs3* is a central suppressor of the JAK-STAT signaling, while *Tnfaip3* (A20) directly inhibits NF-κB activation. Both *Nfkbia* and *Nfkbie* encode inhibitory proteins that prevent nuclear translocation of NF-κB transcription factors. These feedback mechanisms are essential for limiting inflammatory responses and preventing excessive immune activation [152, 153].

In addition, genes associated with alternative and reparative myeloid activation states were upregulated as well, including *Chil3*, *Arg1*, *Lgals3*, *Mrc1*, *Lpl* and *Stab1*. These genes are associated with phagocytosis, lipid handling, debris clearance and tissue remodeling. *Chil3* and *Arg1* are classical markers of reparative macrophages, while *Mrc1* (CD206) and *Lgals3* are associated with enhanced phagocytosis and tissue remodeling after brain injury [40]. Such reparative macrophage and microglial states are known to limit excessive inflammation while promoting structural recovery [40, 154, 155].

The upregulation of inflammatory mediators, regulatory feedback inhibitors and reparative gene programs suggests that the immune cells in the AAV-BR1-CD73-treated animals adopt a coordinated activation state rather than an uncontrolled pro-inflammatory profile. Such mixed transcriptional programs are characteristic of myeloid cells post stroke as they have to counterbalance the complex neuroinflammatory response [29, 30]. While some of these molecules, such as *Il1b*, *Tnf*, *Mmp8* and *Mmp19*, may also contribute to tissue damage, they also play an important role in extracellular matrix remodeling and repair post stroke [21, 156, 157].

The transcriptional analysis of infiltrating immune cells suggests that endothelial CD73 expression does not simply dampen immune activation or prevent infiltration into the brain parenchyma after stroke but rather initiates a shift in immune cells activation and feedback

regulators. This aligns with previous studies showing that monocytes and macrophages undergo extensive context-dependent reprogramming after entering the ischemic brain [158]. It also aligns with the concept of adenosine generated via the CD39 / CD73 cascade, that might counterbalance pro-inflammatory cytokines production while promoting resolution [68, 140, 159].

Flow cytometry analysis demonstrated an increased infiltration of monocytes / macrophages in AAV-BR1-CD73-treated animals. This would also explain the upregulation of “M2-like” associated properties such as phagocytosis, debris clearance and tissue protection, observed in the transcriptional analysis. This observation further supports that adenosine signaling promotes resolution and repair, as well as that the ATP-adenosine axis is a key regulator of neuroinflammation and stroke outcome [74, 108].]. So, the combined transcriptomic and FACS data suggest that endothelial CD73 expression alters the immune response rather than just the number of infiltrating cells.

However, these interpretations must be considered with caution. The immune transcriptomic analyses were performed using bulk RNA sequencing, which averages gene expression across heterogeneous cell populations. As a result, it is not possible to definitively assign specific transcriptional programs to distinct immune cell populations and subpopulations nor to directly confirm polarization towards “M2-like” macrophage and microglia. Therefore, while the data of this study support the hypothesis that endothelial CD73 promotes a more regulated and reparative immune response post stroke, these conclusions remain largely speculative. Approaches, such as single-cell or single-nucleus RNA sequencing, are required in order to identify immune cell subtypes and activation states responsible for the observed protective effect.

4.4. Implications for translational stroke research and human relevance

The data presented in this study demonstrate that increasing extracellular adenosine via the CD39/CD73 axis CD73 in the brain endothelium has huge implications on the outcome of stroke. Although this study does not answer the question of why two enzymes with such a fundamental impact on the immune response (CD39 & CD73) are expressed reciprocally when comparing the BBB of humans ($CD39^{low}$/ $CD73^{high}$) and mice ($CD39^{high}$/$CD73^{low}$), it demonstrates the huge therapeutic potential of boosting the conversion of extracellular ATP

into adenosine in ischemic stroke. From a therapeutic perspective, the endothelium offers several practical advantages as a target. The luminal surface of brain endothelial cells is accessible through the bloodstream, meaning that systemic administration, as shown in this study, can manipulate vascular signaling pathways and interactions without the need of invasive strategies. While the AAV-BR1-CD73 vector used in this study provides a powerful experimental tool to enhance endothelial CD73 expression in mice selectively, the AAV-mediated delivery of CD73 or CD39 is unlikely in a clinical setting of acute stroke in humans, as AAV-based gene delivery requires too much time for transgene expression.

Nevertheless, the present findings offer important mechanistic insights and support the development of targeted delivery of CD73, or even together with CD39, using nanobody-based approaches that allow rapid and transient expression. This study provides proof of principle that selective (over)expression of endothelial CD73 can influence stroke outcome and strengthen the BBB as a promising therapeutic target in ischemic stroke.

4.5. Limitations of the study

The relatively small number of biological replicates used for transcriptomic analyses constitutes another limitation of this study. The data revealed consistent trends and allowed the identification of related pathways, yet the sample size might increase the masking of other more subtle DEGs and reduce the statistical power. Also the lack of depletion of macrophages, which would be required to directly test whether the observed "M2-like" macrophage population contributes to the protective effects associated with endothelial CD73 expression, is missing in this study.

Another limitation of this study is the focus on the late acute phase of stroke, with outcome analyses performed at 48 hours after tMCAO. While this time point allows the evaluation of early infarct development, acute survival and initial immune responses, it does not investigate the intermediate and long-term effects of endothelial CD73 expression [160, 161]. Stroke pathology evolves over days to weeks and involves secondary inflammatory processes, tissue remodeling, angiogenesis and functional recovery. It therefore remains unclear whether the strong protective effects observed in the acute phase will persist, diminish or change over time.

Additional limitation is the exclusive use of male mice. There are significant sex-dependent differences in stroke pathophysiology that have been observed, which may affect stroke severity and recovery [162-164]. These differences are due to hormonal regulations, immune responses, vascular functions and gene expressions that differ between the two genders. For example, estrogen-dependent signaling has been shown to modulate vascular integrity and immune cell activation [165]. The current study was also only performed in young adult mice, although stroke primarily affects older patients. Therefore, follow-up studies are needed to evaluate the effects of CD73 expression at the BBB at later time-points, in both female and male mice of different ages. All these factors can influence infarct size, immune response and recovery. It will therefore be necessary to determine whether the protective effects of endothelial CD73 are observed across these biologically relevant conditions and whether certain patient groups may benefit more strongly than others [166-168].It is important to emphasize that the present study was designed to focus on a single sex in order to reduce biological variability and limit the number of mice required for statistical analyses under the 3R values. Using only male mice allowed a more controlled assessment of the direct effects of endothelial CD73 expression on stroke outcome, without additional variability from hormonal cycling or sex-dependent immune responses.

4.6. Future directions

Given the ambiguous bulk RNAseq data generated so far, single-cell or single-nucleus RNA sequencing should be performed to assess the transcriptional changes of the brain endothelium and the composition of the immune cell compartment in more detail.

The downstream mechanism of CD73 expression in the BBB in stroke also needs to be investigated further. Identifying which adenosine receptor or receptors may show an altered activation under this experimental conditions will prove essential to further understand this protective effect and reveal even more purinergic signaling-related therapeutic targets.

From a translational aspect, future work should focus on nanobodies that target endothelial cells and enable the overexpression of CD73 or CD39, which would be the less expressed counterpart of CD73 in humans. It is also interesting to investigate the potential therapeutic effect of the overexpression of both CD39 and CD73. Furthermore, the combination of named

nanobodies in combination with established reperfusion therapies may prove to enhance protection and resolution even more. The study of potential systemic side-effects would also be essential in order to avoid peripheral damage.

5. Summary

5.1. Summary (English, one page)

Ischemic stroke remains one of the leading causes of death and neurological disability worldwide. Despite the development of current treatment options, many patients continue to suffer from chronic neurological and psychological impairments. During ischemic stroke, the sudden interruption of blood supply leads to deprivation of oxygen and nutrients in the affected brain region. This results in disruption of BBB and the development of secondary injury. The breakdown of the blood-brain barrier (BBB) enables the infiltration of peripheral immune cells into the brain, which contributes to a complex neuroinflammatory response. Ischemic injury also triggers the release and accumulation of extracellular ATP, creating a strongly pro-inflammatory environment that can further exacerbate tissue damage. Within the purinergic signaling cascade, extracellular ATP can be degraded to ADP and AMP by CD39, while CD73 subsequently converts AMP into adenosine. In contrast to ATP, adenosine exerts anti-inflammatory and tissue protective effects.

In mice, CD73 expression in brain endothelial cells is relatively low compared to humans and in order to address this limitation, the AAV-BR1-CD73 vector was generated to enable targeted expression of CD73 in the brain endothelium of mice.

The aim of this study was therefore to investigate whether targeted endothelial expression of CD73 in mice could positively influence stroke outcome. Initially, *in vitro* experiments were performed to validate AAV-mediated CD73 expression and to confirm the enzymatic activity of CD73 by demonstrating its ability to degrade AMP. Then, *in vivo* experiments were conducted to determine the best suitable AAV dose that achieved efficient expression without inducing side effects such as hepatotoxicity.

Finally, the effect of endothelial CD73 expression was investigated in the murine stroke model of transient middle cerebral artery occlusion (tMCAO). Mice were systemically injected with either AAV-BR1-CD73 or a control vector, AAV-BR1-empty, which contains the same capsid but lacks a transgene. Using magnetic resonance imaging (MRI) and flow cytometry, endothelial CD73 expression was found to be associated with reduced infarct sizes, improved survival and altered recruitment of immune cells in the ischemic brain.

To further investigate the underlying mechanisms, transcriptomic analysis of isolated immune cells after tMCAO was performed. These analyses revealed alterations in immune related signaling pathways, suggesting that endothelial CD73 expression influences the post ischemic immune response.

Overall, this study demonstrates that adenosine generated via CD73 acts as an active regulator of immune responses following ischemic stroke. These findings highlight the importance of purinergic signaling at the BBB and suggests that the purinergic signaling at the BBB represents indeed a promising therapeutic target for stroke.

5.2. Zusammenfassung (German, one page)

Der ischämische Schlaganfall zählt weiterhin zu den häufigsten Ursachen für Tod und neurologische Behinderungen weltweit. Trotz der Entwicklung moderner Behandlungsmöglichkeiten leiden viele Patientinnen und Patienten weiterhin unter langfristigen neurologischen und psychischen Einschränkungen. Beim ischämischen Schlaganfall führt die plötzliche Unterbrechung der Blutversorgung zu einem Mangel an Sauerstoff und Nährstoffen in der betroffenen Hirnregion. Dies führt zu einer Störung der Blut-Hirn-Schranke (BBB) und zur Entstehung sekundärer Gewebeschäden. Der Zusammenbruch der Blut-Hirn-Schranke ermöglicht das Eindringen peripherer Immunzellen in das Gehirn, was zu einer komplexen neuroinflammatorischen Reaktion beiträgt. Darüber hinaus führt die ischämische Schädigung zur Freisetzung und Akkumulation von extrazellulärem ATP, wodurch ein stark proinflammatorisches Milieu entsteht, das die Gewebeschädigung weiter verstärken kann. Innerhalb der purinergen Signalkaskade kann extrazelluläres ATP durch das Enzym CD39 zu ADP und anschließend zu AMP abgebaut werden, während CD73 AMP weiter zu Adenosin umwandelt. Im Gegensatz zu ATP besitzt Adenosin antiinflammatorische und gewebeschützende Eigenschaften.

Bei Mäusen ist die Expression von CD73 in Gehirnendothelzellen im Vergleich zum Menschen relativ gering ausgeprägt. Um diese Limitation zu adressieren, wurde der Vektor AAV-BR1-CD73 entwickelt, der eine gezielte Expression von CD73 im Gehirnendothel von Mäusen ermöglicht.

Ziel dieser Studie war es daher zu untersuchen, ob eine gezielte endotheliale Expression von CD73 bei Mäusen den Ausgang eines Schlaganfalls positiv beeinflussen kann. Zunächst wurden in vitro Experimente durchgeführt, um die AAV-vermittelte Expression von CD73 zu validieren und die enzymatische Aktivität von CD73 durch den Nachweis des AMP-Abbaus zu bestätigen. Anschließend wurden in vivo Experimente durchgeführt, um eine geeignete AAV-Dosis zu bestimmen, die eine effiziente Expression ermöglicht, ohne Nebenwirkungen wie beispielsweise Hepatotoxizität zu verursachen.

Schließlich wurde der Effekt der endothelialen CD73-Expression im murinen Schlaganfallmodell der transienten Okklusion der Arteria cerebri media (tMCAO) untersucht. Die Mäuse wurden systemisch entweder mit AAV-BR1-CD73 oder mit einem Kontrollvektor, AAV-BR1-empty, injiziert, der das gleiche Kapsid enthält, jedoch kein Transgen trägt. Mithilfe von Magnetresonanztomographie (MRT) und Durchflusszytometrie konnte gezeigt werden, dass die endotheliale CD73-Expression mit kleineren Infarktgrößen, verbessertem Überleben sowie einer veränderten Rekrutierung von Immunzellen im ischämischen Gehirn assoziiert war. Um die zugrunde liegenden Mechanismen weiter zu untersuchen, wurde eine transkriptomische Analyse isolierter Immunzellen nach tMCAO durchgeführt. Diese Analysen zeigten Veränderungen in immunrelevanten Signalwegen und legen nahe, dass die endotheliale CD73-Expression die Immunantwort nach ischämischem Schlaganfall beeinflusst.

Insgesamt zeigt diese Studie, dass durch CD73 generiertes Adenosin als aktiver Regulator von Immunantworten nach ischämischem Schlaganfall wirkt. Diese Ergebnisse unterstreichen die Bedeutung der purinergen Signalübertragung an der Blut-Hirn-Schranke und deuten darauf

hin, dass diese einen vielversprechenden therapeutischen Ansatz für die Behandlung des Schlaganfalls darstellen könnte.

6. List of Abbreviations

AAV - Adeno-associated virus

AF700 - Alexa Fluor 700

AMP - Adenosine monophosphate

APC - Allophycocyanin

Arg1 - Arginase 1

ATP - Adenosine triphosphate

BAMs - Border-associated macrophages

b-actin - Beta-actin

bEND.3 - Mouse brain endothelial cell line

B220 - B cell marker (CD45R)

BBB - Blood-brain barrier

BCA - Bicinchoninic acid

BSA - Bovine serum albumin

bGHpA - Bovine growth hormone polyadenylation signal

BMDC - Bone marrow-derived cells

BUV395 - Brilliant Ultraviolet 395

BUV737 - Brilliant Ultraviolet 737

BV605 - Brilliant Violet 605

BV650 - Brilliant Violet 650

BV710 - Brilliant Violet 710

BV785 - Brilliant Violet 785

CAG - Cytomegalovirus early enhancer/chicken β-actin promoter

CCA - Common carotid artery

cDNA - Complementary deoxyribonucleic acid

CD4 - Cluster of differentiation 4

CD6 - Cluster of differentiation 6

CD14 - Cluster of differentiation 14

CD31 - Cluster of differentiation 31

CD39 - Ectonucleoside triphosphate diphosphohydrolase 1

CD45 - Cluster of differentiation 45

CD73 - Ecto-5'-nucleotidase

Chil3 - Chitinase-like protein 3

CMV - Cytomegalovirus promoter

CNS - Central nervous system

Csf3r - Colony-stimulating factor 3 receptor

Ct - Cycle threshold

Cxcl2 - C-X-C motif chemokine ligand 2

DAMP - Damage-associated molecular pattern

DEG - Differentially expressed gene

DNA - Deoxyribonucleic acid

DNBs - DNA nanoballs

DNBSEQ - DNA nanoball sequencing platform

DPBS - Dulbecco's phosphate-buffered saline

DWI - Diffusion-weighted imaging

EC - Endothelial cell

ECG - Electrocardiogram

ECM - Extracellular matrix

EDTA - Ethylenediaminetetraacetic acid

ECA - External carotid artery

ESI - Electrospray ionization

F10 - Coagulation factor X

F4/80 - Mouse macrophage marker

FACS - Fluorescence-activated cell sorting

FBS - Fetal bovine serum

FDR - False discovery rate

FITC - Fluorescein isothiocyanate

Gb - Gigabase

GO - Gene ontology

HBMEC - Human brain microvascular endothelial cell

HEK - Human embryonic kidney

HEK 293T - Human embryonic kidney 293T cells

HIF-1α - Hypoxia-inducible factor 1 alpha

HILIC - Hydrophilic interaction liquid chromatography

HPLC - High-performance liquid chromatography

ICA - Internal carotid artery

IFN-γ - Interferon gamma

IL - Interleukin

IL-1 - Interleukin 1

IL-17 - Interleukin 17

Il1b - Interleukin 1 beta

Il1rn - Interleukin 1 receptor antagonist

ITR - Inverted terminal repeat

ITRs - Inverted terminal repeats

kDa - Kilodalton

LC-MS/MS - Liquid chromatography-tandem mass spectrometry

Lcn2 - Lipocalin 2

Lgals3 - Galectin 3

log2FC - Log2 fold change

Lpl - Lipoprotein lipase

Ly6G - Lymphocyte antigen 6 complex, locus G

MACS - Magnetic-activated cell sorting

MCA - Middle cerebral artery

MCAO – Middle cerebral artery occlusion

mBMEC - Mouse brain microvascular endothelial cell

Mefv - Mediterranean fever gene

MHC II - Major histocompatibility complex class II

Mmp8 - Matrix metalloproteinase 8

Mmp19 - Matrix metalloproteinase 19

MOI - Multiplicity of infection

MRM - Multiple reaction monitoring

Mrc1 - Mannose receptor C-type 1

MRI - Magnetic resonance imaging

mRNA - Messenger ribonucleic acid

Near-IR - Near infrared

NETs - Neutrophil extracellular traps

NF-κB - Nuclear factor kappa B

Nfkbia - NF-κB inhibitor alpha

Nfkbie - NF-κB inhibitor epsilon

NK - Natural killer (cells)

NK cell - Natural killer cell

NK1.1 - Natural killer cell marker 1.1

OPCs - Oligodendrocyte precursor cells

P1 - Adenosine (P1) receptor family

P2X - Ionotropic purinergic receptor family

P2Y - Metabotropic purinergic receptor family

P2Y12 - Purinergic receptor P2Y12

PBS - Phosphate-buffered saline

PBS-MK - Phosphate-buffered saline supplemented with magnesium and potassium ions

PCR - Polymerase chain reaction

PE150 - Paired-end 150 base pair sequencing

PerCP-Cy5.5 - Peridinin-chlorophyll protein-Cyanine 5.5

pFastBac1 - Baculovirus transfer vector plasmid

qPCR - Quantitative polymerase chain reaction

Rep/Cap - Replication and capsid genes

RNA - Ribonucleic acid

RNA-seq - RNA sequencing

ROS - Reactive oxygen species

RT - Room temperature

S100a8 - S100 calcium-binding protein A8

S100a9 - S100 calcium-binding protein A9

Saa3 - Serum amyloid A3

SCIEX - SCIEX mass spectrometry platform

scRNA - Single-cell RNA

scRNA-seq - Single-cell RNA sequencing

SEM - Standard error of the mean

Sf9 cells - Spodoptera frugiperda insect cells

SMA - Spinal muscular atrophy

SMN1 - Survival motor neuron 1

snRNA - Single-nucleus RNA

Socs3 - Suppressor of cytokine signaling 3

SPF - Specific pathogen-free

Stab1 - Stabilin 1

T cell - T lymphocyte

TCRgd - Gamma delta T-cell receptor

TGF - Transforming growth factor

Th1 - T helper type 1 cells

Th17 - T helper type 17 cells

tMCAO - Transient middle cerebral artery occlusion

TLR - Toll-like receptor

TNF - Tumor necrosis factor

TNF-α - Tumor necrosis factor alpha

Tnfaip3 - TNF alpha-induced protein 3

Tregs - Regulatory T cells

Tris - Tris(hydroxymethyl)aminomethane

vg - Viral genome

vg/dg - Viral genomes per diploid genome

vs. - Versus

Wfdc17 - WAP four-disulfide core domain protein 17

WPRE - Woodchuck hepatitis virus posttranscriptional regulatory element

γδ T cells - Gamma delta T cells

7. References

1. Feigin, V.L., et al., *World Stroke Organization: Global Stroke Fact Sheet 2025.* Int J Stroke, 2025. **20**(2): p. 132-144.
2. Markus, H.S., *The global burden of stroke.* International Journal of Stroke, 2023. **18**(6): p. 632-633.
3. Li, X.Y., et al., *Global, regional, and national burden of ischemic stroke, 1990-2021: an analysis of data from the global burden of disease study 2021.* EClinicalMedicine, 2024. **75**: p. 102758.
4. Fan, J., et al., *Global Burden, Risk Factor Analysis, and Prediction Study of Ischemic Stroke, 1990-2030.* Neurology, 2023. **101**(2): p. e137-e150.
5. Katan, M. and A. Luft, *Global Burden of Stroke.* Semin Neurol, 2018. **38**(2): p. 208-211.
6. *Global, regional, and national burden of stroke and its risk factors, 1990-2021: a systematic analysis for the Global Burden of Disease Study 2021.* Lancet Neurol, 2024. **23**(10): p. 973-1003.
7. Quinn, T., et al., *A Systematic Literature Review on the Burden of Disease for Patients With Moderate to Severe Acute Ischemic Stroke.* Medicine (Baltimore), 2025. **104**(3): p. e41249.
8. Zhou, J., et al., *A systematic review and meta-analysis of health utility values among patients with ischemic stroke.* Front Neurol, 2023. **14**: p. 1219679.
9. *Tissue plasminogen activator for acute ischemic stroke.* N Engl J Med, 1995. **333**(24): p. 1581-7.
10. Raha, O., et al., *Advances in mechanical thrombectomy for acute ischaemic stroke.* BMJ Med, 2023. **2**(1): p. e000407.
11. Pinter, D., et al., *Relevance of Cognition and Emotion for Patient-Reported Quality of Life After Stroke in Working Age: An Observational Cohort Study.* Front Neurol, 2022. **13**: p. 869550.
12. Kusec, A., et al., *Long-term psychological outcomes following stroke: the OX-CHRONIC study.* BMC Neurol, 2023. **23**(1): p. 426.
13. Liu, L., et al., *Prevalence and natural history of depression after stroke: A systematic review and meta-analysis of observational studies.* PLoS Med, 2023. **20**(3): p. e1004200.
14. Sweeney, M.D., et al., *Blood-Brain Barrier: From Physiology to Disease and Back.* Physiol Rev, 2019. **99**(1): p. 21-78.
15. Nian, K., et al., *Blood-Brain Barrier Damage in Ischemic Stroke and Its Regulation by Endothelial Mechanotransduction.* Front Physiol, 2020. **11**: p. 605398.
16. Obermeier, B., R. Daneman, and R.M. Ransohoff, *Development, maintenance and disruption of the blood-brain barrier.* Nat Med, 2013. **19**(12): p. 1584-96.
17. McConnell, H.L., et al., *The Translational Significance of the Neurovascular Unit.* J Biol Chem, 2017. **292**(3): p. 762-770.
18. Armulik, A., et al., *Pericytes regulate the blood-brain barrier.* Nature, 2010. **468**(7323): p. 557-61.
19. Iadecola, C., *The Neurovascular Unit Coming of Age: A Journey through Neurovascular Coupling in Health and Disease.* Neuron, 2017. **96**(1): p. 17-42.
20. Wang, L., et al., *Neurovascular Unit: A critical role in ischemic stroke.* CNS Neurosci Ther, 2021. **27**(1): p. 7-16.

21. Sorokin, L., *The impact of the extracellular matrix on inflammation.* Nat Rev Immunol, 2010. **10**(10): p. 712-23.
22. Daneman, R. and A. Prat, *The blood-brain barrier.* Cold Spring Harb Perspect Biol, 2015. **7**(1): p. a020412.
23. Sandoval, K.E. and K.A. Witt, *Blood-brain barrier tight junction permeability and ischemic stroke.* Neurobiol Dis, 2008. **32**(2): p. 200-19.
24. Knowland, D., et al., *Stepwise recruitment of transcellular and paracellular pathways underlies blood-brain barrier breakdown in stroke.* Neuron, 2014. **82**(3): p. 603-17.
25. Jin, R., G. Yang, and G. Li, *Molecular insights and therapeutic targets for blood-brain barrier disruption in ischemic stroke: critical role of matrix metalloproteinases and tissue-type plasminogen activator.* Neurobiol Dis, 2010. **38**(3): p. 376-85.
26. del Zoppo, G.J., *The neurovascular unit in the setting of stroke.* J Intern Med, 2010. **267**(2): p. 156-71.
27. Engelhardt, B. and R.M. Ransohoff, *Capture, crawl, cross: the T cell code to breach the blood-brain barriers.* Trends Immunol, 2012. **33**(12): p. 579-89.
28. Engelhardt, B., P. Vajkoczy, and R.O. Weller, *The movers and shapers in immune privilege of the CNS.* Nat Immunol, 2017. **18**(2): p. 123-131.
29. Iadecola, C. and J. Anrather, *The immunology of stroke: from mechanisms to translation.* Nat Med, 2011. **17**(7): p. 796-808.
30. Chamorro, Á., et al., *The immunology of acute stroke.* Nat Rev Neurol, 2012. **8**(7): p. 401-10.
31. Hu, X., et al., *Microglia/macrophage polarization dynamics reveal novel mechanism of injury expansion after focal cerebral ischemia.* Stroke, 2012. **43**(11): p. 3063-70.
32. Ransohoff, R.M. and B. Engelhardt, *The anatomical and cellular basis of immune surveillance in the central nervous system.* Nat Rev Immunol, 2012. **12**(9): p. 623-35.
33. Prinz, M. and J. Priller, *Microglia and brain macrophages in the molecular age: from origin to neuropsychiatric disease.* Nat Rev Neurosci, 2014. **15**(5): p. 300-12.
34. Ginhoux, F., et al., *Fate mapping analysis reveals that adult microglia derive from primitive macrophages.* Science, 2010. **330**(6005): p. 841-5.
35. Ajami, B., et al., *Local self-renewal can sustain CNS microglia maintenance and function throughout adult life.* Nat Neurosci, 2007. **10**(12): p. 1538-43.
36. Nimmerjahn, A., F. Kirchhoff, and F. Helmchen, *Resting microglial cells are highly dynamic surveillants of brain parenchyma in vivo.* Science, 2005. **308**(5726): p. 1314-8.
37. Eggen, B.J., et al., *Microglial phenotype and adaptation.* J Neuroimmune Pharmacol, 2013. **8**(4): p. 807-23.
38. Salter, M.W. and B. Stevens, *Microglia emerge as central players in brain disease.* Nat Med, 2017. **23**(9): p. 1018-1027.
39. Berns, K.I., *Parvovirus replication.* Microbiol Rev, 1990. **54**(3): p. 316-29.
40. Cherry, J.D., J.A. Olschowka, and M.K. O'Banion, *Neuroinflammation and M2 microglia: the good, the bad, and the inflamed.* J Neuroinflammation, 2014. **11**: p. 98.
41. Van Hove, H., et al., *A single-cell atlas of mouse brain macrophages reveals unique transcriptional identities shaped by ontogeny and tissue environment.* Nat Neurosci, 2019. **22**(6): p. 1021-1035.
42. Prinz, M., D. Erny, and N. Hagemeyer, *Ontogeny and homeostasis of CNS myeloid cells.* Nat Immunol, 2017. **18**(4): p. 385-392.
43. Goldmann, T., et al., *Origin, fate and dynamics of macrophages at central nervous system interfaces.* Nat Immunol, 2016. **17**(7): p. 797-805.
44. Sofroniew, M.V. and H.V. Vinters, *Astrocytes: biology and pathology.* Acta Neuropathol, 2010. **119**(1): p. 7-35.

45. Liddelow, S.A. and B.A. Barres, *Reactive Astrocytes: Production, Function, and Therapeutic Potential.* Immunity, 2017. **46**(6): p. 957-967.
46. Sofroniew, M.V., *Molecular dissection of reactive astrogliosis and glial scar formation.* Trends Neurosci, 2009. **32**(12): p. 638-47.
47. Anrather, J. and C. Iadecola, *Inflammation and Stroke: An Overview.* Neurotherapeutics, 2016. **13**(4): p. 661-670.
48. Jayaraj, R.L., et al., *Neuroinflammation: friend and foe for ischemic stroke.* J Neuroinflammation, 2019. **16**(1): p. 142.
49. Gelderblom, M., et al., *Temporal and spatial dynamics of cerebral immune cell accumulation in stroke.* Stroke, 2009. **40**(5): p. 1849-57.
50. Denorme, F., et al., *Neutrophil extracellular traps regulate ischemic stroke brain injury.* J Clin Invest, 2022. **132**(10).
51. Ren, T., et al., *Targeting microglial PPARα ameliorates the outcome of ischemic stroke by enhancing interaction with infiltrating peripheral monocytes/macrophages.* Cell Rep, 2025. **44**(7): p. 115875.
52. Chen, S., et al., *Macrophages in immunoregulation and therapeutics.* Signal Transduct Target Ther, 2023. **8**(1): p. 207.
53. Han, D., H. Liu, and Y. Gao, *The role of peripheral monocytes and macrophages in ischemic stroke.* Neurol Sci, 2020. **41**(12): p. 3589-3607.
54. Dufort, C., et al., *Monocyte-derived macrophages and their roles in ischemic stroke.* J Cereb Blood Flow Metab, 2026: p. 271678x251414082.
55. Liesz, A., et al., *Regulatory T cells are key cerebroprotective immunomodulators in acute experimental stroke.* Nat Med, 2009. **15**(2): p. 192-9.
56. Telec, M., et al., *Circulating CD4+, CD8+, and double-negative T cells in ischemic stroke and stroke-associated infection: a prospective case-control study.* Front Cell Neurosci, 2025. **19**: p. 1547905.
57. Shichita, T., et al., *Pivotal role of cerebral interleukin-17-producing gammadeltaT cells in the delayed phase of ischemic brain injury.* Nat Med, 2009. **15**(8): p. 946-50.
58. Piepke, M., et al., *IL-17A-producing γδ T cells: A novel target in stroke immunotherapy.* Eur J Immunol, 2024. **54**(12): p. e2451067.
59. Wang, L., et al., *γδ T Cell in Cerebral Ischemic Stroke: Characteristic, Immunity-Inflammatory Role, and Therapy.* Frontiers in Neurology, 2022. **Volume 13 - 2022**.
60. Gan, Y., et al., *Ischemic neurons recruit natural killer cells that accelerate brain infarction.* Proc Natl Acad Sci U S A, 2014. **111**(7): p. 2704-9.
61. Burnstock, G., *Purinergic Signalling: Therapeutic Developments.* Front Pharmacol, 2017. **8**: p. 661.
62. Idzko, M., D. Ferrari, and H.K. Eltzschig, *Nucleotide signalling during inflammation.* Nature, 2014. **509**(7500): p. 310-7.
63. Wang, L., et al., *Purinergic signaling: a potential therapeutic target for ischemic stroke.* Purinergic Signal, 2023. **19**(1): p. 173-183.
64. Cisneros-Mejorado, A., et al., *Purinergic signaling in Stroke and Multiple Sclerosis: Prospects for therapies.* Neuropharmacology, 2026. **284**: p. 110783.
65. Di Virgilio, F., et al., *The P2X7 Receptor in Infection and Inflammation.* Immunity, 2017. **47**(1): p. 15-31.
66. Xu, W., Y. Huang, and R. Zhou, *NLRP3 inflammasome in neuroinflammation and central nervous system diseases.* Cell Mol Immunol, 2025. **22**(4): p. 341-355.
67. Rivera, A., I. Vanzulli, and A.M. Butt, *A Central Role for ATP Signalling in Glial Interactions in the CNS.* Curr Drug Targets, 2016. **17**(16): p. 1829-1833.
68. Antonioli, L., et al., *CD39 and CD73 in immunity and inflammation.* Trends Mol Med, 2013. **19**(6): p. 355-67.

69. Zimmermann, H., M. Zebisch, and N. Sträter, *Cellular function and molecular structure of ecto-nucleotidases.* Purinergic Signal, 2012. **8**(3): p. 437-502.
70. Lee, N.T., et al., *Role of Purinergic Signalling in Endothelial Dysfunction and Thrombo-Inflammation in Ischaemic Stroke and Cerebral Small Vessel Disease.* Biomolecules, 2021. **11**(7).
71. Gratal, P., et al., *Purinergic System Signaling in Metainflammation-Associated Osteoarthritis.* Frontiers in Medicine, 2020. **Volume 7 - 2020**.
72. Wang, Y., et al., *Purinergic signaling: A gatekeeper of blood-brain barrier permeation.* Front Pharmacol, 2023. **14**: p. 1112758.
73. Eltzschig, H.K., M.V. Sitkovsky, and S.C. Robson, *Purinergic signaling during inflammation.* N Engl J Med, 2012. **367**(24): p. 2322-33.
74. Haskó, G. and B.N. Cronstein, *Adenosine: an endogenous regulator of innate immunity.* Trends Immunol, 2004. **25**(1): p. 33-9.
75. Wala, K., et al., *Modulation of Blood-Brain Barrier Permeability by Activating Adenosine A2 Receptors in Oncological Treatment.* Biomolecules, 2021. **11**(5).
76. Kim, D.G. and M.S. Bynoe, *A2A adenosine receptor modulates drug efflux transporter P-glycoprotein at the blood-brain barrier.* J Clin Invest, 2016. **126**(5): p. 1717-33.
77. Shen, J., et al., *CD39 and CD73: biological functions, diseases and therapy.* Mol Biomed, 2025. **6**(1): p. 97.
78. Koziak, K., et al., *Analysis of CD39/ATP diphosphohydrolase (ATPDase) expression in endothelial cells, platelets and leukocytes.* Thromb Haemost, 1999. **82**(5): p. 1538-44.
79. Synnestvedt, K., et al., *Ecto-5'-nucleotidase (CD73) regulation by hypoxia-inducible factor-1 mediates permeability changes in intestinal epithelia.* J Clin Invest, 2002. **110**(7): p. 993-1002.
80. Colgan, S.P., et al., *Physiological roles for ecto-5'-nucleotidase (CD73).* Purinergic Signal, 2006. **2**(2): p. 351-60.
81. Regateiro, F.S., S.P. Cobbold, and H. Waldmann, *CD73 and adenosine generation in the creation of regulatory microenvironments.* Clin Exp Immunol, 2013. **171**(1): p. 1-7.
82. Schädlich, I.S., et al., *Nt5e deficiency does not affect post-stroke inflammation and lesion size in a murine ischemia/reperfusion stroke model.* iScience, 2022. **25**(6): p. 104470.
83. Feoktistov, I. and I. Biaggioni, *Role of adenosine A(2B) receptors in inflammation.* Adv Pharmacol, 2011. **61**: p. 115-44.
84. Thompson, L.F., et al., *Crucial role for ecto-5'-nucleotidase (CD73) in vascular leakage during hypoxia.* J Exp Med, 2004. **200**(11): p. 1395-405.
85. Eltzschig, H.K., S.K. Bonney, and T. Eckle, *Attenuating myocardial ischemia by targeting A2B adenosine receptors.* Trends Mol Med, 2013. **19**(6): p. 345-54.
86. Zhang, X., et al., *Hypoxia-inducible factor-1alpha protects the liver against ischemia-reperfusion injury by regulating the A2B adenosine receptor.* Bioengineered, 2021. **12**(1): p. 3737-3752.
87. Sixt, M., et al., *Endothelial cell laminin isoforms, laminins 8 and 10, play decisive roles in T cell recruitment across the blood-brain barrier in experimental autoimmune encephalomyelitis.* J Cell Biol, 2001. **153**(5): p. 933-46.
88. Atchison, R.W., B.C. Casto, and W.M. Hammon, *ADENOVIRUS-ASSOCIATED DEFECTIVE VIRUS PARTICLES.* Science, 1965. **149**(3685): p. 754-6.
89. Berns, K.I. and C. Giraud, *Biology of adeno-associated virus.* Curr Top Microbiol Immunol, 1996. **218**: p. 1-23.

90. Daya, S. and K.I. Berns, *Gene therapy using adeno-associated virus vectors.* Clin Microbiol Rev, 2008. **21**(4): p. 583-93.
91. Naso, M.F., et al., *Adeno-Associated Virus (AAV) as a Vector for Gene Therapy.* BioDrugs, 2017. **31**(4): p. 317-334.
92. Kaplitt, M.G., et al., *Safety and tolerability of gene therapy with an adeno-associated virus (AAV) borne GAD gene for Parkinson's disease: an open label, phase I trial.* Lancet, 2007. **369**(9579): p. 2097-105.
93. Wu, Z., A. Asokan, and R.J. Samulski, *Adeno-associated virus serotypes: vector toolkit for human gene therapy.* Mol Ther, 2006. **14**(3): p. 316-27.
94. Asokan, A., D.V. Schaffer, and R.J. Samulski, *The AAV vector toolkit: poised at the clinical crossroads.* Mol Ther, 2012. **20**(4): p. 699-708.
95. Foust, K.D., et al., *Intravascular AAV9 preferentially targets neonatal neurons and adult astrocytes.* Nat Biotechnol, 2009. **27**(1): p. 59-65.
96. Mendell, J.R., et al., *Single-Dose Gene-Replacement Therapy for Spinal Muscular Atrophy.* N Engl J Med, 2017. **377**(18): p. 1713-1722.
97. Wang, D., P.W.L. Tai, and G. Gao, *Adeno-associated virus vector as a platform for gene therapy delivery.* Nat Rev Drug Discov, 2019. **18**(5): p. 358-378.
98. Kwon, J.M., et al., *Intrathecal onasemnogene abeparvovec for treatment-experienced patients with spinal muscular atrophy: a phase 3b, open-label trial.* Nat Med, 2025.
99. Deverman, B.E., et al., *Cre-dependent selection yields AAV variants for widespread gene transfer to the adult brain.* Nat Biotechnol, 2016. **34**(2): p. 204-9.
100. Körbelin, J., et al., *A brain microvasculature endothelial cell-specific viral vector with the potential to treat neurovascular and neurological diseases.* EMBO Molecular Medicine, 2016. **8**(6): p. 609-625.
101. Hudry, E. and L.H. Vandenberghe, *Therapeutic AAV Gene Transfer to the Nervous System: A Clinical Reality.* Neuron, 2019. **101**(5): p. 839-862.
102. Abbott, N.J., L. Rönnbäck, and E. Hansson, *Astrocyte-endothelial interactions at the blood-brain barrier.* Nat Rev Neurosci, 2006. **7**(1): p. 41-53.
103. Maheshri, N., et al., *Directed evolution of adeno-associated virus yields enhanced gene delivery vectors.* Nat Biotechnol, 2006. **24**(2): p. 198-204.
104. Kotterman, M.A. and D.V. Schaffer, *Engineering adeno-associated viruses for clinical gene therapy.* Nat Rev Genet, 2014. **15**(7): p. 445-51.
105. Marsic, D., et al., *Vector design Tour de Force: integrating combinatorial and rational approaches to derive novel adeno-associated virus variants.* Mol Ther, 2014. **22**(11): p. 1900-9.
106. Stamataki, M., et al., *Identification of AAV variants with improved transduction of human vascular endothelial cells by screening AAV capsid libraries in non-human primates.* Gene Ther, 2025. **32**(5): p. 529-541.
107. Hiefner, J., et al., *A liquid chromatography-tandem mass spectrometry based method for the quantification of adenosine nucleotides and NAD precursors and products in various biological samples.* Front Immunol, 2023. **14**: p. 1250762.
108. Schädlich, I.S., et al., *The role of the ATP-adenosine axis in ischemic stroke.* Semin Immunopathol, 2023. **45**(3): p. 347-365.
109. Lein, E.S., et al., *Genome-wide atlas of gene expression in the adult mouse brain.* Nature, 2007. **445**(7124): p. 168-76.
110. Hodge, R.D., et al., *Conserved cell types with divergent features in human versus mouse cortex.* Nature, 2019. **573**(7772): p. 61-68.
111. Di Virgilio, F., et al., *Extracellular ATP: A powerful inflammatory mediator in the central nervous system.* Neuropharmacology, 2023. **224**: p. 109333.

112. Arnaud-Sampaio, V.F., et al., *Using Cytometry for Investigation of Purinergic Signaling in Tumor-Associated Macrophages.* Cytometry A, 2020. **97**(11): p. 1109-1126.
113. Gao, H., et al., *CD73: a new immune checkpoint for leukemia treatment.* Front Immunol, 2025. **16**: p. 1486868.
114. Niemelä, J., et al., *IFN-beta regulates CD73 and adenosine expression at the blood-brain barrier.* Eur J Immunol, 2008. **38**(10): p. 2718-26.
115. Mills, J.H., et al., *Human brain endothelial cells are responsive to adenosine receptor activation.* Purinergic Signal, 2011. **7**(2): p. 265-73.
116. Airas, L., et al., *Mechanism of action of IFN-beta in the treatment of multiple sclerosis: a special reference to CD73 and adenosine.* Ann N Y Acad Sci, 2007. **1110**: p. 641-8.
117. Petrovic-Djergovic, D., et al., *Tissue-resident ecto-5' nucleotidase (CD73) regulates leukocyte trafficking in the ischemic brain.* J Immunol, 2012. **188**(5): p. 2387-98.
118. Pinsky, D.J., et al., *Elucidation of the thromboregulatory role of CD39/ectoapyrase in the ischemic brain.* J Clin Invest, 2002. **109**(8): p. 1031-40.
119. Lee, N.T., et al., *Development of endothelial-targeted CD39 as a therapy for ischemic stroke.* J Thromb Haemost, 2024. **22**(8): p. 2331-2344.
120. Fredholm, B.B., et al., *International Union of Pharmacology. XXV. Nomenclature and classification of adenosine receptors.* Pharmacol Rev, 2001. **53**(4): p. 527-52.
121. Ohta, A. and M. Sitkovsky, *Role of G-protein-coupled adenosine receptors in downregulation of inflammation and protection from tissue damage.* Nature, 2001. **414**(6866): p. 916-20.
122. Melani, A., A.M. Pugliese, and F. Pedata, *Adenosine receptors in cerebral ischemia.* Int Rev Neurobiol, 2014. **119**: p. 309-48.
123. Pedata, F., et al., *The role of ATP and adenosine in the brain under normoxic and ischemic conditions.* Purinergic Signal, 2007. **3**(4): p. 299-310.
124. Lopes Pinheiro, M.A., et al., *Immune cell trafficking across the barriers of the central nervous system in multiple sclerosis and stroke.* Biochim Biophys Acta, 2016. **1862**(3): p. 461-71.
125. Mills, J.H., et al., *CD73 is required for efficient entry of lymphocytes into the central nervous system during experimental autoimmune encephalomyelitis.* Proc Natl Acad Sci U S A, 2008. **105**(27): p. 9325-30.
126. Fredholm, B.B., *Adenosine receptors as drug targets.* Exp Cell Res, 2010. **316**(8): p. 1284-8.
127. Antonioli, L., et al., *Anti-CD73 in cancer immunotherapy: awakening new opportunities.* Trends Cancer, 2016. **2**(2): p. 95-109.
128. Bynoe, M.S., et al., *Adenosine receptor signaling: a key to opening the blood-brain door.* Fluids Barriers CNS, 2015. **12**: p. 20.
129. Abdullahi, W., D. Tripathi, and P.T. Ronaldson, *Blood-brain barrier dysfunction in ischemic stroke: targeting tight junctions and transporters for vascular protection.* Am J Physiol Cell Physiol, 2018. **315**(3): p. C343-c356.
130. Yang, C., et al., *Neuroinflammatory mechanisms of blood-brain barrier damage in ischemic stroke.* Am J Physiol Cell Physiol, 2019. **316**(2): p. C135-c153.
131. Kadry, H., B. Noorani, and L. Cucullo, *A blood-brain barrier overview on structure, function, impairment, and biomarkers of integrity.* Fluids Barriers CNS, 2020. **17**(1): p. 69.
132. Li, X., et al., *Effect of hypoxia/reoxygenation on CD73 (ecto-5'-nucleotidase) in mouse microvessel endothelial cell lines.* Microvasc Res, 2006. **72**(1-2): p. 48-53.

133. Zhou, Y., et al., *Inactivation of endothelial adenosine A(2A) receptors protects mice from cerebral ischaemia-induced brain injury.* Br J Pharmacol, 2019. **176**(13): p. 2250-2263.
134. Melani, A., et al., *Low doses of the selective adenosine A2A receptor agonist CGS21680 are protective in a rat model of transient cerebral ischemia.* Brain Res, 2014. **1551**: p. 59-72.
135. Von Lubitz, D.K., R.C. Lin, and K.A. Jacobson, *Cerebral ischemia in gerbils: effects of acute and chronic treatment with adenosine A2A receptor agonist and antagonist.* Eur J Pharmacol, 1995. **287**(3): p. 295-302.
136. Lacoste, B., et al., *The Blood-Brain Barrier: Composition, Properties, and Roles in Brain Health.* Cold Spring Harb Perspect Biol, 2025. **17**(5).
137. Komarova, Y.A., et al., *Protein Interactions at Endothelial Junctions and Signaling Mechanisms Regulating Endothelial Permeability.* Circ Res, 2017. **120**(1): p. 179-206.
138. Haskó, G., et al., *Adenosine receptors: therapeutic aspects for inflammatory and immune diseases.* Nat Rev Drug Discov, 2008. **7**(9): p. 759-70.
139. Antonioli, L., et al., *Immunity, inflammation and cancer: a leading role for adenosine.* Nat Rev Cancer, 2013. **13**(12): p. 842-57.
140. Allard, B., et al., *The ectonucleotidases CD39 and CD73: Novel checkpoint inhibitor targets.* Immunol Rev, 2017. **276**(1): p. 121-144.
141. Sitkovsky, M.V., et al., *Physiological control of immune response and inflammatory tissue damage by hypoxia-inducible factors and adenosine A2A receptors.* Annu Rev Immunol, 2004. **22**: p. 657-82.
142. Haskó, G. and P. Pacher, *A2A receptors in inflammation and injury: lessons learned from transgenic animals.* J Leukoc Biol, 2008. **83**(3): p. 447-55.
143. Yu, L., et al., *Selective inactivation or reconstitution of adenosine A2A receptors in bone marrow cells reveals their significant contribution to the development of ischemic brain injury.* Nat Med, 2004. **10**(10): p. 1081-7.
144. Li, Y., et al., *Mouse spinal cord compression injury is reduced by either activation of the adenosine A2A receptor on bone marrow-derived cells or deletion of the A2A receptor on non-bone marrow-derived cells.* Neuroscience, 2006. **141**(4): p. 2029-39.
145. Orihuela, R., C.A. McPherson, and G.J. Harry, *Microglial M1/M2 polarization and metabolic states.* Br J Pharmacol, 2016. **173**(4): p. 649-65.
146. Joós, G., et al., *Involvement of adenosine A3 receptors in the chemotactic navigation of macrophages towards apoptotic cells.* Immunol Lett, 2017. **183**: p. 62-72.
147. Zhuang, H., et al., *Overexpressed CD73 attenuates GSDMD-mediated astrocyte pyroptosis induced by cerebral ischemia-reperfusion injury through the A2B/NF-κB pathway.* Exp Neurol, 2025. **386**: p. 115152.
148. Vogl, T., A.L. Gharibyan, and L.A. Morozova-Roche, *Pro-inflammatory S100A8 and S100A9 proteins: self-assembly into multifunctional native and amyloid complexes.* Int J Mol Sci, 2012. **13**(3): p. 2893-2917.
149. Allan, S.M., P.J. Tyrrell, and N.J. Rothwell, *Interleukin-1 and neuronal injury.* Nat Rev Immunol, 2005. **5**(8): p. 629-40.
150. Jha, M.K., et al., *Diverse functional roles of lipocalin-2 in the central nervous system.* Neurosci Biobehav Rev, 2015. **49**: p. 135-56.
151. Emsley, H.C., et al., *A randomised phase II study of interleukin-1 receptor antagonist in acute stroke patients.* J Neurol Neurosurg Psychiatry, 2005. **76**(10): p. 1366-72.
152. Lawrence, T., *The nuclear factor NF-kappaB pathway in inflammation.* Cold Spring Harb Perspect Biol, 2009. **1**(6): p. a001651.
153. Hayden, M.S. and S. Ghosh, *Regulation of NF-κB by TNF family cytokines.* Semin Immunol, 2014. **26**(3): p. 253-66.

154. Hu, X., et al., *Microglial and macrophage polarization—new prospects for brain repair.* Nat Rev Neurol, 2015. **11**(1): p. 56-64.
155. Lalancette-Hébert, M., et al., *Selective ablation of proliferating microglial cells exacerbates ischemic injury in the brain.* J Neurosci, 2007. **27**(10): p. 2596-605.
156. Rosenberg, G.A., *Matrix metalloproteinases in neuroinflammation.* Glia, 2002. **39**(3): p. 279-91.
157. Jin, R., G. Yang, and G. Li, *Inflammatory mechanisms in ischemic stroke: role of inflammatory cells.* J Leukoc Biol, 2010. **87**(5): p. 779-89.
158. Li, X., et al., *Single-cell transcriptomic analysis of the immune cell landscape in the aged mouse brain after ischemic stroke.* J Neuroinflammation, 2022. **19**(1): p. 83.
159. Pasquini, S., et al., *Adenosinergic System Involvement in Ischemic Stroke Patients' Lymphocytes.* Cells, 2020. **9**(5).
160. Liu, F. and L.D. McCullough, *The middle cerebral artery occlusion model of transient focal cerebral ischemia.* Methods Mol Biol, 2014. **1135**: p. 81-93.
161. Yoon, N., et al., *Investigation of long-term metabolic alteration after stroke in tMCAO (transient middle cerebral artery occlusion) mouse model using metabolomics approach.* Neurosci Lett, 2022. **774**: p. 136492.
162. Liu, F., et al., *Changes in experimental stroke outcome across the life span.* J Cereb Blood Flow Metab, 2009. **29**(4): p. 792-802.
163. Ospel, J., et al., *Sex and Gender Differences in Stroke and Their Practical Implications in Acute Care.* J Stroke, 2023. **25**(1): p. 16-25.
164. Leppert, M.H., et al., *Systematic Review of Sex Differences in Ischemic Strokes Among Young Adults: Are Young Women Disproportionately at Risk?* Stroke, 2022. **53**(2): p. 319-327.
165. McCullough, L.D. and P.D. Hurn, *Estrogen and ischemic neuroprotection: an integrated view.* Trends Endocrinol Metab, 2003. **14**(5): p. 228-35.
166. Manwani, B. and L.D. McCullough, *Sexual dimorphism in ischemic stroke: lessons from the laboratory.* Womens Health (Lond), 2011. **7**(3): p. 319-39.
167. Bushnell, C., et al., *Sex differences in the evaluation and treatment of acute ischaemic stroke.* Lancet Neurol, 2018. **17**(7): p. 641-650.
168. Ritzel, R.M., et al., *Aging alters the immunological response to ischemic stroke.* Acta Neuropathol, 2018. **136**(1): p. 89-110.

8. Acknowledgements

First and foremost, I would like to thank my supervisor, PD Dr. Jakob Körbelin, for his continuous guidance, scientific input and support throughout this project. His expertise, encouragement and trust were essential for the completion of this work. I am especially grateful to him for introducing me to the fascinating world of AAVs and for sparking my enthusiasm for gene therapy. His patience in explaining complex concepts, his openness to new ideas and his dedication to scientific excellence have profoundly shaped my development as a researcher. Working under his supervision has been both inspiring and formative. I deeply appreciate the many discussions, insights and opportunities he has provided.

I would also like to sincerely thank Prof. Dr. Tim Magnus for providing a supportive and inspiring scientific environment. His trust and encouragement allowed me to grow scientifically, and I am grateful for the perspectives and guidance he shared along the way.

My sincere thanks also go to PD Dr. Björn Rissiek for his continuous support, scientific input, and helpful discussions during my doctoral studies. His advice, openness and readiness to help were highly valuable at different stages of this project and made many challenges easier to navigate.

My sincere thanks go to all past and present members of our lab for the friendly working atmosphere, scientific exchange and everyday support. In particular, I would like to thank Julia Lüschow (in my mind, she will always be JM) for being my lab companion during that first year when it was just the two of us. I wish her all the best as she enjoys her well-deserved maternity leave. I am also deeply grateful to my fellow lab mates Merrit Johanna Rothe, Zexin Cao, Lilly Rautenberg, and our amazing TA Julie Mendoza for their teamwork, support and the countless discussions and everyday moments that filled our lab with laughter. From the chaos of moving the lab and installing shelves that somehow always ended up slightly crooked, to the legendary bets on that one mysterious bowl, every moment with you made this journey brighter. Your humor, patience and willingness to help turned long days into good memories and made even the toughest challenges feel lighter.

I would also like to thank all past and present members of the ERSI lab for their constant help and support. In particular, I am grateful to my fellow PhD students Jiani, Mamta and Enrico for the mutual encouragement and support that made this journey lighter. I would also like to thank the TAs Lennart, Karo and Tobi, with a special thank you to Lennart for the many tMCAO appointments and the willingness to always help.

Many thanks go to AG Worthmann for their valuable support and collaboration. In particular, I am sincerely grateful to Johanna Hiefner for generously offering her help and for performing the HPLC measurements not once but twice, which greatly contributed to the successful completion of this work.

To my fellow PhD students and postdocs, thank you for the encouragement, the shared frustrations, the laughter and the countless conversations in the hallways and beyond. This journey would not have been the same without your support and companionship. There are too many of you to name individually, but I would like to give a special mention to Lama and Melina, our nearly daily lunches together were a constant source of support and laughter throughout this journey. You all know who you are and I am truly grateful for each of you.

I would like to thank our collaborators and the core facilities for their expertise and assistance. Their contributions were essential for the success of this project.

I am grateful for the financial support provided by the German Research Foundation (DFG) within the Collaborative Research Centre SFB1328, which made this work possible. I also wish to acknowledge the valuable discussions and continuous support from the members of the SFB1328 consortium, whose insights and collaboration greatly enriched this project.

Finally, I would like to thank my family and friends for their unconditional love and support throughout my life. Their encouragement gave me strength during difficult moments and reminded me of what truly matters. I am deeply grateful to my partner for his patience, encouragement and understanding during the ups and downs of this journey. And to our three little dogs, for bringing joy and comfort during the long days and late nights of writing.

This work would not have been possible without all of you. Thank you. Danke. Grazie. 谢谢. ميرسي . Maraming salamat po. धन्यवाद.

Last but certainly not least, I would also like to acknowledge the mice that were sacrificed for this research. Their contribution was essential for advancing our understanding of stroke biology and for the development of potential therapeutic approaches. This work was conducted with the utmost care, responsibility and respect for animal welfare. As the great Jane Goodall said: The least I can do is speak out for those who cannot speak for themselves.

9. Publications

Stamataki M, Rissiek B, Magnus T, Körbelin J.

Microglia targeting by adeno-associated viral vectors.

Front Immunol. 2024;15:1425892.

Stamataki M, Lüschow J, Schlumbohm C, Alawi M, Lunding L, Fuchs E, Trepel M, Schwaninger M, Körbelin J.

Identification of AAV variants with improved transduction of human vascular endothelial cells by screening AAV capsid libraries in non-human primates.

Gene Ther. 2025;32(5):529–541.

10. Declaration of Authorship / Eidesstattliche Versicherung

Ich versichere ausdrücklich, dass ich die Arbeit selbständig und ohne fremde Hilfe, insbesondere ohne entgeltliche Hilfe von Vermittlungs- und Beratungsdiensten, verfasst, andere als die von mir angegebenen Quellen und Hilfsmittel nicht benutzt und die aus den benutzten Werken wörtlich oder inhaltlich entnommenen Stellen einzeln nach Ausgabe (Auflage und Jahr des Erscheinens), Band und Seite des benutzten Werkes kenntlich gemacht habe. Das gilt insbesondere auch für alle Informationen aus Internetquellen. Soweit beim Verfassen der Dissertation KI-basierte Tools („Chatbots“) verwendet wurden, versichere ich ausdrücklich, den daraus generierten Anteil deutlich kenntlich gemacht zu haben. Die „Stellungnahme des Präsidiums der Deutschen Forschungsgemeinschaft (DFG) zum Einfluss generativer Modelle für die Text- und Bilderstellung auf die Wissenschaften und das Förderhandeln der DFG“ aus September 2023 wurde dabei beachtet. Ferner versichere ich, dass ich die Dissertation bisher nicht einem Fachvertreter an einer anderen Hochschule zur Überprüfung vorgelegt oder mich anderweitig um Zulassung zur Promotion beworben habe. Ich erkläre mich damit einverstanden, dass meine Dissertation vom Dekanat der Medizinischen Fakultät mit einer gängigen Software zur Erkennung von Plagiaten überprüft werden kann.

Datum 24.03.2026 Unterschrift